ISSN: 2614-8757 (Print) 2615-2347 (Online)

CHEESA

CHEMICAL ENGINEERING RESEARCH ARTICLES

BOD Analysis & FTIR Spectrum (Fauziah, et al)

VOLUME 5 NO 2, DECEMBER 2022

EDITORIAL BOARD

CHEESA: Chemical Engineering Research Articles

Volume 5 No 2, 2022
ISSN 2614-8757 (Print), ISSN 2615-2347 (Online)
Available online at: http://e-journal.unipma.ac.id/index.php/cheesa

Volume 5 No 2, 2022
ISSN 2614-8757 (Print), ISSN 2615-2347 (Online)
Available online at: http://e-journal.unipma.ac.id/index.php/cheesa

ACKNOWLEDGMENT

CHEESA: Chemical Engineering Research Articles

Our highest gratitude and appreciation go to the reviewers who have reviewed the submitted manuscripts and provided suggestions to us. The reviewers who contributed to this issue are,

1. Prof. Fronthea Swastanti
2. Prof. Rieny Sulistijowati
3. Prof. Mery Napitupulu, Ph.D
4. Prof. Johnner P. Sitompul, Ph.D
5. Prof. Dr. Poedji Loekitowati Hariani
6. Prof. Dedy Suhendra
7. Ronny Purwadi, Ph.D
8. Mujtahid Kaavessina, Ph.D
9. Dr. Agus Budianto
10. Dr. Rhenny Ratnawati
11. Dr. Eng. Dewi Agustina Iryani
12. Dr. Zuhdi Ma'sum
13. Wahyu Prasetyo Utomo
14. Renova Panjaitan
15. Rokiy Alfanaar
16. Cucuk Evi Lusiani

with the seriousness and thoroughness of the reviewers, help us to improve a quality and maintain the quality of writing in the CHEESA: Chemical Engineering Research Articles Volume 5 No 2, December 2022.

Our thanks also go to the various parties who have helped, so that this edition can be published online according to the specified time.

Editorial
CHEESA

Volume 5 No 2, 2022

ISSN 2614-8757 (Print), ISSN 2615-2347 (Online)

Available online at: http://e-journal.unipma.ac.id/index.php/cheesa

TABLE OF CONTENTS

CHEESA: Chemical Engineering Research Articles

CHEESA is a journal that becomes a media of study for chemical and chemical engineering. This journal serves as a media for publication of research in chemistry and chemical engineering aimed at academics, practitioners and community at large. Articles that was published in the CHEESA Journal have gone through editing according to established rules without changing the original manuscript.

Volume 5 No 2, 2022

ISSN 2614-8757 (Print), ISSN 2615-2347 (Online) Available online at: http://e-journal.unipma.ac.id/index.php/cheesa

CHEESA: Chemical Engineering Research Articles
ISSN **2614-8757 (Print)**, ISSN **2615-2347 (Online)**
Available online at: http://e-journal.unipma.ac.id/index.php/cheesa

Research Article

The Effectiveness of Green Scallop Shell Chitosan as Coagulant in Treatment of Tofu Industrial Liquid Waste

Efektivitas Limbah Cangkang Kerang Hijau sebagai Koagulan Dalam Pengolahan Limbah Cair Industri Tahu

Nurlaili Fauziah[1*)], Ma'rifatul Ain[1)], Retno Dewati[1)]
[1)]UPN "Veteran" Jawa Timur, Faculty of Engineering, Chemical Engineering, Indonesia

***correspondence email*:** nurlailifauziah0@gmail.com

Received: 25 June 2022;
Revised: 02 September 2022;
Accepted: 12 September 2022;

doi: *10.25273/cheesa.v5i2.13019.49-58*

Abstract

Tofu waste is gotten after processing soybean, and this waste contains a lot of polluting substances, hence it can pollute rivers and cause health problems. Meanwhile, one method used for treating wastewater into clean water is called the jartest method and its processes include coagulation-flocculation and deposition. This study aims to determine the effectiveness of green mussel shells as coagulants in the treatment of tofu industrial liquid waste. The variables used were 100 mesh green mussel shell powder, 1000 mL of liquid tofu dregs, 150 rpm fast stirring speed for 2 minutes, and 60 rpm slow stirring speed for 15 minutes. Furthermore, chitosan was used with different weight variations in grams (0.5, 0.7, 0.9, 1.1, and 1.3) as well as precipitation time with variations in minutes (20, 30, 40, 50, and 60). The content of Chitosan water was 1.29% and its degree of deacetylation was 65.04%. The result of the preliminary analysis of tofu liquid waste with a coagulant showed BOD, COD, and TSS levels of 965.25mg/L, 435mg/L, and 395mg/L with pH 4 respectively. However, these levels were changed to 195.56mg / L; 299mg/L; and 195.32 mg/L with pH 6 after the final analysis of the liquid waste was conducted.

Keywords: coagulant; green mussel shells; jartest method; tofu industry

Abstrak

Limbah tahu merupakan sisa dari pengolahan kedelai yang terbuang karena tidak terbentuk menjadi tahu. Limbah tahu banyak mengandung pencemar yang dapat mencemari sungai dan menimbulkan gangguan kesehatan. Metode jartest adalah suatu metode pengolahan air limbah menjadi air bersih yang prosesnya meliputi proses koagulasi-flokulasi dan pengendapan. Penelitian ini bertujuan untuk mengetahui efektivitas cangkang kerang hijau sebagai koagulan dalam pengolahan limbah cair industri tahu. Variabel yang digunakan yakni serbuk cangkang kerang hijau 100 mesh, 1000 mL ampas tahu cair, pengadukan cepat 150 rpm selama 2 menit, dan pengadukan lambat 60 rpm selama 15 menit. Variasi berat kitosan yang digunakan dalam gram antara lain 0,5; 0,7; 0,9; 1,1; 1,3; dan waktu pengendapan dalam menit 20, 30, 40, 50, 60. Kadar air kitosan 1,29% dan persentase deasetilasi 65,04%. Analisis awal limbah cair industri tahu dengan koagulan diperoleh kadar BOD, COD, TSS berturut-turut 965,25mg/L; 435mg/L; 395mg/L; dan pH 4. Pada analisis akhir limbah cair industri tahu, diperoleh perubahan kadar BOD, COD, TSS menjadi 195,56mg/L; 299mg/L; 195,32 mg/L dan pH 6.

Kata kunci: *cangkang kerang hijau; industri tahu; koagulan; metode jartest*

1. Introduction

Kenjeran, in Surabaya is one area that has at most 3 tons of shells discarded on the Kenjeran seaside [1]. These discarded shells are partly made up of the green mussel shell, which is a source of minerals with high carbonates. The shells are widely used by local people as decoration while the rest are left on the Kenjeran. Thus, the remaining shells can be converted into chitosan, which can be used as a coagulant for the process of purifying river water and waste. The content of green mussel shells that can produce chitosan is called chitin [2]. Furthermore, these shells contain calcium oxide (CaO), silicon dioxide (SiO_2), iron (III) oxide (Fe_2O_3), magnesium (MgO), and aluminum oxide (Al_2O_3) [3].

One known water contaminant is the tofu waste and it is produced by tofu industries. These industries are fast-growing in big cities and liquid waste is the dominant type of waste from the tofu production process [4]. These wastes contain high protein and thus pollute the environment with a bad smell as soon as they are disposed of without prior processing and this will automatically reduce the quality of the water bodies in which the waste is disposed of [5]. Furthermore, the waste contains both suspended and dissolved solids, which will undergo physical, chemical, and biological changes hence they can cause health problems because they produce toxic substances or create a medium for the growth of microorganisms in the human body [6].

Wastewater left on land will be absorbed by the ground and can accumulate with well water sources. Liquid waste flowing into rivers can contaminates and cause health problems in the form of itching, diarrhea, cholera, intestinal inflammation, and other diseases, especially those related to blood. In addition, the river water will become dirty and cause poor sanitation [7]. Therefore, it is necessary to treat tofu industrial liquid wastes before disposal in order to achieve the quality standards determined by the Indonesian Minister of Environment Number 5 of 2014 [5].

Industrial waste treatment can be performed either by physical, chemical, or biological means. Physical wastewater treatment is carried out in various stages such as filtration, grit chamber, sieving, sedimentation, and equalization. Chemical wastewater treatment includes chemical deposition, gas transfer, adsorption, disinfection, and dechlorination. Meanwhile, the biological treatment is divided into three models, including aerobic, anaerobic, and facultative treatments [8].

The jartest method is a wastewater treatment method whose processes include coagulation, flocculation, and sedimentation. It is used to remove suspended solids that can cause turbidity problems [9]. Coagulation is the process of treating water or wastewater by stabilizing colloidal particles to ensure particle growth during flocculation. Meanwhile, flocculation is a type of wastewater treatment that contacts the colloidal particles resulting from coagulation to become larger flocs hence they can settle quickly [6]. The next process is sedimentation also known as the deposition of coagulant particles. In this process, all streams of solids whose density is greater than the density of water (or liquid) will settle for a certain time and during that time, they are automatically separated from the water. The time required for the

particles to settle is dependent on their sizes as well as the position of the high and low particles from the bottom of the sedimentation tank [10]. Parameters measured in the tofu industrial liquid waste treatment process with the addition of coagulant include wastewater pH, Biological Oxygen Demand (BOD), Chemical Oxygen Demand (COD), and Total Suspended Solid (TSS) [11].

Subsequently, the coagulation and flocculation processes are influenced by the pH level of the wastewater and the type of coagulant used. The appropriate waste pH makes the coagulant work well. The selection of the types of coagulant and flocculant used should be adjusted to the type of colloid contained in the wastewater. These types of coagulants and flocculants are generally oppositely charged to the ionic charge in the wastewater and they function to bind ions in wastewater in order to reduce the repulsion between colloidal particles, hence flocs can be formed [12].

Coagulants play an important role in clean water treatment, especially in terms of reducing turbidity, Total Dissolved Solid (TDS), and Total Suspended Solid (TSS). Alum sulfate, poly-aluminum chloride, ferrous sulfate (FeSO4), and ferric chloride (FeCl3) are examples of commonly used chemical coagulants. Meanwhile, the use of natural ingredients as coagulants is currently being developed because it has several advantages such as being biodegradable, safer for human health, and more economical. Natural coagulants can be found easily because they can be obtained or extracted from local ingredients such as plants or animals [13].

Chitosan is a by-product obtained from the oxidation of chitin hence it can be used as an herbal coagulant in water treatment [14]. The degree of chitosan deacetylation is generally about 60%, and about 90-100% for fully deacetylated chitosans [15]. Furthermore, the advantages of using chitosan as a coagulant include the fact it is non-toxic, biodegradable, multi-electron cation, and easily interacts with other organic substances such as protein, hence it has the potential as a natural coagulant for water treatment [16].

Aulia *et al.*[17] used 1000 mL of tofu industrial liquid waste with a fast stirring speed of 150 rpm for 2 minutes and a slow stirring of 60 rpm for 15 minutes, followed by precipitation for 30 minutes. The result of their study showed that the addition of a green mussel shell coagulant dose at 0.7 grams or 700 mg/L can reduce the COD and TSS levels to 1339.59 mg/L and 119mg/L with a removal efficiency of 73.09% and 90.846% respectively.

Following this, Farihin *et al.* [18] used 100 mL of PT. Sido Muncul, Tbk liquid waste with variations in the dose of green mussel shell chitosan per liter of waste, such as 150 mg/L, 200 mg/L, 250 mg/L, and 300 mg/L. The best results were obtained at a variation of 250 mg/L with fast stirring of 100 rpm for 1 minute followed by slow stirring of 20 rpm for 15 minutes and precipitation for 30 minutes. Based on the results, this bio-coagulant reduced the COD concentration from 5082.86 mg/L to 1636.43 mg/L, reduce the TSS concentration from 2270 mg/L to 365 mg/L, and set aside the Turbidity concentration value from 621.1 NTU to 194.9 NTU.

Therefore, this research was carried out to determine the efficiency of green mussel shell waste as a coagulant in the tofu industrial liquid waste treatment as

well as to observe the effectiveness of this natural coagulant in reducing pH, Biological Oxygen Demand (BOD), Chemical Oxygen Demand (COD), and Total Suspended Solid (TSS) levels.

2. Research Methods

2.1 Research Place

This research was conducted at the waste treatment laboratory in the UPN "Veteran" Jawa Timur.

2.2 Tools and materials

The raw material used in this research is the green mussel shell waste, which was obtained from the Kenjeran area, Surabaya. Meanwhile, the tofu liquid waste was obtained from the A Hok tofu factory.

The tools used include oven, pH meter, heating reactor, BOD bottle, stative and clamps, burette, Erlenmeyer, COD meter, beaker glass, and sieve. The series of research tools are shown in Figures 1 and 2.

2.3 Research procedure

2.3.1 Green Mussel Shell Preparation

Green mussel shells were washed and dried in the sun, then it was mashed and sieved to obtain a size of 100 mesh.

2.3.2 Chitosan Preparation

2.3.2.1 Deproteination stage

The green mussel shell powder was added to a 3% NaOH solution with a ratio of 1:6 (w:v). The solution was then heated to 80-90^{o}C and stirred using a magnetic stirrer. After which, the solids were washed with distilled water until the pH is neutral and then dried in the oven.

2.3.2.2 Demineralization stage

The result of the deproteination stage in the form of green mussel shell powder was then added to a 1.25N HCl solution with a ratio of 1:10 (w:v) and also stirred using a magnetic stirrer at a temperature of 70-80^{o}C. The resulting solids were also washed at neutral pH and then dried to obtain dry chitin.

2.3.2.3 Deacetylation stage

Further, the demineralized dry chitin was dissolved in a 45% NaOH solution with a ratio of 1:20 (w:v) at 140^{o}C and stirred with a magnetic stirrer. The resulting solids were then dried at 80^{o}C to obtain the chitosan.

2.3.2.4 Chitosan analysis stage

The water content and FTIR (Fourier Transform InfraRed) of the green mussel shell chitosan were then analyzed.

2.3.3 Waste Treatment

The tofu industrial liquid waste sample collected was fresh and still in the temporary waste storage tank. Furthermore, the sample's pH, BOD, COD, and TSS levels were analyzed.

At most 1000 mL of tofu industrial liquid waste and green mussel shell coagulant with weight variations of 0.5 grams; 0.7 grams; 0.9 grams; 1.1 grams; and 1.3 grams was coagulated at a stirring speed of 150 rpm for 2 minutes at a glass beaker. After which, the flocculation process was carried out for 15 minutes by reducing the stirring speed to 65 rpm.

The further stage was the deposition process of the colloidal particles which resulted from flocculation (slow stirring), with variations in the precipitation time of 20, 30, 40, 50, and 60 minutes for each variation in chitosan weight. The treated wastewater was then analyzed for pH, BOD, COD, and TSS.

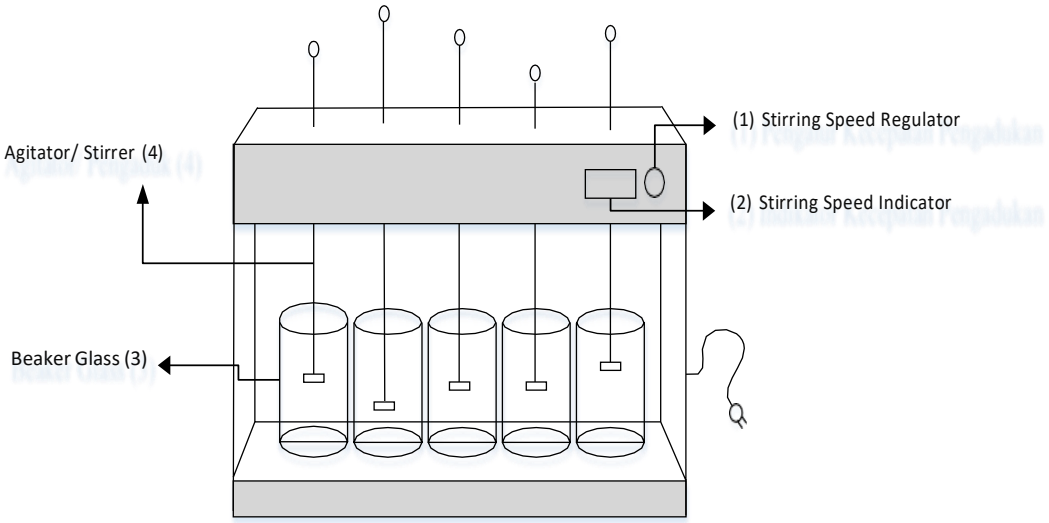

Figure 1. The series of coagulation-flocculation process tools

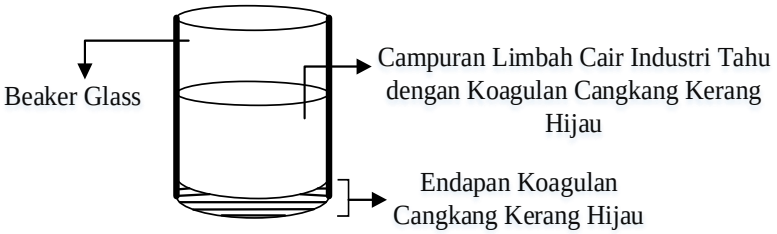

Figure 2. The series of sedimentation process

3. Results and Discussion

The process of producing coagulant from chitin involves several stages. First, is the deproteination. This stage aims to reduce the protein content with a dilute alkaline solution. Secondly, the demineralization stage is aimed at reducing the mineral content by using low acidity to obtain the chitin. Lastly, the deacetylation stage aims to completely remove the structure of acetyl chitin by heating it in a strongly alkaline solution at a high concentration [19].

Before the deproteination stage, Chitin was a proteinate. To make it protein-free, the material was dissolved in a 3% NaOH solution. The deproteination process uses high temperatures and stirring to accelerate the binding of the ends of the protein chains using NaOH hence the protein degradation and precipitation process were perfect. Furthermore, the purpose of washing with distilled water was to dissolve the Na-proteinate formed during the reaction hence it was lost during the filtering and washing process [20]. The reaction that occurs in the deproteination step is shown in Figure 3.

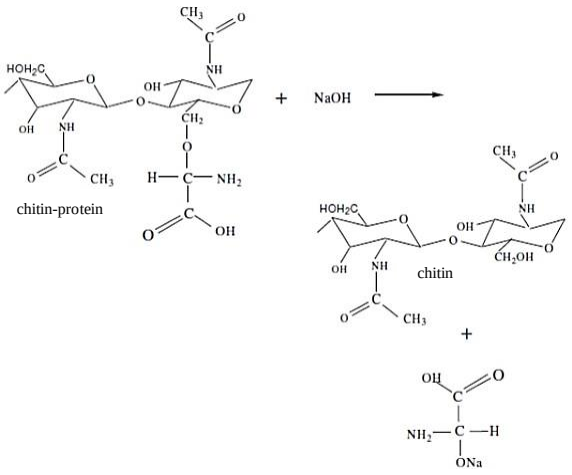

Figure 3. Deproteination stage reaction

The application of Chitin contained in green mussel shells into the main mineral content of $CaCO_3$ dissolved in a 1.25N HCl solution will produce chitin solids, calcium chloride, carbon dioxide gas, and water. The demineralization process using HCl dissolved the minerals contained in the green mussel shells, thus drastically reducing the mineral contents in the chitin. When the deproteinized chitin was dissolved in HCl, a CO_2 gas bubble was formed which indicated the ongoing mineral release process [20]. The reaction in the demineralization stage is shown in Figure 4.

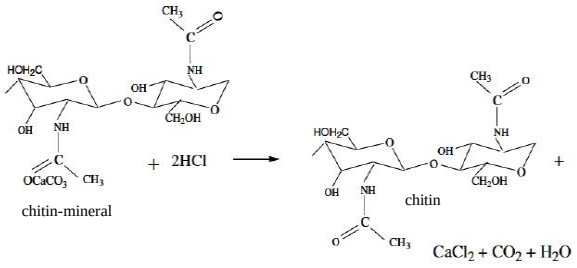

Figure 4. Demineralization stage reaction

Chitin was the amide and NaOH was the base. At first, an addition reaction occurred, the OH^- group entered the $NHCOCH_3$ group, then the elimination of the CH_3COO^- group produced an amine, namely chitosan. Furthermore, the deacetylation process, which was conducted using a high concentration of base and high temperature affected the degree of deacetylation. The formation reaction of the chitosan from chitin was a hydrolysis reaction of an amide [20]. The reaction in the deacetylation stage is shown in Figure 5.

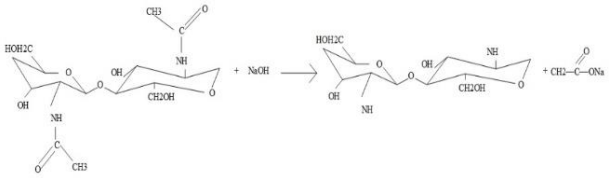

Figure 5. Deacetylation stage reaction

The preparation of chitosan from green mussel shells was carried out by analyzing the water content and the degree of deacetylation. Its water content was 1.29% and the degree of deacetylation was obtained from the FTIR spectrum analysis results shown in Figure 6.

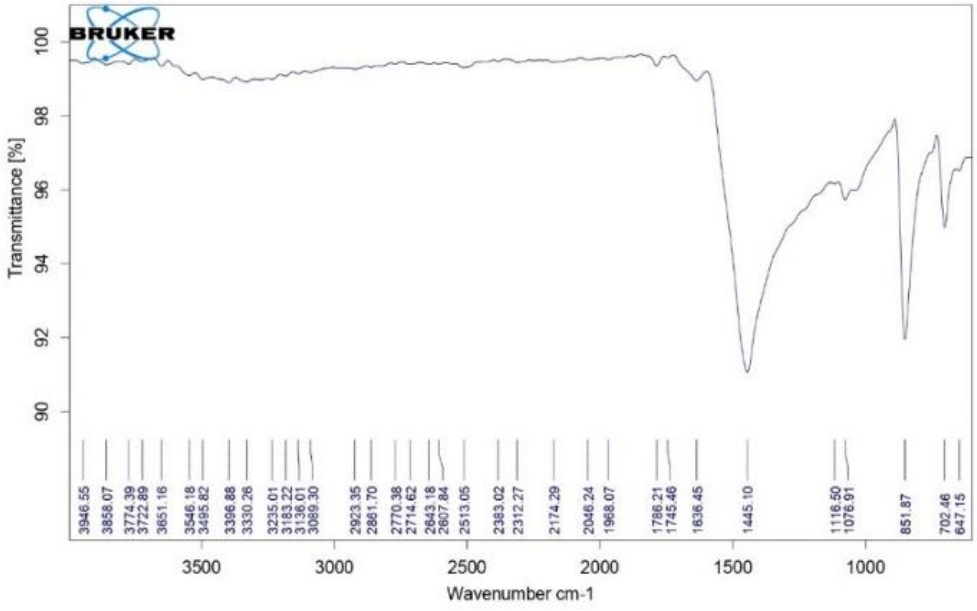

Figure 6. FTIR spectrum of green mussel shell chitosan

The degree of deacetylation was calculated by giving infrared light to the chitosan sample, then the light absorption rate was recorded. Additionally, the amide and hydroxyl groups were at wavelengths of 1655cm^{-1} and 3450 cm^{-1} respectively. Based on the infrared absorption recording results shown in Figure 6, the absorbance value of chitosan obtained at the two aforementioned wavelengths was 1.047 and 2.252 respectively, hence the degree of deacetylation obtained was 65.04%.

Following this, the obtained chitosan had a water content of 1.29% and a degree of deacetylation of 65.04%. This result is different from that of Aulia *et al.* [17] in whose study crab shell chitosan was used with a water content of 2.21% and a degree of deacetylation of 87.64%. The water content of the chitosan in green mussel shells is, however, lower than that of crab shells. This is influenced by the drying time as well as the amount and surface of the chitosan to be dried [21].

Accordingly, the degree of deacetylation in crab shell chitosan is higher than that of the green mussel shell because of the crab shell coagulant's ability to separate more nitrogen-bound acetyl groups in the structure of chitin compounds, thereby increasing the ratio of amino groups in the chitosan [16].

Table 1. The initial analysis results of the tofu industrial liquid waste before going through the treatment process

Parameter	Unit	Concentration
BOD	mg/L	965.25
COD	mg/L	435.56
TSS	mg/L	395
pH		4

Table 1 shows the initial analysis results of the tofu industrial liquid waste before undergoing the treatment process. The waste had BOD, COD, and TSS levels of 965.25 mg/L, 435.56 mg/L, and 395 mg/L respectively with pH 4. Furthermore, the waste was then processed using the jartest method with the green mussel shell chitosan as a coagulant. The analysis results of the BOD concentration in tofu industrial liquid waste that had undergone treatment are shown in Figure 7.

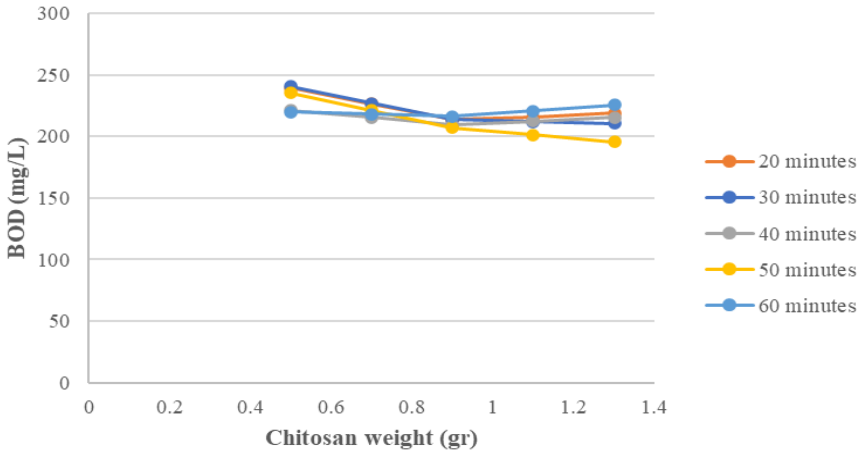

Figure 7. Analysis results of BOD level (mg/L) vs chitosan weight (grams)

Figure 7 shows that green mussel shell coagulant can reduce the BOD level. The best results were obtained from the addition of 1.3 grams of chitosan with a precipitation time of 50 minutes, where the BOD level was reduced by 195.56 mg/L from an initial concentration of 965.25 mg/L. However, the BOD produced was still far from the quality standards outlined by the Minister of Environment Regulation Number 5 of 2014 at 150 mg/L [5]. This was due to the inaccurate speed and delay in stirring, hence the floc was not formed in the wastewater and precipitation occurred easily. In addition, the high BOD level has an impact on the death of aquatic organisms such as fish due to a lack of dissolved oxygen [22].

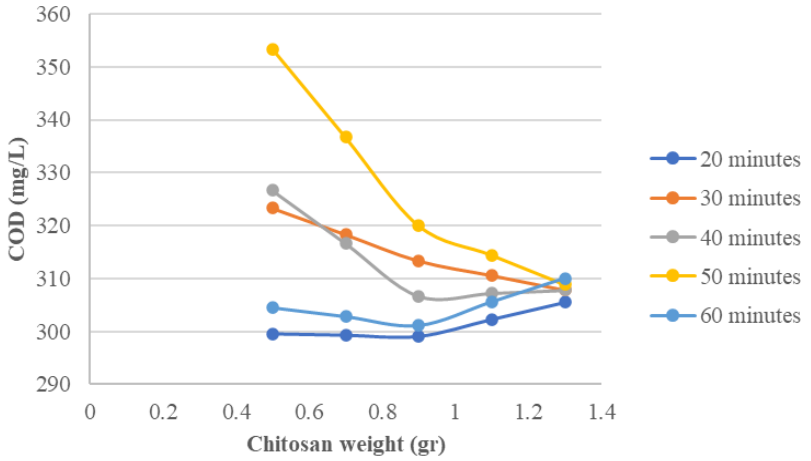

Figure 8. Analysis results of COD level (mg/L) vs chitosan weight (grams)

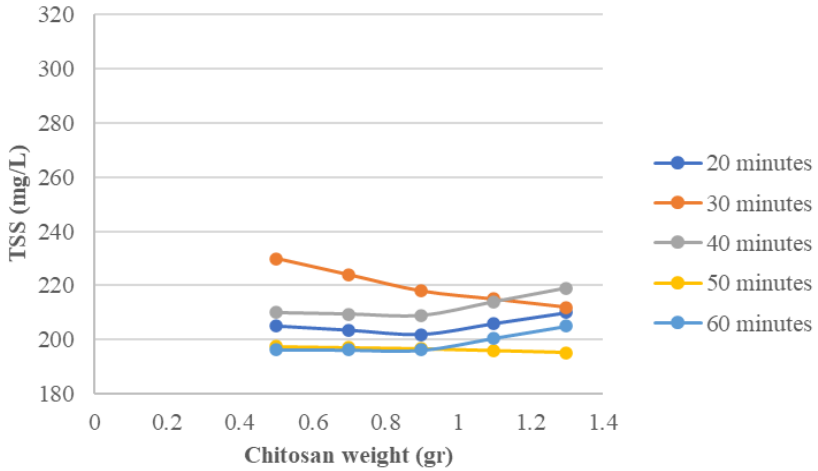

Figure 9. Graph for analysis of TSS level (mg/L) vs chitosan weight (grams)

The COD analysis in Figure 8 show that the green mussel shell coagulant can reduce the COD level. The best results were obtained with the addition of 0.9 grams of chitosan at 20 minutes of precipitation time which reduced the COD level by 299 mg/L from the initial level of 435.56 mg/L. These results met the quality standards of the tofu industrial liquid waste from the Minister of the Environment Regulation Number 5 of 2014, which is a maximum limit of 300

mg/L COD [5].

The COD level in the wastewater decreased as the concentration of organic matter decreased. A low COD level indicates that the amount of oxygen present can oxidize the organic matter in the wastewater properly [23].

Figure 9 shows that the green mussel shell coagulant reduced the TSS level of the tofu industrial liquid waste. The best results were obtained with the addition of 1.3 grams of chitosan at 50 minutes of precipitation time which reduced the TSS level by 195.32 mg/L from the initial level of 395 mg/L. This result also met the quality standards of tofu industrial liquid waste determined by the Minister of Environment Regulation Number 5 of 2014, which is a maximum limit of 200 mg/L [5].

4. Conclusion

Based on the observation results obtained, it can be concluded that the coagulant of mussel shell waste is quite effective in processing the liquid waste of tofu factories. The initial levels of BOD, COD, and TSS were 965.25 mg/L; 435.56 mg/L; and 395 mg/L respectively with pH 4. However, the processing carried out using the jartest method with the addition of coagulant produced pH 6 with BOD, COD, and TSS levels of 195.56 mg/L; 299 mg/L; and 195.32 mg/L, respectively. Conclusively, green mussel shell coagulant can reduce the BOD, COD, and TSS levels of tofu industrial liquid waste. The decrease in BOD level, however, did not meet the quality standards of the tofu industrial liquid waste.

References

[1] Rokhmadhoni, R. A. (2019). *Kulit Kerang Sebagai Media Alternatif Filter Anaerobik Untuk Mengolah Air Limbah Domestik*. *Institut Teknologi Sepuluh November*.

[2] Yuda, P., Bandem, P. D., & Zulfita, D. (2019). The Improvement Chemical Property of Peatlands By fertilizer mussel shell (Polymesoda erosa) To cultivation of the Sweet Corn. *Journal of Geotechnical and Geoenvironmental Engineering ASCE*, 120(11), 259.

[3] Firyanto R., Soebiyono, Rif'an, M. (2019). Pemanfaatan kitosan dari limbah cangkang kerang hijau (Perna viridis) sebagai adsorban logam Cu. *Jurnal Teknik Kimia*, 23(1), 1–6.

[4] Saenab, S., Henie, M., Al, I., Rohman, F., & Arifin, A. N. (2018). Pemanfaatan Limbah Cair Industri Tahu Sebagai Pupuk Organik Cair (POC) Guna Mendukung Program Lorong Garden (Longgar) Kota Makassar. *Prosiding Seminar Nasional Megabiodiversitas Indonesia*, 4(1), 31–38.

[5] Sayow, F., Polii, B. V. J., Tilaar, W., & Augustine, K. D. (2020). Analisis Kandungan Limbah Industri Tahu Dan Tempe Rahayu Di Kelurahan Uner Kecamatan Kawangkoan Kabupaten Minahasa. *Agri-Sosioekonomi*, 16(2), 245. doi: 10.35791/agrsosek.16.2.2020.28758

[6] Coniwanti, P., Mertha, I. D., & Eprianie, D. (2013). Pengaruh Beberapa Jenis Koagulan Terhadap Pengolahan Limbah Cair Industri Tahu dalam Tinjauannya Terhadap Turbidity, TSS dan COD. *Jurnal Teknik Kimia*, 19(3), 22–30.

[7] Setyawati, H., Sinaga, E. J., Wulandari, L. S., & Sandy, F. (2018). Efektifitas Biji Kelor Dan Tawas Sebagai Koagulan Pada Peningkatan Mutu Limbah Cair Industri Tahu. *Jurnal Teknik Kimia*, 12(2), 47–51. doi: 10.33005/tekkim.v12i2.1084

[8] Dahruji, Wilianarti, P. F., & Hendarto, T. (2016). Studi Pengolahan Limbah Usaha Mandiri Rumah Tangga dan Dampak Bagi Kesehatan di Wilayah Kenjeran, Surabaya. *Aksiologiya: Jurnal Pengabdian Kepada Masyarakat*, 1(1), 36–44. doi: 10.30651/aks.v1i1.304

[9] Setyawati, H., LA, S. S., & Sari, S. A. (2019). Penerapan Penggunaan Serbuk Biji Kelor Sebagai Koagulan Pada Proses Koagulasi Flokulasi Limbah Cair Pabrik Tahu Di Sentra Industri Tahu Kota Malang. *Industri Inovatif : Jurnal Teknik Industri*, 8(1), 21-31. doi: 10.36040/industri.v8i1.669

[10] Cahyana, G. H. (2022). Flotasi vs Sedimentasi. *Majalah Bulanan Air Minum: SAINSTEK*, 50–51.

[11] Husaini, Cahyono, S. S., Suganal, S., & Hidayat, K. N. (2018). Perbandingan Koagulan Hasil Percobaan Dengan Koagulan Komersial Menggunakan Metode Jar Test. *Jurnal Teknologi Mineral dan Batubara*, 14(1), 31–46. doi: 10.30556/jtmb.vol14.no1.2018.387

[12] Welasih, T. (2008). Penurunan BOD dan COD limbah industri kertas dengan air laut sebagai koagulan. *Jurnal Teknik Kimia*, 4, 1–13.

[13] Prihatinningtyas, E., & Jasalesmana, T. (2021). Studi penurunan kekeruhan dengan aplikasi ekstrak tapioka sebagai koagulan alam pada pengolahan air bersih the study of turbidity removal by using tapioca extract as natural coagulant on water treatment. *Jurnal Riset Teknologi Industri*, 15(2), 200–208.

[14] Meicahayanti, I., Marwah, M., & Setiawan, Y. (2018). Efektifitas Kitosan Limbah Kulit Udang dan Alum Sebagai Koagulan dalam Penurunan TSS Limbah Cair Tekstil. *Jurnal Chemurgy*, 2(1), 1–5. doi: 10.30872/cmg.v2i1.1630

[15] Rahayu, L. H., & Purnavita, S. (2017). Optimasi Pembuatan Kitosan Dari Kitin Limbah Cangkang Rajungan (Portunus pelagicus) Untuk Adsorben Ion Logam Merkuri. *Reaktor*, 11(1), 45. doi: 10.14710/reaktor.11.1.45-49

[16] Ihsani, S. L., & Widyastuti, C. R. (2014). Sintesis Biokoagulan Berbasis Kitosan Dari Kulit Udang Untuk Pengolahan Air Sungai Yang Tercemar Limbah Industri Jamu Dengan Kandungan Padatan Tersuspensi Tinggi. *Jurnal Bahan Alam Terbarukan*, 3(2), 66–70. doi: 10.15294/jbat.v3i2.3700

[17] Aulia, Z., Sutrisno, E., & Hadiwidodo, M. (2016). Pemanfaatan Limbah Cangkang Kepiting Sebagai Biokoagulan Untuk Menurunkan Parameter Pencemar COD dan TSS Pada Limbah Industri Tahu. *Jurnal Teknik Lingkungan*, 5(2), 1–12.

[18] Farihin, F. M., Wardhana, I. W., & Sumiyati, S. (2015). Studi Penurunan COD, TSS, dan Turbidity Dengan Menggunakan Kitosan dari Limbah Cangkang Kerang Hijau (Perna viridis) Sebagai Biokoagulan Dalam Pengolahan Limbah Cair PT.Sido Muncul Tbk, Semarang. *Jurnal Teknik Lingkungan*, 7(1), 37–72.

[19] Sinardi, Soewondo, P., & Suprihanto, N. (2013). Pembuatan, karakterisasi dan aplikasi kitosan dari cangkang kerang hijau (Mytulus virdis linneaus) sebagai koagulan penjernih air. *Konferensi Nasional Teknik Sipil 7*, 2, 24–25. Retrieved from http://sipil.ft.uns.ac.id/konteks7/index_qa.php

[20] Laili, N., Fitri, E., & Rusmini, D. (n.d.). Characterization of Chitosan from Simping Shells (Placuna placenta) Waste. *UNESA Journal of Chemistry*, 109.

[21] Rahmawati, W., Herasari, D., & Husniati. (2012). Produksi Kitosan Dari Bahan Baku Cangkang Udang Enzim Kitin Deasetilase. *Prosiding SNSMAIP*, 3(978), 535–540.

[22] Daroini, T. A., & Arisandi, A. (2020). Analisis Bod (Biological Oxygen Demand) Di Perairan Desa Prancak Kecamatan Sepulu, Bangkalan. *Juvenil*, 1(4), 558–566. Retrieved from https://journal.trunojoyo.ac.id/juvenil/article/view/8994

[23] Harahap, M. R., Amanda, L. D., & Matondang, A. H. (2020). Analisis Kadar Cod (Chemical Oxygen Demand) Dan Tss (Total Suspended Solid) Pada Limbah Cair Dengan Menggunakan Spektrofotometer Uv-Vis. *Amina*, 2(2), 79–83.

CHEESA: Chemical Engineering Research Articles
ISSN **2614-8757 (Print)**, ISSN **2615-2347 (Online)**
Available online at: http://e-journal.unipma.ac.id/index.php/cheesa

Research Article

Ultrasonic-Assisted Flavonoid Extraction from Ant Nest

Ekstraksi Flavonoid Sarang Semut Berbantu Gelombang Ultrasonik

Nita Indriyani[1*)], Yusnita La Goa[1)], Muthmainnah Ely[1)], Elton Mendy[1)]
[1)]Universitas Pendidikan Muhammadiyah Sorong, Faculty of Science and Technology, Chemical Engineering, Indonesia

***correspondence email*:** nitaindriyani@unimudasorong.ac.id

Received: 23 March 2022;
Revised: 16 August 2022;
Accepted: 20 September 2022;

doi: *10.25273/cheesa.v5i2.12231.59-64*

Abstract

The extraction of active substances from ant nests can be affected by various extraction methods, whether conventional or sonication. Sample extraction was carried out by maceration and ultrasonic methods with the use of solvents to yield flavonoid compounds. The solvents used were aquadest, 70% ethanol and n-hexane, with a material-to-solvent ratio of 1:50 (w/v). The highest flavonoid content of 14% was obtained by ultrasonic-assisted extraction method, with aquadest as the solvent and at operating conditions of 24 minutes at a temperature of 40°C. Due to their high aquadest solubility and the presence of one or more sulphate ions that are bound to the hydroxyl phenol or sugar, the flavonoids produced are classified as flavonoid sulphate.

Keywords: ant nest; extraction; flavonoid; ultrasonic; maceration

Abstrak

Berbagai macam metode ekstraksi baik konvensional maupun sonikasi dapat memberikan pengaruh yang berbeda pada ektraksi zat aktif pada sarang semut. Penelitian ini mencoba berbagai macam metode ekstraksi dan penggunaan pelarut untuk mengekstraksi senyawa flavonoid sarang semut. Ekstraksi sampel dilakukan dengan metode maserasi dan ultrasonik. Adapun pelarut yang digunakan aquadest, etanol 70%, dan n-hexane. Rasio bahan dengan pelarut 1:50 (b/v). Kadar flavonoid tertinggi diperoleh dengan metode ekstraksi berbantu gelombang ultrasonik, yaitu 14% pada kondisi operasi 24 menit, suhu 40°C dengan pelarut air. Flavonoid yang dihasilkan termasuk pada golongan flavonoid sulfat. Senyawa flavonoid sulfat memiliki sifat mudah larut dalam air dan memuat satu ion sulfat atau lebih, yang terikat pada hidroksil fenol atau gula.

Kata Kunci*: ekstraksi; flavonoid; maserasi; sarang semut; ultrasonik,*

1. Introduction

Ant nest is a tuber plant native to Papua. It is a typical Indonesian plant with a high content of flavonoids and tannins [1]. Previous research on *Myrmecodia pendans* reported that ant nests have antibacterial properties, and the extract is effective against gram-positive and gram-negative bacteria [2].

Ant nest Plants contain chemical compounds from the flavonoid and tannin groups known to cure various diseases.

Flavonoids have antibacterial, antiviral and anticancer properties [3]. Previous research also reported that ant nests contain many antioxidants and immunostimulants that help increase immunity. Furthermore, immunostimulants protect and assist the body's cells to perform their functions properly [2].

The mechanism for the extraction of bioactive substances from plants involves organic solvents penetrating the plant cell walls and dissolving the bioactive substances. This results in a concentration difference between organic solvents outside the cell and bioactive substances in cells. Therefore, the solution with a higher concentration diffuses out of the cell, and the process continues until there is a balance between the concentration of the active substance inside and outside the cell. [4].

One of the extraction methods that can be used is sonication extraction (ultrasonic), which involves the extraction of bioactive substances into the solvent using ultrasonic waves [5]. In the ultrasonic reactor (sonicator), ultrasonic waves are used to form cavitation bubbles in the solution. The cavitation bubbles that burst close to the cell wall produce shock waves and liquid jets, causing the cell walls of bioactive substances to rupture. This rupture causes the cell components to leak out and mix with the solution.

Various extraction methods, including conventional methods and sonication, can have different effects on the extraction of active substances in ant nests. Crisnaningtyas & Rachmadi reported that antibacterial substances extracted from ant nests by leaching method and ethanol solvent did not produce an inhibitory reaction, which could be attributed to the use of volatile ethanol [6]. This research aimed to determine and compare the effect of ultrasonic-assisted extraction and conventional extraction (maceration). Furthermore, the purpose of this research was to determine the effect of the type of solvent on the extraction.

2. Research Methods

2.1 Tools and Materials

The materials used in this research include ant nest from Maibo Village, 70% ethanol, n-hexane, and aquadest. The tools used include a digital ultrasonic sonicator CD-2840A Krisbow, beaker, measuring flask, cooler, thermometer, analytical balance, and stirrer.

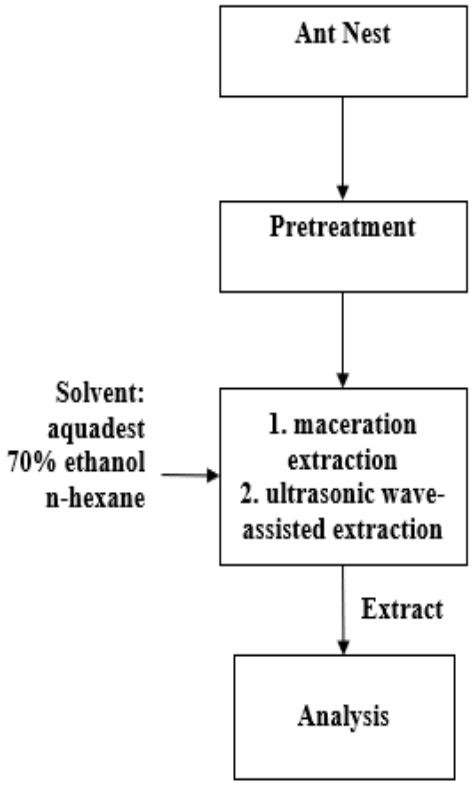

Figure 1. Process Flow Chart

2.2 Extraction

2.2.1 Maceration Method

A total of 2 grams of ant nest powder was measured into a beaker and 100 ml of three different solvents (ethanol 70%, n-hexane, aquadest) were then added with a

sample-solvent ratio of 1:50 (w/v), respectively. The mixture was then stirred and covered. Furthermore, the Immersion process lasted 3 hours at a temperature of 30, 40 and 50°C, respectively. After 3 hours, the filtrate and residue were filtered.

2.2.2 Ultrasonic Method

A total of 2 grams of ant nest powder was measured into a beaker and 100 mL of three different solvents (ethanol 70%, n-hexane, aquadest) with a sample-solvent ratio of 1:50 (w/v) were added, respectively. The sample was then inserted into the Krisbow digital ultrasonic sonicator CD-2840A at 50 Hz. The operation was carried out at temperatures of 30, 40 and 50°C with a time of 16, 24, and 32 minutes, respectively.

3. Results and Discussion

3.1 Chemical Compound Content

Table 1 shows the phytochemical test results for flavonoid content using ultrasonic-assisted extraction at a temperature of 40°C for 24 minutes. The phytochemical test result using three different solvents shows that the ant nest using aquadest and ethanol as solvents contains flavonoid compounds and tannins. This is consistent with the results by Soeksmanto *et al.* [7] which showed that the phytochemical test results of the water extract of the ant nest *Myrmecodia pendens* type contained flavonoids and tannins, while the aqueous extract of the *Myrmecodia tuberosa* type contained flavonoids and anthocyanidins [3].

Table 1. Phytochemical test results

Group	Aquadest	Ethanol	n-hexane
Alkaloid	-	-	-
Flavonoid	+	+	-
Tannin	+	+	-

3.2 Solvent Effect

The effect of solvents on the yield of flavonoids is shown in Table 2 and Figure 2. Figure 2 is the result of the extraction of ant nests assisted by ultrasonic waves at a temperature of 40°C, for 24 minutes. Flavonoids are plant pigments with red, yellow, and orange-yellow colors. In Table 2 and Figure 2, it can be seen that the extraction result with water solvent shows red color. Based on the results obtained, high flavonoid content is found in ant nest extract with water as a solvent. Therefore, the flavonoid compounds produced are classified as flavonoid sulphate due to their solubility in water and the presence of one or more sulphate ions, which are bound to the hydroxyl phenol or sugar. Structurally, this compound is a bisulphate because it exists as a salt, namely flavone-O-SO_3K. This bisulphate part is generally bound to the free phenolic hydroxyl or sugar [2] [8]. This compound has a limited distribution, such as in angiosperms that have an ecological relationship with aquatic habitats. Therefore, the ant nest contains sulphate flavonoids because it is an angiosperm.

Table 2. Effect of extraction solvent

Method	Solvent	Color
Maceration	aquadest	dark red
	70% ethanol	bright red
	n-hexane	bright yellow
Ultrasonic	aquadest	dark red
	70% ethanol	pretty dark red
	n-hexane	bright yellow

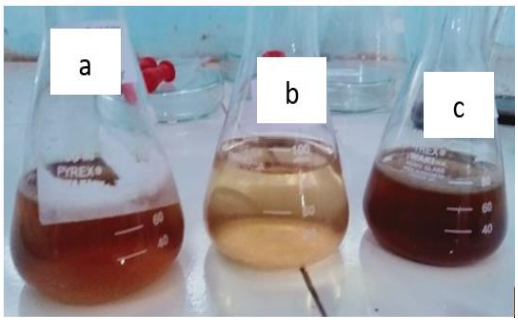

Figure 2. Results of ultrasonic-assisted extraction: a) 70% ethanol, b) n-hexane, c) aquadest

3.3 Effect of Extraction Temperature and Time

The effect of temperature and extraction time on flavonoid content is shown in Figure 3. Figure 3 shows that the highest flavonoid content of 14% was achieved in 24 minutes and at 40ºC. These results are similar to those reported by Handayani *et al.* who stated that the best extraction time for soursop leaves using ultrasonic states is 20 minutes [9]. The higher the extraction temperature and time, the lower the flavonoid content produced. The increase in temperature and longer extraction time resulted in lower yields [4] [10]. According to Ibrahim *et al.*, an increase in extraction temperature should be considered because high temperatures, long extraction times, and exceeding the optimum limit can cause compound loss in solution due to oxidation [11]. Flavonoid compounds are not resistant to temperatures above 50ºC, resulting in structural changes and low extract. Andriani *et al.* reported that too low temperature and short extraction time resulted in low flavonoid content [12]. This is due to the incomplete flavonoid compounds extracted from the material.

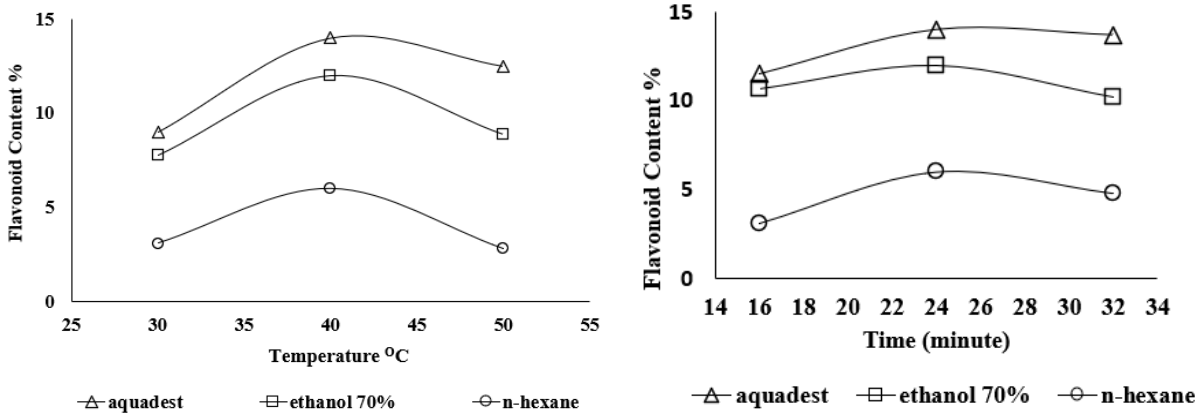

Figure 3. Graph of ultrasonic-assisted extraction on flavonoid content: (a) the effect of temperature, (b) the effect of extraction time

3.4 Effect of Extraction Method

Figure 4 shows the effect of the extraction method on the flavonoid content. A high yield of 14% flavonoid content was produced using the ultrasonic method with water as a solvent. The ultrasonic process was carried out in 24 minutes at 40ºC. However, the maceration method with water as a solvent and at the same temperature conditions of 40ºC for 3 hours produced a 10% yield. Figure 4 shows that the ultrasonic process produces a high yield compared to the maceration process. This is because ultrasonic waves in water will cause the growth and destruction of microbubbles, resulting in high temperatures and pressures, which trigger the formation of free radicals

through the thermal dissociation of water and oxygen [5] [13] [14].

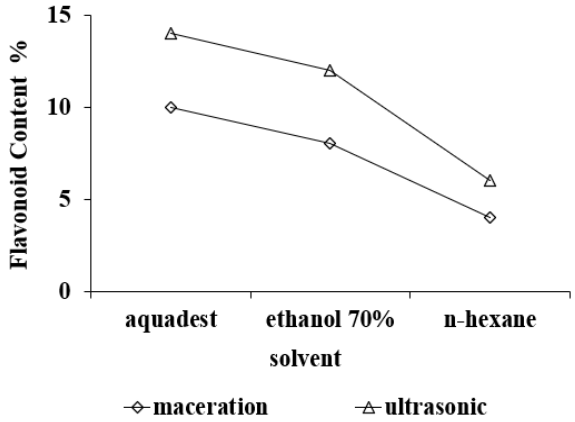

Figure 4. Comparison of ultrasonic extraction method with maceration

The use of ultrasonic waves creates a cavitation effect that can break down the cell walls of the material, allowing bioactive compounds to be easily extracted with maximum results in a relatively short processing time [15][16]. The advantage of ultrasonic-assisted extraction is that it increases the extract yield compared to conventional extraction methods such as maceration.

4. Conclusion

Based on this research, water as a solvent produces the highest flavonoid content. The flavonoids produced are classified as flavonoid sulphate due to their high solubility in water and the presence of one or more sulphate ions, which are bound to the hydroxyl phenol or sugar. Furthermore, the ultrasonic-assisted extraction method yielded the highest flavonoid content of 14% in 24 minutes and at 40^{o}C temperature.

5. Acknowledgments

The author wishes to express gratitude to PP Muhammadiyah Higher Education Research and Development Council for the Batch V of 2021 Muhammadiyah Research Grants.

References

[1] Wabia, E., & Siburian, R. (2019). Profil Tempat Tumbuh Sarang Semut (Myrmecodia Spp.) Di Distrik Manokwari Selatan Papua Barat. Retrieved from http://repository.unipa.ac.id:8080/xmlui/handle/123456789/393

[2] Mardany, M. P., Chrystomo, L. Y., & Karim, A. K. (2016). Skrining Fitokimia dan Uji Aktivitas Sitotoksik dari Tumbuhan Sarang Semut (Myrmecodia beccarii Hook.f.) Asal Kabupaten Merauke. *Jurnal Biologi Papua*, 8(1), 13-22. doi: 10.31957/jbp.41

[3] Parubak, A. S. (2019). Senyawa Flavonoid Yang Bersifat Antibakteri Dari Akway (Drimys becariana Gibbs). *Chemistry Progress*, 6(1). doi: 10.35799/cp.6.1.2013.2069

[4] Sayuti, M. (2017). Pengaruh Perbedaan Metode Ekstraksi, Bagian Dan Jenis Pelarut Terhadap Rendemen Dan Aktifitas Antioksidan Bambu Laut (Isis Hippuris). *Technology Science and Engineering Journal*, 1(3), 166-174.

[5] Kusnadi, J., Andayani, D. W., Zubaidah, E., & Arumingtyas, E. L. (2019). Ekstraksi Senyawa Bioaktif Cabai Rawit (Capsicum Frutescens L.) Menggunakan Metode Ekstraksi Gelombang Ultrasonik. *Jurnal Teknologi Pertanian*, 20(2), 79–84. doi: 10.21776/ub.jtp.2019.020.02.1

[6] Crisnaningtyas, F., & Rachmadi, A. T. (2010). Pemanfaatan sarang semut (Myrmecodia pendens) asal kalimantan selatan sebagai antibakteri. *Jurnal Riset Industri Hasil Hutan*, 2(2), 31–35.

[7] Soeksmanto, A., Subroto, M. A., Wijaya, H., & Simanjuntak, P. (2010). Anticancer activity test for extracts of Sarang semut plant (Myrmecodya pendens) to HeLa and MCM-B2 cells. *Pakistan journal of biological sciences: PJBS*, 13(3), 148–151.

[8] Harborne, J. B. (1987). Metode fitokimia: Penuntun cara modern menganalisis tumbuhan. *Bandung: Penerbit ITB*, 78.

[9] Handayani, H., Sriherfyna, F. H., & Yunianta, Y. (2016). Ekstraksi Antioksidan Daun Sirsak Metode Ultrasonic Bath (Kajian Rasio Bahan: Pelarut Dan Lama Ekstraksi). *Jurnal Pangan dan Agroindustri*, 4(1), 262-272.

[10] Margaretta, S., Handayani, S. D., Indraswati, N., & Hindarso, H. (2013). Ekstraksi senyawa phenolic Pandanus amaryllifolius roxb. sebagai antioksidan alami. *Widya Teknik*, 10(1), 20–30.

[11] Ibrahim, A. M., Yunianta, Y., & Sriherfyna, F. H. (2014). Pengaruh Suhu dan Lama Waktu Ekstraksi terhadap Sifat Kimia dan Fisik pada Pembuatan Minuman Sari Jahe Merah (Zingiber officinale var. Rubrum) dengan Kombinasi Penambahan Madu sebagai Pemanis. *Jurnal Pangan dan Agroindustri*, 3(2), 530-541.

[12] Andriani, M., Permana, I., & Widarta, I. R. (2019). Pengaruh Suhu dan Waktu Ekstraksi Daun Belimbing Wuluh (Averrhoa bilimbi L.) Terhadap Aktivitas Antioksidan dengan Metode Ultrasonic-Assisted Extraction (UAE). *Jurnal Ilmu dan Teknologi Pangan*, 8(3), 330–340.

[13] Ratnawati, R., & Indriyani, N. (2020). Kinetics and Thermodynamics Study of Ultrasound-Assisted Depolymerization of k-Carrageenan in Acidic Solution. *Bulletin of Chemical Reaction Engineering & Catalysis*, 15(1), 280–289. doi: 10.9767/bcrec.15.1.6738.280-289

[14] Abi-Khattar, A.-M., Boussetta, N., Rajha, H. N., Abdel-Massih, R. M., Louka, N., Maroun, R. G., … Debs, E. (2022). Mechanical damage and thermal effect induced by ultrasonic treatment in olive leaf tissue. Impact on polyphenols recovery. *Ultrasonics Sonochemistry*, 82, 105895. doi: 10.1016/j.ultsonch.2021.105895

[15] Suhendra, C. P., Widarta, I. W. R., & Wiadnyani, A. (2019). Pengaruh konsentrasi etanol terhadap aktivitas antioksidan ekstrak rimpang ilalang (Imperata cylindrica (L) Beauv.) pada ekstraksi menggunakan gelombang ultrasonik. *Jurnal Ilmu dan Teknologi Pangan*, 8(1), 27–35.

[16] Wen, C., Zhang, J., Zhang, H., Dzah, C. S., Zandile, M., Duan, Y., … Luo, X. (2018). Advances in ultrasound-assisted extraction of bioactive compounds from cash crops – A review. *Ultrasonics Sonochemistry*, 48, 538–549. doi: 10.1016/j.ultsonch.2018.07.018

CHEESA: Chemical Engineering Research Articles
ISSN **2614-8757 (Print)**, ISSN **2615-2347 (Online)**
Available online at: http://e-journal.unipma.ac.id/index.php/cheesa

Research Article

Determination of Content and Oil Losses in Meal through Palm Kernel Pressing Process at PT XYZ Belawan

Penentuan Kadar dan Kehilangan Minyak pada Meal dalam Proses Pressing Palm Kernel di PT XYZ Belawan

Dimas Frananta Simatupang[1*)], Maulidna[1)], Utami Nanda Agfira[1)], Anna Angela Sitinjak[2)], Merta Simbolon[3)]
[1)]Politeknik Teknologi Kimia Industri Medan, Chemical Engineering, Indonesia
[2)]Politeknik Teknologi Kimia Industri Medan, Mechanical Engineering, Indonesia
[3)]Universitas Musamus Merauke, Physics Education, Indonesia

**correspondence email*: difratas@ptki.ac.id

Received: 17 May 2021;
Revised: 22 September 2022;
Accepted: 26 September 2022;

doi: *10.25273/cheesa.v5i2.9255.65-73*

Abstract

PT XYZ Belawan has a kernel crushing plant unit that produces Crude Palm Kernel Oil (CPKO) with 700 tons/day capacity. Palm kernel processing is carried out in two pressing stages. The first stage or first press produces oil and cake, while the second stage or second press produces oil and meal. The meal still contains 7-8% of the oil content. This study is aimed to determine the amount of CPKO yield, oil content, and oil losses in a meal during the pressing palm kernel process. The method used was the calculation of the mass balance in each process flow. The mass balance calculation is carried out after collecting the secondary data from the factory, including the analysis of water content, solids, FFA, and oil content. Based on the calculation results, CPKO yield was 48.10% of the average kernel mass rate of 714.7155 tons and met the plant standard of at least 44%. Furthermore, the average yield of oil content from the meal was 7.45% and oil losses were 3.86%.

Keywords: CPKO; mass balance; oil loss; palm kernel pressing

Abstrak

PT XYZ Belawan memiliki unit pabrik kernel crushing plant yang menghasilkan minyak inti kelapa sawit (Crude Palm Kernel Oil/CPKO) dengan kapasitas 700 ton/hari. Proses pengolahan inti kelapa sawit dilaksanakan dengan dua tahap pengepressan (pressing). Tahap pertama atau first press yang menghasilkan minyak dan cake sedangkan tahap kedua atau second press yang menghasilkan minyak dan meal. Meal masih mengandung kadar minyak sebanyak 7-8%. Tujuan penelitian ini adalah untuk menentukan banyaknya rendemen CPKO, kadar minyak dan kehilangan minyak pada meal selama proses pressing palm kernel. Metode yang digunakan adalah perhitungan neraca massa pada setiap aliran proses. Perhitungan neraca massa dilaksanakan setelah pengumpulan data sekunder dari pabrik, meliputi: analisis kadar air, padatan, FFA, dan kadar minyak. Berdasarkan hasil perhitungan diperoleh rendemen CPKO sebanyak 48,1105% dari rata-rata laju massa kernel 714,7155 ton dan memenuhi standar pabrik minimal 44%. Selanjutnya diperoleh hasil rata-rata kadar minyak yang dihasilkan dari meal sebanyak 7,45% dan kehilangan minyak sebanyak 3,86%.

Kata kunci*: CPKO; kehilangan minyak; neraca massa; pressing palm kernel*

1. Introduction

Palm fruit, one of the essential commodities in plantation corps, is produced by oil palm plantations [1]. This is because it can be processed and used to produce palm oil (Crude Palm Oil/CPO) and palm kernel oil (Crude Palm Kernel Oil/CPKO) products [2]. This product is a non-oil and gas foreign exchange source for Indonesia [3]. In addition to CPO, which is the dominant product for the palm oil processing industry in Indonesia [4], CPKO has also received particular attention as a product of economic value [5], which is used as a lubricant and emulsifier and is widely used in the paint manufacture materials [6],such as soaps and candles, as well as raw materials in the biodiesel manufacture [7].

Oil that is produced from palm fruit consists of two types, which are the raw material of fruit flesh (mesocarp), which is produced through a boiling and pressing process [8], and is known as crude palm oil (CPO) [9]. Also, the raw material of palm kernel which is known as palm kernel oil (PKO) [10]. A by-product of PKO is palm kernel meal or pellets. The meal is a palm kernel that has undergone a process of extraction and drying [11]. The composition of palm kernel oil is almost similar to oil that is derived from palm oil. Both of these oils can be made into various types of products. The oil processing include refinery and extraction. The results of the processing from the refinery and extraction unit is producing several kinds of oil, including oil that is ready to use and oil that must be processed again to become other products such as food products, like cocoa butter substitute, shortening, margarine, and non-food products, including fatty acid, fatty alcohol and fatty methyl ester [12].

In every treatment process, the company always prioritizes quality and optimizes the amount of CPO and CPKO yields. One of the management systems that can be applied to obtain the optimal amount of oil yield is suppressing the occurrence of oil losses during the production process [13]. Oil yield is related to oil loss, in which if the oil loss is high, the oil yield becomes lower and vice versa [14]. The amount of oil loss can be reduced by treating the residual waste dregs [15]. Generally, to reduce the oil content in the waste residue is by adjusting the pressure. Too high pressure will result in a higher number of broken seeds [16] and can damage the screw press [17]. Palm oil mills (POM) must always ensure that it works based on the appropriate standards or regulations during the process.

PT XYZ Belawan is a factory that manufactures oil from palm fruit raw materials located in Belawan, North Sumatra, Indonesia. This factory has a kernel crushing plant (KCP) unit with a production capacity of 700 tons/day, which is one of the CPKO-producing factories that produces palm kernel expeller (PKE) by-products. Palm kernel processing in the KCP unit is carried out through a weighing station, receiving palm kernels (intake station), storing palm kernels (seed silo), pressing, and storing meals (flat silo). The pressing process is divided into two processes: the first press and the second press. In the first press, the palm kernel is treated with pressure, producing oil and cake. In the second press, the cake from the first press is pressed to produce oil and meal as the output material [18].

The investigation of oil loss in CPKO processing at PT XYZ was carried out using the seven tools method, which focuses on case studies (library studies) and direct field

studies. The results of the qualitative descriptive study concluded that the company suffered losses due to high oil losses for four months of 8.92% [19]. In addition to CPKO, oil loss is also occurred in CPO, which was analyzed using statistical process control methods at PT Bastian Olah Sawit Tungkal Palembang. The results of this study concluded that the loss of CPO exceeded the maximum threshold [20].

In processing palm kernel, paying attention and determining the amount of CPKO obtained in several raw materials entering the factory is necessary. Furthermore, the amount of oil loss during the processing process is also significant in determining whether to meet factory standards and avoid losses. Based on that reason, this study was conducted to calculate the CPKO yield obtained in the processing of raw materials, the oil content obtained from the meal, and the value of oil loss obtained in the pressing palm kernel process.

2. Research Methods

The initial data collection in this study began with secondary data from PT XYZ Belawan factory in the Palm Kernel pressing process, which included the number of processed kernels (tons) per day, the number of CPKO (tons) per day, and the number of the meal (tons) per day. Then, secondary data collection was carried out for six days of observation with the conditions and parameters of factory production following the quality standards set by the company.

2.1 Tools and Materials

Some of the tools used in this study include a Soxhlet extraction set, extraction flask, electro mantle, desiccator, oven, kernel grinder, NIR-InfraAlyzer 2000, rotary evaporator, spectrophotometer, and analytical balance. The materials used are the kernel, meal, n-hexane p.a, potassium hydroxide, ethanol p.a, and phenolphthalein indicators.

2.2 Analysis of Water Content and Solid Content

Determination of water content and solid content from the sample was done using a NIR-InfraAlyzer 2000 spectrophotometer. Samples of sorting, cake, and meal were crushed manually [21] with mortal first [22]. For CPKO samples, there was no special pre-treatment carried out, because the sample was in a liquid phase. Furthermore, the sample was put into a sample drawer inside the NIR-InfraAlyzer 2000 spectrophotometer. The instrument was turned on and operated with the SESAME program. The analysis system was chosen by adjusting the desired parameter. After that, the scan icon was clicked and waited for a few moments to get the spectrums. The water and solid content values were obtained directly through the data collection features and icon prediction.

2.3 Analysis of FFA Content

The acid-base titration method generally analyzed free fatty acid (FFA) [23]. However, the sample in this study was immediately analyzed with a NIR-InfraAlyzer 2000 spectrophotometer. The mashed kernel was placed in the rotating sample cup and operated on the device using the SESAME program and the FFA icon selection.

2.4 Analysis of Oil Content

The oil content of kernel and meal samples was determined using the solid-liquid soxhlet extraction method [24].

Samples were weighed as much as 100 grams, and then mashed with a kernel grinder. Paper thimble was made of filter paper and cotton then the extraction flask was weighed to a constant weight. 10 grams of smooth samples were weighed and put into the paper thimble. 150 ml of n-hexane solvents were added to the flask extraction. Soxhlet extraction tools are set up in such a way as electro mantle as a heater. Extraction was done for 6 hours. The extraction result was evaporated with a rotary evaporator to get oil and evaporate the solvent. Furthermore, the extraction flask is inserted into the oven at 103 ^{o}C for 1 hour. The oil-containing flask is then placed in a desiccator for 30 minutes and weighed to a constant weight. The yield/oil content is calculated using an equation (1).

$$\text{Oil Content} = \frac{\text{Extraction Oil Mass}}{\text{Sample Mass}} \text{ x } 100\% \quad \textbf{.....(1)}$$

2.5 Calculation of Mass Balance

The mass balance is a proper calculation of all the materials that enter, accumulate, and come out within a specific time [25]. Material equilibrium (mass balance) can be formulated in the conservative system [26] in the palm kernel pressing process, as shown in Figure 1. F^1 is the mass rate of the kernel that enters the first press (tons/day), F^2 is the CPKO mass rate that comes out of the first press (tons/day), F^3 is the mass rate of cake that comes out of the first press and will enter the second press (tons/day), F^4 is the mass rate of CPKO that comes out of second press (tons/day), and F^5 is the mass rate of Palm Kernel Meal (PKM) that comes out of second press (tons/day). Each process' component balance includes water, oil, FFA, and solid content. The total mass balance of both first press and the total mass balance in the second press is formulated through equation (2). By calculating the mass balance, the values of F^2, F^3, and F^5 can be determined as well as the value of water, oil, FFA, and solid content from the meal that comes out after going through the second press unit.

$$F^1 = F^2 + F^3 \quad \textbf{.....(2)}$$

$$F^3 = F^4 + F^5 \quad \textbf{.....(3)}$$

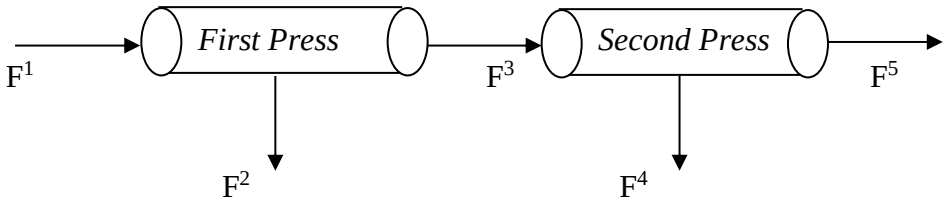

Figure 1. Mass balance of pressing palm kernel process

2.6 Determination of Oil Loss

To obtain the amount of oil loss in the meal, first determine the amount of oil using equation (4) and assigns the percentage of oil loss using equation (5).

$$A = B \text{ x } C \quad \textbf{.....(4)}$$

A is the amount of oil in the meal (tons); B is the oil content (%), and C is the amount of meal production (tons). The value of B is obtained by calculating the mass balance after going through a process in the second press.

$$\%OI = A/D \text{ x } 100\% \quad \textbf{.....(5)}$$

%OI is the percentage of oil loss, and D is the number of processed kernels (tons) [27].

3. Result and Discussion

Secondary data that was obtained directly from the factory at the palm kernel pressing unit is essential as material in the

mass balance calculation. This secondary data is daily production data observed for six consecutive days with the same conditions according to the company quality standards. Daily production data is shown in Table 1. The average number of kernels processed by PT XYZ Belawan was 714.7155 tons/day with an average CPKO production of 343.7067 tons/day, and the average meal production from the second press was 371.0088 tons/day. This data found that the average CPKO yield was 48.1105% for one production. Therefore, the CPKO yield value exceeded the minimum and met the factory standards with an average production standard of 44%.

Table 1. Secondary data and percentage of CPKO yield

No	Observation Day	Processed Kernel (tons)	CPKO Production (tons)	% Yield	Number of *meal* (tons)
1	First	703.5400	348.2755	49.5033	355.2645
2	Second	700.0640	355.1769	50.7349	344.8871
3	Third	704.7470	332.2315	47.1420	372.5155
4	Fourth	731.7690	341.8084	46.7099	389.9606
5	Fifth	741.7110	349.8802	47.1720	391.8308
6	Sixth	706.4620	334.8678	47.4007	371.5942
	Average	714,7155	343.7067	48.1105	371.0088

3.1 Determination of Water, Solid, and FFA Content

Kernel samples were analyzed using the NIR-InfraAlyzer 2000 spectrophotometer with specific settings for analyzing water, solid, and FFA content. Data on water, solid, and FFA contents in the kernel and the first press output of CPKO are shown in Table 2. Meanwhile, data on water, solid, and FFA contents in the first press output of cake and the second press output of CPKO are shown in Table 3. Data on both tables were then used as values on the component balance to calculate the oil content of meal and the percentage of oil loss.

Rantawi *et al.* research [28] shows a linear correlation between the value of water content in the kernel and the quality of the FFA content in the PKO produced. The higher the water content, the higher the FFA content in the PKO. However, the value of water content in kernel varies to the value of the FFA content in the second press output of CPKO. The reason was possible because in this study, the first and second press output of CPKO were still in crude extract and not pure PKO, in which it is causing bias in measuring the FFA content.

The value of water content in the kernel and solid content in CPKO according to Indonesian National Standard (SNI) 01-0024-1987 is a maximum of 8% and 6% [29]. Therefore, referring to the Indonesian National Standard (SNI), the water content value in the kernel and the solid content value in CPKO remained below the maximum limit. This was similar to the research results of Daulay *et al.* [30], which revealed that the quality of the kernel from the factory under study met the SNI requirements for the kernel water content, but the solid content was still above the SNI limit.

3.2 Determination of Oil Content

Oil content in the kernel, first press output of CPKO, first press output of cake, and second press output of CPKO were determined by the soxhlet method. The

results of the analysis of oil content are shown in Table 4. The average oil content value in the kernel reached 50% of the total kernel. The acquisition of this value showed that the kernel used as the raw material at PT XYZ Belawan factory was satisfactory, because the oil content exceeded the minimum SNI limit of 46%.

Table 2. Data on water, FFA, solid contents in kernel and first press output of CPKO

No	Observation Day	Kernel			First Press Output of CPKO		
		Water Content (%)	FFA Content (%)	Solid Content (%)	Water Content (%)	FFA Content (%)	Solid Content (%)
1	First	7.59	2.55	38.97	8.85	2.30	3.00
2	Second	6.78	2.31	39.96	8.80	2.19	3.01
3	Third	7.67	2.38	39.62	8.90	2.25	3.15
4	Fourth	7.32	2.05	40.26	8.95	2.03	3.47
5	Fifth	7.74	2.03	39.97	8.98	2.00	3.60
6	Sixth	7.59	2.15	39.98	8.92	2.10	3.35

Table 3. Data on water, FFA, solid contents in first press output of cake and second press output of CPKO

No	Observation Day	First Press Output of Cake			Second Press Output of CPKO		
		Water Content (%)	FFA Content (%)	Solid Content (%)	Water Content (%)	FFA Content (%)	Solid Content (%)
1	First	6.58	1.15	77.57	12.80	0.47	2.37
2	Second	5.01	1.18	80.01	12.70	0.56	1.94
3	Third	6.80	1.12	77.18	12.85	0.35	2.25
4	Fourth	6.21	1.10	77.34	12.90	0.40	2.30
5	Fifth	6.90	1.13	76.22	14.20	0.33	2.52
6	Sixth	6.65	1.06	77.19	12.87	0.45	2.20

Table 4. Oil content data distribution

No	Observation Day	Oil Content (%)			
		Kernel	First Press Output of CPKO	First Press Output of Cake	Second Press Output of CPKO
1	First	50.89	85.85	14.70	84.36
2	Second	50.95	86.00	13.80	84.80
3	Third	50.33	85.70	14.90	84.55
4	Fourth	50.37	85.55	15.35	84.40
5	Fifth	50.26	85.42	15.75	82.95
6	Sixth	50.28	85.63	15.10	84.48

Table 5. Data distribution of oil content in meal and oil loss

No	Observation Day	Oil Content in *Meal* (%)	Oil Loss (%)
1	First	7.78	3.92
2	Second	7.98	3.93
3	Third	7.37	3.89
4	Fourth	7.31	3.89
5	Fifth	7.11	3.75
6	Sixth	7.19	3.78
	Average	7,45	3.86

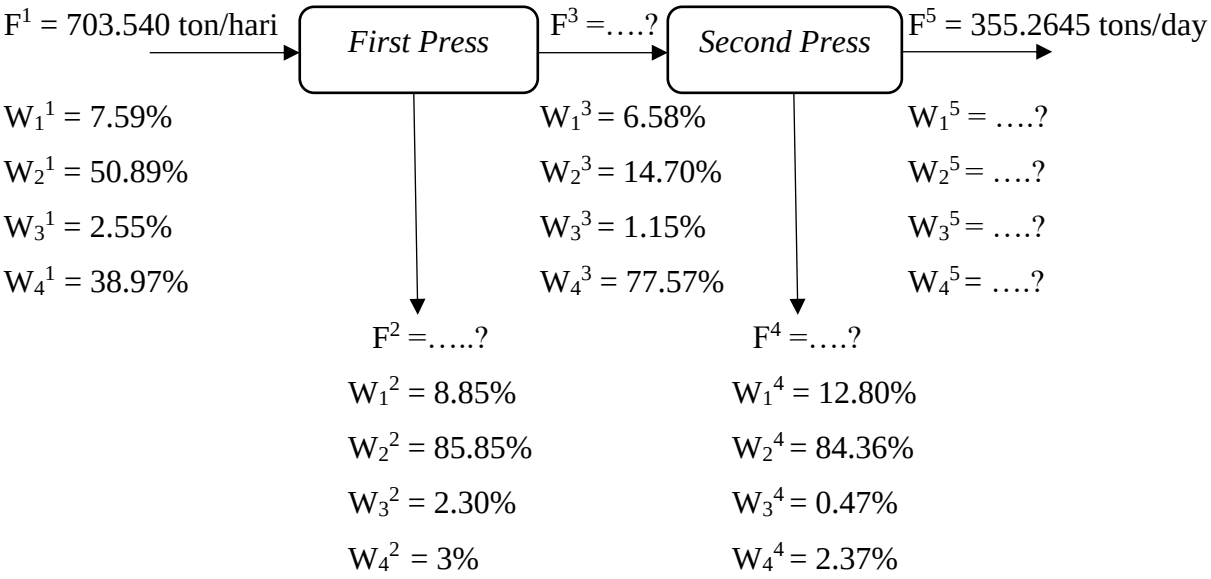

Figure 2. Mass balance scheme of palm kernel pressing with data distribution from the first day of observation

3.3 Determination of Oil Loss in Meal

In this study, the secondary data on the number of meal production from PT XYZ Belawan factory is shown in Table 1. Meanwhile, the amount of oil and the percentage of oil loss in the Palm Kernel pressing process is shown in Table 5. The average oil content in the meal was 7.45%, with the percentage of oil loss of 3.86%. The maximum standard value of PT XYZ Belawan factory for the percentage of oil loss was 3%, so the percentage value of oil loss has crossed the standard limit. Many factors were thought to have contributed to this case, such as minor damage to the pressing unit and the high oil levels in the Palm Kernel Expeller. However, if referred to several studies, it was found that the percentage of oil loss in the pressing unit was < 8% [19,27]. Hence, based on this standard, the percentage of oil loss remained within the normal limits.

4. Conclusion

Based on the results of sample analysis and calculation using the mass balance principle, it can be concluded that the average CPKO yield produced was 48.1105% of the average kernel processed 714.7155 tons/day. This value meets the minimum factory standard with a minimum percent yield of 44%. Furthermore, the value of oil content in meal and oil loss was obtained with an average of 7.45% and 3.86% respectively.

References

[1] Rinaldi, R., Pranoto, S., & Afriza, R. (2017). Studi Eksperimen Karakteristik Mekanik Material Screw Press Kapasitas 10-14 Ton/Jam di Lingkungan Pabrik Kelapa Sawit. *Jurnal Surya Teknika*, 5(01), 6–18. doi: 10.37859/jst.v5i01.350

[2] Purwanti, A., & Rahmawati. (2019). Analisis Proses Pemisah Kadar Produksi Crude Palm Oil (CPO) Di Ptp Nusantara 1 Tanjung Seumantoh-Aceh Tamiang. *Jurnal Hadron*, 1(1), 5–8.

[3] Dianto, F. (2017). *Pengelolalaan Panen Kelapa Sawit Pelantaran Agro Estate*. Bogor: IPB.

[4] Larasati, N., Chasanah, S., Machmudah, S., & Winardi, S. (2016). Studi Analisa Ekonomi Pabrik CPO (Crude Palm Oil) dan PKO (Palm Kernel Oil) Dari Buah Kelapa Sawit. *Jurnal Teknik ITS*, 5(2). doi: 10.12962/j23373539.v5i2.16851

[5] Ezeoha, S. L., Akubuo, C. O., Odigboh, E. U., & Arallo, M. (2017). Performance evaluation of Magnus screw press (Model MS-100) for palm kernel oil extraction. *Nigerian Journal of Technology*, 36(2), 636. doi: 10.4314/njt.v36i2.40

[6] Yunos, N. S. H. M., Baharuddin, A. S., Md Yunos, K. F., Hafid, H. S., Busu, Z., Mokhtar, M. N., … Som, A. M. (2015). The physicochemical characteristics of residual oil and fibers from oil palm empty fruit bunches. *BioResources*, 10(1), 14–29. doi: 10.15376/biores.10.1.14-29

[7] Bello, E. I., Oguntuase, B., Osasona, A., & Mohammed, T. I. (2015). Characterization and engine testing of palm kernel oil biodiesel. *European Journal of Engineering and Technology*, 3(3), 1–14.

[8] Sulaiman, & Randa, R. (2018). Pengaruh Temperatur Terhadap Efisiensi Sterilizer Dan Kualitas Minyak Yang Dihasilkan. *Menara Ilmu*, XII(10), 1–8.

[9] Majid, R. A., Mohammad, A. W., & May, C. Y. (2012). Properties of residual palm pressed fibre oil. *Journal of Oil Palm Research*, 24(APRIL), 1310–1317.

[10] Rahardja, I. B., & Ramadhan, A. I. (2020). Identification of Palm Oil Mill Throughput Capacity of 60 tons/hour (Case Study at XYZ Palm Oil Mill). *Journal of Applied Science and Advanced Technology Journal Homepage*, 83–86. Retrieved from https://jurnal.umj.ac.id/index.php/JASAT/article/view/6345

[11] Ezeoha, S. L., Akubuo, C. O., & Ani, A. O. (2012). Indigenous Design and Manufacture of Palm Kernel Oil Screw Press in Nigeria: Problems and Prospects. *International Journal of Applied Agricultural Research*, 7(2), 67–82. Retrieved from http://www.ripublication.com/ijaar.htm

[12] Kasmin, H., Lazim, A. M., & Awang, R. (2016). Effect of Heat Treatments on the Yield, Quality and Storage Stability of Oil Extracted From Palm Fruits. *Malaysian Journal of Analytical Science*, 20(6), 1373–1381. doi: 10.17576/mjas-2016-2006-16

[13] Jaeba, K. A., Lestari, E. T., & Adelino, M. I. (2021). Oil Losses Pada Fibre From Press Cake Di Pt. Amp Plantation Unit Pom. *Jurnal Teknologi Dan Sistem Informasi Bisnis*, 3(1), 234–239. doi: 10.47233/jteksis.v3i1.220

[14] Asarta, C. J., & Schmidt, J. R. (2020). The effects of online and blended experience on outcomes in a blended learning environment. *Internet and Higher Education*, 44(June 2018), 100708. doi: 10.1016/j.iheduc.2019.100708

[15] Zulkefli, F., Othman, N., Syahlan, S., Zaini, M. R., & Bakar, M. A. (2017). Fresh Fruit Bunch Quality and Oil Losses in Milling Processes As Factors That Affect the Extraction Rate of Palm Oil. *International Journal of Agriculture*, 5(June), 99–103.

[16] Hasballah, I. T., & Siahaan, E. W. B. (2018). Pengaruh Tekanan Screw Press Pada Proses Pengepresan Daging Buah Menjadi Crude Palm Oil. *Darma Agung*, XXVI, 722–729.

[17] Louis, E. S., Akubuo, C. O., & Odigboh, E. U. (2020). Effect of some kernel factors on palm kernel oil extraction using a screw press. *Agricultural Engineering International: CIGR Journal*, 22(1), 156–161.

[18] PT. XYZ. (2019). *Katalog PT. XYZ Belawan*. Sumatera Utara.

[19] Ulimaz, A., Hidayah, S. N., & Ningsih, Y. (2021). Analisis Oil Losses pada Proses Pengolahan Minyak Inti Kelapa Sawit di PT . XYZ dengan Metode Seven Tools Oil Losses Analysis of Palm Kernel Oil Processing Using Seven Tools Method. *Jurnal Teknologi Agroindustri*, 8(2), 124–134.

[20] Alfian, A., Wardana, A., Yasmin, & Lya. (2016). Analisis Kehilangan Minyak Pada Crude Palm Oil Dengan Metode Statistical Process Control Pada PT Bastian Olah Sawit Tungkal Palembang. *Jurnal Ilmiah Teknik Industri*, 1(5), 36–40.

[21] Yulianto. (2020). Analisis Quality Control Mutu Minyak Kelapa Sawit Di Pt. Perkebunan Lembah Bhakti Aceh Singkil. *Amina*, 1(2), 72–78. doi: 10.22373/amina.v1i2.36

[22] Tarigan, J., & Simatupang, D. F. (2019). Uji Kualitas Minyak Goreng Bekas Pakai Dengan Penentuan Bilangan Asam, Bilangan Peroksida Dan Kadar Air. *Ready Star* , 2(1), 6–10.

[23] Simatupang, D. F., Tarigan, J., & Mansyur. (2020). The effect of active carbon adsorbents from some wastes in reducing free fatty acids and acid number to improve vco quality. *IOP Conference Series: Materials Science and Engineering*, 885(1), 6–11. doi: 10.1088/1757-899X/885/1/012011

[24] Ramirez-Niño, M. Á., Jiménez-Forero, J. A., Bernal-Salazar, J. P., & Osorio-Dueñas, M. D. (2018). Characterization of oil extracted from the kernel of the fruit of cumare's palm

(Astrocaryum chambira barret). *Revista Facultad Nacional de Agronomia Medellin*, 71(1), 8415–8422. doi: 10.15446/rfna.v71n1.69589

[25] Simatupang, D. F., Saragih, G., & Simbolon, D. M. C. (2021). Studi Penentuan Perolehan dan Kehilangan Minyak dari Lumpur Buangan Proses pada Unit Decanter di Pabrik Kelapa Sawit PT. SPTG. In *Seminar Nasional Teknologi Industri VII* (pp. 376–382).

[26] Simatupang, D. F., Yunianto, & Sihaloho, E. D. W. (2021). Analisa Kebutuhan Batu Bara pada Unit Dryer dalam Pengeringan Pupuk NPK di PT AGS Medan. *CHEESA: Chemical Engineering Research Articles*, 4(1), 11–17. doi: 10.25273/cheesa.v4i1.7830.11-17

[27] Wahyudi, J., Renjani, R. A., & Hermantoro. (2012). Analisis Oil Losses pada Fiber dan Broken Nut di Unit Screw Press dengan Variasi Tekanan. *Prosiding Seminar Nasional PERTETA*, (July), 399–404.

[28] Rantawi, A. B., Mahfud, A., & Situmorang, E. R. (2017). Korelasi Antara Kadar Air pada Kernel Terhadap Mutu Kadar Asam Lemak Bebas Produk Palm Kernel Oil Yang Dihasilkan (Studi Kasus pada PT XYZ). *Industrial Engineering Journal*, 6(1), 36–42.

[29] Dewan Standardisasi Nasional. (1987). Crude palm kernel fatty acid (SNI 01-0024-1987). Indonesia. Retrieved from http://lib.kemenperin.go.id/neo/detail.php?id=223728

[30] Daulay, H. B., Sudibyo, P. I., & Subha, M. H. (2019). Profile and Consistency of Kernel Quality Pt. Daria Dharma Pratama Lubuk Bento Palm Oil Processing Industry. *Jurnal Agroindustri*, 9(2), 109–116. doi: 10.31186/j.agroindustri.9.2.109-116

CHEESA: Chemical Engineering Research Articles
ISSN **2614-8757 (Print)**, ISSN **2615-2347 (Online)**
Available online at: http://e-journal.unipma.ac.id/index.php/cheesa

Research Article

Enhancement of the Quality of Onion Drying Using Tray Dryer

Peningkatan Kualitas Pengeringan Bawang Merah Menggunakan Tray Dryer

Siska Nuri Fadilah[1)], Achri Isnan Khamil[1)], Maktum Muharja[1*)], Rizki Fitria Darmayanti[1)], Viqhi Aswie[2)]
[1)]Universitas Jember, Department of Chemical Engineering, Faculty of Engineering, Kalimantan street 37 Jember 68121, Indonesia
[2)]MAN 1 Kota Sukabumi, Pramuka street No. 04, Sukabumi 43144, Indonesia

**correspondence email*: maktum@unej.ac.id

Received: 22 September 2022;
Revised: 22 November 2022;
Accepted: 23 November 2022;

doi: *10.25273/cheesa.v5i2.13968.74-81*

Abstract

Previous reports showed that there has been a continuous increase in the annual production of onion in Indonesia, and it is inversely proportional to the market price. The price drop is often caused by the high water content, which makes it easy to rot. Preservation of onions through a tray dryer is a good preservation method because it is effective and does not require much energy. Therefore, this study aims to determine the effect of variations in time, material thickness, and air velocity on the drying rate of onions. The samples were sliced to a size of 2 - 5 mm, followed by drying for 60 min using a tray dryer with different air rates between 4 - 7 m/s, and the rate of the process was observed every 15 min. The results showed that the drying time reduced the humidity in the chamber. The highest rate of 0.525 g/min was obtained at the peak air rate of 7 m/s. ANOVA results revealed that variations in time, onion thickness, and flow rate have a significant effect on increasing the drying rate of onions. This indicates that the method can be an effective and efficient solution to optimize the drying of the commodity.

Keywords: drying; humidity; onion; tray dryer

Abstrak

Produksi bawang merah di Indonesia selalu mengalami kenaikan setiap tahunnya, tetapi peningkatan ini berbanding terbalik dengan harganya di pasaran. Penurunan harga disebabkan oleh kandungan air yang tinggi, sehingga mudah membusuk. Pengawetan bawang merah melalui pengeringan tray dryer saat ini menjadi pilihan karena efektif dan tidak membutuhkan energi yang besar. Penelitian ini bertujuan untuk mengetahui pengaruh variasi waktu, ketebalan bahan dan kecepatan udara terhadap laju pengeringan bawang merah. Penelitian dilakukan dengan pengirisan bawang merah berukuran 2 - 5 mm, kemudian dikeringkan selama 60 menit menggunakan tray dryer dengan variasi laju udara 4 – 7 m/s. Pengamatan laju pengeringan dilakukan setiap 15 menit. Hasil penelitian menunjukkan waktu pengeringan dapat menurunkan kelembaban udara. Laju pengeringan tertinggi sebesar 0,525 g/menit didapatkan saat laju udara tertinggi 7 m/s. Hasil ANOVA menunjukkan bahwa variasi waktu, ketebalan bahan, dan laju udara berpengaruh secara signifikan terhadap peningkatan laju pengeringan bawang merah. Dengan demikian, metode ini menjadi solusi yang efektif dan efisien untuk mengoptimalkan pengeringan bawang merah.

Kata kunci*: bawang merah; kelembaban; pengeringan; tray dryer*

1. Introduction

Onion (*Allium ascalonicum*) is one of the horticultural commodities with sufficient potential to be developed into a superior commodity [1]. It also contains beneficial chemicals, such as natural fiber, various vitamins, organic acids, phenolic compounds, and antioxidants. Furthermore, every 100 g of red onion contains 84.18 g of water, 0.93 g of fiber, and 2.43 g protein [2]. Previous reports showed there has been an annual increase of 5.11% in its production volume over the years [3]. However, this increase is inversely proportional to the market price, due to the high water content of onions, which accelerates microbial growth and spoilage [4]. This indicates that a method is needed to extend its shelf life, increase added value, and diversify of the products.

One of the common food preservation techniques is drying, which is the simplest process to reduce the water content of a material [5]. Drying onion to a certain moisture content can extend shelf life, hence, it is an alternative to keep the price of the commodity from falling during the harvest season [6]. Furthermore, one of the end results of this process is a powder product. Traditional drying is often carried out using sunlight, but it is considered less effective due to uncertain weather conditions [7]. It can also be performed with vacuum frying, but the process has some drawbacks, such as high energy demand and operating temperatures. This method is often used in vacuum frying for large-scale industrial drying only [8]. Drying can also be carried out using an electric-powered oven, but the operating costs are very high and the operation as well as maintenance require skilled personnel [4]. One of the technologies with the simplest and easiest technique is a multilevel tray dryer, which uses hot air in an enclosed space. The mechanism involves direct drying because the hot air is in contact with the material [1]. This technology can be applied to food ingredients that are sensitive to heat and are easily moldy.

Drying with a tray dryer is relatively efficient in energy consumption, suitable for small-scale industries, and the operating temperature is not too high. Manfaati et al. [2] reported onions drying (species Bima) using a tray dryer with variations in temperature and time. The results also showed that the moisture content was reduced to 4% at the optimum temperature, indicating that the both resultsvariables greatly affected the process. Prasetyaningsih & Mulyanti [9], carried out a similar experiment using variations in thickness, flow rate, and temperature. The results showed that the thinner the material, the greater the temperature and drying rate, which facilitated the decrease in moisture content and shortened the time required.

Based on the review of previous studies, several factors are involved in the drying process using a tray dryer. Findings also showed temperature, time, material thickness, and air flow rate are the most problematic factors. Although several studies have explored the use of the tray dryer, but none of them dicussed variations in time, flow rate, and material thickness simultaneously, which are very important. Therefore, it is necessary to determine the relationship of these three parameters with the drying process to obtain the optimum conditions for optimization. Therefore, this study aims to determine the optimum point through an optimization process based on analysis of variations of temperature, time, flow rate, and thickness of the material to

reduce the water content of shallots and increase their shelf life.

2. Research Methods

2.1 Materials

Fresh onions were obtained from the Tanjung market, Jember, with uniform humidity. Physiologically, the samples used were red onions with good quality.

2.2 Experimental procedure

The main instrument used in this study is a tray dryer model SF-25H with a size of 250 mm, capacity of 42 m^3/min, 190 W power, 280 r/min speed, 220-240 V voltage, and 50 Hz frequency, as shown in Figure 1. The description of the instruments in Figure 1 is as follows; heater power button (1), temperature control (2), fan power button (3), fan speed control button (4), temperature button (5), temperature displays (6), sensor of dry bulb temperature before and after tray (7 and 9), wet bulb temperature sensor before and after tray (8 and 10), analytical balance inside dryer (11), and tray (12). The rectangular tray dryer was equipped with perforated metal shelves. The rack was used to accommodate the material, which needs to be dried. The tray dryer was also equipped with a thermometer, a fan to regulate air circulation, as well as an anemometer (HoldPeak HP-866B, Taiwan), which was used to measure the fan air velocity. Furthermore, several supporting tools were used, including a stop watch to adjust the drying time, a ruler to measure the thickness of the sample, a knife to cut raw materials, and a digital scale (GSF G-4405, China) to measure the mass of the sample.

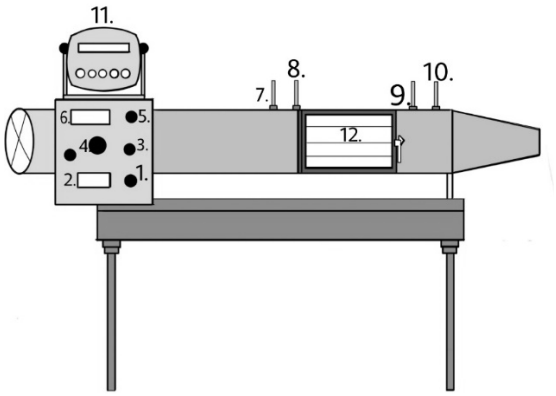

Figure 1. Schematic diagram of tray dryer

The union was peeled, sliced, and its thickness was then measured. Furthermore, slices with a fixed thickness of ± 2 mm were used for experiments with time variables and fan air flow rates. For the thickness variable, the onion was sliced into sizes of 2, 3, 4, and 5 mm. The tray dryer was then heated to a temperature of 55 °C, and a total of 50 g of the material was weighed. The onions were then rearranged on a perforated tray lined with aluminum foil to ensure that the samples were not piling up on each other. The tray containing the ingredients was inserted into the dryer. The fan air rate was set at 5.0 m/s for experiments using variations in time and thickness, while others with different fan air rates were set at 4, 5, 6, and 7 m/s. Sampling of mass data was carried out every 15, 30, 45 and 60 min for time variations. Meanwhile, for the thickness and fan air rate variables, sample mass data were collected after drying for 60 min. The last step was to calculate the values of T1, T2, T3 and T4 on the temperature reader every time the sample was weighed.

2.3 Statistical analysis

One-way analysis of variance (ANOVA) was carried out to analyze the effect of the variables on the drying rate

using MINITAB 16. The level of significance of 95% was selected to determine the effect of the factors. Sig stands for significance, which indicates statistical research error. The best study significance (sig) was obtained when the value was less than 5% (0.05) [10-12]. Determination of humidity can be performed using psychrometric charts through dry and wet bulb temperature data.

3. Results and Discussion

3.1 Humidity in a chamber of tray dryer

When a wet solid sample comes in contact with a air whose humidity is lower than its water content, it releases some of the moisture until it a balance point is achieved. Therefore, the humidity in the drying chamber affects the effectiveness of the process, and the level in the chamber is presented in Figure 2.

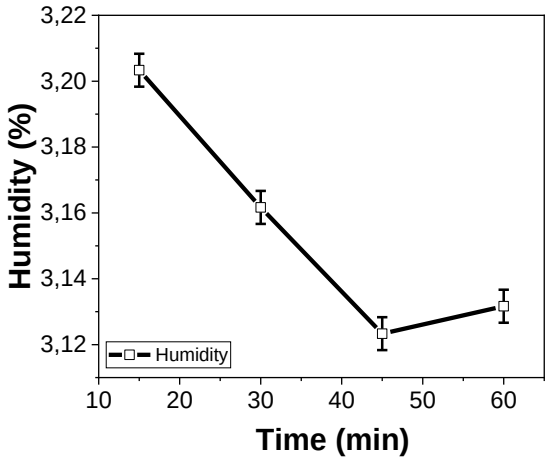

Figure 2. Effect of time on the humidity in a chamber of tray dryer

The optimal humidity level was 3.123% at 45 min. The results showed that the long drying time can significantly reduce the humidity in the chamber with sig value of 0.00<0.05. This is because the extended time causes longer contact with heating air, which allows more water in the material and chamber to be evaporated [8]. It can also lead to increased precipitation (condensation) of water molecules in the air, and this decreases its charges [13]. This is in line with a previous study, which revealed that the higher the temperature of the drying air, the higher the heat energy, which causes more mass of the liquid to be evaporated [14].

3.2 Effect of time on drying rate

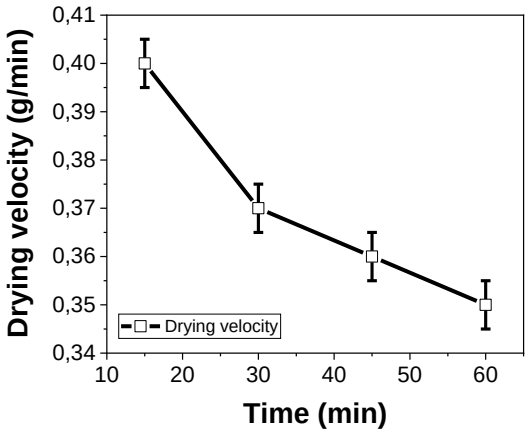

Figure 3. Effect of time on drying rate

Figure 3 shows that a long drying time can reduce the rate of the process significantly (P<0.05). At the beginning of drying, there was a large decrease in the rate until the 30th min. This was because the moisture content of the material was still high at the start of the process, and it was easily evaporated. At the end of drying, namely 30 to 60 min, the water bound to the material has decreased slowly, which caused reduced evaporation and slow rate [15]. The highest drying rate was obtained in the first 15 min, namely 0.4 g/min. According to Sari et al. [16], the time is inversely proportional to the rate of the process. The decrease in rate is proportional to that of the water content of the material. Reduction of moisture takes place continuously with the length of drying time. This is also in line with Sari

and Prabawa [17] that the longer the time, the lower the drying rate.

3.3 Effect of thickness on drying rate

Figure 4 shows a graph of the relationship between onions thickness and drying rate. Furthermore, the thicker the material, the longer the time required to evaporate the moisture content. This is because the mass of water in the middle of the thick pile has difficulty reaching the surface. The thickness of material causes airflow to accumulate in the center of the material [18]. It also affects the drying rate significantly, based on the ANOVA results with a sig value of 0.01 <0.05.

The process of drying onions at a temperature of 55 °C, an air rate of 5 m/s for 60 min with thickness of 2, 3, 4, and 5 mm occurred at rates of 0.183, 0.150, 0.117, and 0.133 g/min, respectively. The highest value was obtained when the thickness of the material was 2 mm. This indicates that the thinner the onion, the greater the reduction in water content. A thin material has a larger surface area, which causes greater contact with the heating medium, thereby accelerating the evaporation time of the water content [19].

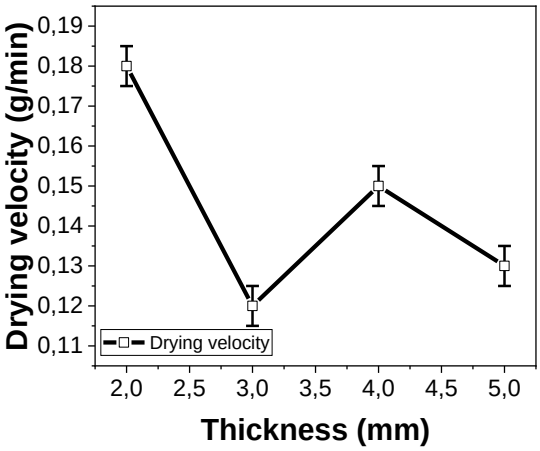

Figure 4. Effect of onions thickness on drying rate

In this study, there was a discrepancy with the literature, namely at a thickness of 4 and 5 mm, the drying rate was predicted to be smaller than 3 mm. This decrease occurred due to the transfer of water vapor by diffusion or through capillary. Furthermore, the diffusion was caused by the difference in the concentration of water vapor between the inner and the surface solids. It often occurs in solids that are not porous, such as paste, soap, gelatin, glue, flour, wood, leather, paper, textiles, and various foodstuffs. Movement of vapor through capillaries was observed because when the water was evaporated, meniscus was formed, which produces tension in its surface. This causes the build up of capillary forces that displaces water through the pores to surface. Vapor movement through capillaries occur in porous solids and granular form, such as clay, sand, soil, and minerals [20].

3.4 Effect of air flow rate on drying rate

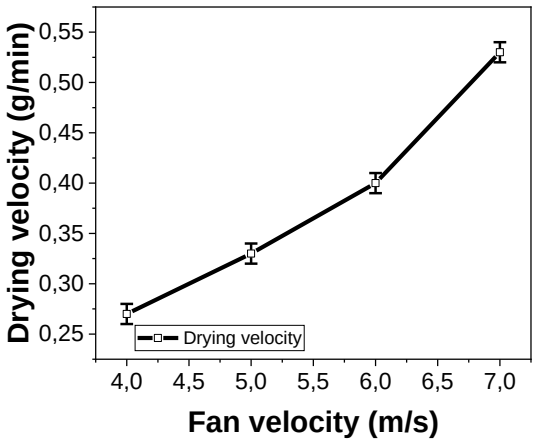

Figure 5. Effect of air flow rate on drying rate

Figure 5 shows that the drying rate increased significantly (sig value of 0.012<0.05) along with the air velocity. The highest rate of 0.525 g/min was obtained at the highest fan velocity of 7 m/s. This phenomenon was due to the increase in the air rate, which caused

increment in the diffusion of hot air into the material to be dried, thereby increasing the amount of water that can evaporate [21]. Additionally, the drying process involves the movement of heat from the medium to material as well as mass transfer to the media dryer. The process starts when hot air flows across solid sheet surface. Displacement of heat occurred by conduction through the tray hot or radiation from the surface of the heated material. Hot air flowing released some of the heat, and this causes evaporation/mass transfer of water from air-dried sample until it reaches an equilibrium state. Large amounts of air can carry large amounts of water vapor, which increase the drying rate and produce good quality dry products [22]. Previous study conducted by Hasibuan, et al. (2020) stated that the fan air rate facilitated the process [23]. Further studies also need to develop a drying kinetics model. Process design and the best-operating conditions can be determined quickly, measurably, and accurately with the availability of kinetics data.

4. Conclusion

In improving the quality of drying onions using a tray dryer, the time variable can reduce the humidity in the chamber. Furthermore, air flow rate, material thickness, and time affect the drying rate. By using a temperature of 55 °C, the optimum rate of the process was obtained during the first 15 min of the experiment, namely 0.4 g/min. Furthermore, the optimum thickness with the best drying rate was 2 mm at 0.183 g/min. The fan air rate of 7 m/s was the best and the process occurred at a rate of 0.533 g/min. The results also showed that the relative humidity of the material increased along with the fan air velocity and decreased with with an increase in drying time. The significance values for each of the parameters used, such as time, material thickness, and flow rate were $0.00<0.05$; $0.01<0.05$; and $0.012<0.05$, respectively, which indicates they met the statistical validity of the data.

In conducting this study, the air humidity must be kept dry to ensure that the drying process takes place optimally. There is also a need to review other parameters, such as temperature and pressure to obtain the optimum conditions as well as for larger scale.

References

[1] Manfaati, R., Baskoro, H., & Rifai, M. M. (2019). Pengaruh Waktu dan Suhu terhadap Proses Pengeringan Bawang Merah menggunakan Tray Dryer. *Fluida*, 12(2), 43–49. doi: 10.35313/fluida.v12i2.1596

[2] Manfaati, R., Baskoro, H., & Rifai, M. M. (2020). Characterization of Drying Shallots (Allium cepa L.) Using Tray Dryer. *CHEESA: Chemical Engineering Research Articles*, 3(2), 71–78. doi: 10.25273/cheesa.v3i2.7660.71-78

[3] Statistika, B. P. (2021). Provinsi Jawa Barat Dalam Angka 2021.

[4] Yanti, A. T. Y., Abizard, A., Fitriani, Al Fatih, M., & Anggara, M. (2021). Mesin Pengering Bawang Merah Menggunakan Double Blower dan Sensor Suhu DHT22 Arduino di Desa Brangkolong Kecamatan Plampang, Sumbawa. *Jurnal Teknik dan Sains*, 2(1), 1–7.

[5] Darianto, Amrinsyah, & Sitohang, H. T. S. (2019). Analisa Pengaruh Waktu dan Turbulensi Asap Pada Mesin Pengering Ikan Lele. *Journal of Mechanical Engineering Manufactures Materials and Energy*, 3(2), 130–142. doi: 10.31289/jmemme.v3i2.3029

[6] Dewayani, W., Samsuri, R., Septianti, E., & Halil, W. (2019). Kajian Jenis Pengeringan dan Beberapa Bahan Pengisi terhadap Kualitas Bubuk Bawang Merah Varietas Pikatan. *Jurnal Pengkajian dan Pengembangan Teknologi Pertanian*, 22(3), 251–262. doi: 10.21082/jpptp.v22n3.2019.p251-262

[7] Zamharir, Sukmawaty, & Priyati, A. (2016). Analysis of Heat Energy Utilizationin Onion (Allium ascalonicum, L.) Drying using Green Houses Gasses (GHG) Dryer. *Jurnal Ilmiah Rekayasa Pertanian dan Biosistem*, 4(2), 264–274.

[8] Purnamasari, I., Meidinariasty, A., & Hadi, R. N. (2019). Prototype Alat Pengering Tray Dryer Ditinjau dari Pengaruh Temperatur dan Waktu Terhadap Proses. *Jurnal Kinetika*, 10(03), 25–28.

[9] Prasetyaningsih, Y., & Mulyanti, S. (2018). Pengaruh Suhu dan Laju Alir Pengeringan pada Bawang Putih Menggunakan Tray Dryer. *Prosiding Seminar Nasional Teknik Kimia "Kejuangan" Pengembanagn Teknologi Kimia untuk Pengolahan Sumber Daya Alam Indonesia*, (April), 1–6.

[10] Muharja, M., Umam, D. K., Pertiwi, D., Zuhdan, J., Nurtono, T., & Widjaja, A. (2019). Enhancement of sugar production from coconut husk based on the impact of the combination of surfactant-assisted subcritical water and enzymatic hydrolysis. *Bioresource Technology*, 274(November 2018), 89–96. doi: 10.1016/j.biortech.2018.11.074

[11] Muharja, M., Fadhilah, N., Darmayanti, R. F., Sangian, H. F., Nurtono, T., & Widjaja, A. (2020). Effect of severity factor on the subcritical water and enzymatic hydrolysis of coconut husk for reducing sugar production. *Bulletin of Chemical Reaction Engineering & Catalysis*, 15(3), 786–797. doi: 10.9767/BCREC.15.3.8870.786-797

[12] Muharja, M., Albana, I., Zuhdan, J., Bachtiar, A., & Widjaja, A. (2019). Reducing Sugar Production in Subcritical Water and Enzymatic Hydrolysis using Plackett- Burman Design and Response Surface Methodology. *Jurnal Teknik ITS*, 8(2), 56–61. doi: 10.12962/j23373539.v8i2.49727

[13] Adha, F., Mustaqimah, & Agustina, R. (2018). Study of Thin Layer Drying Turmeric (Curcuma domestica VAL.) Characteristics Using Tray Dryer. *Jurnal Ilmiah Mahasiswa Pertanian*, 3(1), 1–11.

[14] Rahayuningtyas, A., & Kuala, S. I. (2016). Pengaruh Suhu dan Kelembaban Udara pada Proses Pengeringan Singkong (Studi Kasus: Pengering Tipe Rak). *Jurnal Penelitian dan Pengabdian Masyarakat*, 4(1), 99–104.

[15] Ummah, N., Purwanto, Y. A., & Suryani, A. (2018). Penentuan Konstanta Laju Pengeringan Bawang Merah (Allium ascalonicum L.) Iris Menggunakan Tunnel Dehydrator. *Warta IHP: Journal of Agro-based Industry*, 33(2), 49–56.

[16] Sari, D. K., Kustiningsih, I., & Lestari, R. S. D. (2017). Pengaruh Suhu dan Waktu Pengeringan terhadap Mutu Rumput Laut Kering. *Jurnal Teknika*, 13(1), 43–50.

[17] Sari, D. K., & Prabawa, S. (2019). Effect of drying time and temperature on the characteristics of fig leaf tea (Ficus carica l.). *Jurnal Teknologi Hasil Pertanian*, 12(2), 68–77.

[18] Ridhatullah, M. A., & Hasibuan, R. (2019). Effect of Material Thickness and Amount of Desiccant on Drying Rate of Ginger (Zingiber officinale Roscoe) at Solar Dryer Integrated with Desiccant. *Jurnal Teknik Kimia*, 08(2), 61–66. doi: https://doi.org/10.32734/jtk.v8i2.1882

[19] Elfiana, E., Usman, U., Sami, M., Ridwan, R., Intan, S. K., Rahmawati, C. A., & Pardi, P. (2021). Desiminasi Oven Drying Vacuum (ODV) Untuk Pengeringan Rempah Bandrek Siap Saji Di Desa Kumbang Kecamatan Syamtalira Aron Kabupaten Aceh Utara. *Proceeding Seminar Nasional Politeknik Negeri Lhokseumawe*, 5(1), 147–154.

[20] Yando, A. M., & Paramita, V. (2017). Studi Pengaruh Suhu Dan Ketebalan Irisan Terhadap Kadar Air , Laju Pengeringan Dan Karakteristik Fisik Ubi Kayu Dan Ubi Jalar. *Metana*, 13(1), 23–29. doi: https://doi.org/10.14710/metana.v13i1.17514

[21] Effendy, S., Syarif, A., Wardani, D. K., & Amalia, I. (2019). Prototype Rotary Dryer Dengan Bahan Bakar Biomassa Prototype Rotary Dryer With Biomass Fuels Reviewed From the Influence of Air Flow Rate and. *Jurnal Kinetika*, 10(01), 1–6.

[22] Sari, D. K., & Lestari, R. S. D. (2016). Pengaruh Laju Alir Udara Pengering terhadap Pengeringan Kulit Manggis. *Teknika: Jurnal Sains dan Teknologi*, 12(1), 35. doi: 10.36055/tjst.v12i1.6614

[23] Hasibuan, R., Pane, Y. M., & Hanief, S. (2020). Effect of Air Velocity and Thickness to Drying Rate and Quality Temulawak (Curcum Xanthorrhiza Roxb) using Combination Solar Moleculer Sieve Dryer, *Proceedings of the International Conference of Science, Technology, Engineering, Environmental and Ramification Researches*, 389–394. doi: 10.5220/0010103503890394

[24] Alimny, A. N., Muharja, M., & Widjaja, A. (2019). Kinetics of Reducing Sugar Formation from Coconut Husk by Subcritical Water Hydrolysis. *Journal of Physics: Conference Series*, 1373(1), 12006. doi: 10.1088/1742-6596/1373/1/012006

[25] Fachri, B. A., Rizkiana, M. F., & Muharja, M. (2020). A Kinetic Study on Supercritical Carbon-dioxide Extraction of Indonesian A Kinetic Study on Supercritical Carbon-dioxide Extraction of Indonesian Trigona sp . Propolis. *IOP Conf. Series: Materials Science and Engineering*, 742(012001), 1–5. doi: 10.1088/1757-899X/742/1/012001

CHEESA: Chemical Engineering Research Articles
ISSN **2614-8757 (Print)**, ISSN **2615-2347 (Online)**
Available online at: http://e-journal.unipma.ac.id/index.php/cheesa

Research Article

Quality Evaluation of Bioplastic from Glutinous Rice Starch Reinforced with Bamboo Leaf Powder

Pengujian Kualitas Bioplastik dari Pati Beras Ketan Berpenguat Serbuk Daun Bambu

Uma Fadzilia Arifin[1*)], Nais Pinta Adetya[2)], Wisnu Pambudi[1)], Wahyu Ratnaningsih[1)]
[1)]Politeknik ATK Yogyakarta, Departement of Plastics and Rubber Processing Technology
[2)]Politeknik ATK Yogyakarta, Departement of Leather Processing Technology
Prof. Dr. Wirdjono Prodjodikoro street, Sewon, Bantul, Yogyakarta 55188, Indonesia

****correspondence email*:** umafadzilia67@gmail.com

Received: 29 October 2022;
Revised: 06 December 2022;
Accepted: 08 December 2022;

doi: *10.25273/cheesa.v5i2.14235.82-91*

Abstract

Plastics are widely used in various aspects of life due to their variety of superior properties. However, they contribute a negative impact on the environment, which leads to the search for an alternative solution such as the production of bioplastics as biodegradable plastics. Therefore, this study aims to evaluate the psycho-mechanic quality of bioplastic from glutinous rice starch reinforced with bamboo leaf powder. The bioplastic synthesis process was carried out using 0, 1, 3, 5, and 7% (w/w) variations of bamboo leaf powder on glutinous rice starch, respectively. The results showed that the best bioplastic composition was the addition of 3% (w/w) bamboo leaf powder to glutinous rice starch. This indicated that the addition of bamboo leaf powder in bioplastics can enhance the thickness, hardness, and tensile strength significantly. Meanwhile, the value of density, water vapor transmission rate, and elongation showed a slight increase, and the bioplastic also degraded more than 70% for 7 days.

Keywords: bioplastic; bamboo leaf powder; glutinous rice starch; psycho-mechanic properties

Abstrak

Plastik menawarkan berbagai sifat unggul sehingga banyak digunakan dalam berbagai aspek kehidupan. Namun, beberapa plastik berdampak negatif terhadap lingkungan. Bioplastik dapat menjadi solusi alternatif sebagai plastik yang mudah teruarai secara alami. Tujuan penelitian ini yaitu untuk mengetahui kualitas fisik-mekanik komposit bioplastik pati ketan berpenguat serbuk daun bambu dengan mempertimbangkan komposisi terbaik. Pati ketan yang mengandung amilopektin tinggi berperan sebagai matriks dalam produksi bioplastik. Sedangkan serbuk daun bambu merupakan sumber biosilika yang digunakan sebagai bahan pengisi. Penelitian ini dilakukan proses sintesis bioplastik dengan variasi pati daun bambu pada pati ketan masing-masing 0, 1, 3, 5 dan 7% (b/b). Hasil penelitian menunjukkan bahwa komposisi bioplastik terbaik adalah penambahan serbuk daun bambu 3% (b/b) pada pati ketan. Kesimpulannya, penambahan serbuk daun bambu sebagai bahan pengisi pada bioplastik pati ketan mampu meningkatkan ketebalan, kekerasan dan kekuatan tarik secara signifikan. Bioplastik juga mengalami degradasi secara alami lebih dari 70% selama 7 hari.

Kata kunci*: bioplastik; serbuk daun bambu; tepung ketan; sifat fisik-mekanik.*

1. Introduction

The use of plastics cannot be avoided by human life because of their variety of superior properties. Generally, plastics are light, strong, durable, corrosion-resistant, flexible, inert, not easily broken, easy to obtain, color, as well as shape, and can be widely applied in various temperature ranges [1]. There is currently a significant increase in plastics production annually due to their wide application in various aspects of life.

Plastics provide millions of benefits but they also have various disadvantages that affect the environment. The burning of plastics can produce toxic gases, namely dioxins [2]. This is because several plastics are also not easy to recycle and are being disposed of into the environment both landfill and ocean. Based on data from the Ministry of Environment and Forestry of the Republic of Indonesia [3], approximately 6,300 million tons of plastic waste has been generated globally per year with an estimated 79% in landfills or accumulated in the environment. They take years to decompose by the activities of organisms and can cause environmental damage [4]. One of the alternative solutions to overcome this problem is the production of bioplastic as biodegradable plastics.

Bioplastics are organic-based plastics that can be decomposed by microorganisms into carbon dioxide in aerobic processes or methane in anaerobic processes in a relatively short time [2]. They are polymers composite made from renewable sources such as polysaccharides, proteins, lipids, or current substances derived by several microorganisms [5]. Bioplastics have properties that refer to the conventional ones, therefore, they can replace the plastic function.

The bamboo leaf is one of the agricultural wastes, which is only burned or used as compost materials [6]. Bamboo is a source of biosilica [7], with a silica content of about 17-23%, higher than the 9.3-13.5% in rice husks [6]. According to Warsiki *et al*. [8], the physical and mechanical properties of bioplastic composites can be improved by using silica as a reinforcement. Therefore, bamboo leaf powder is a source of biosilica that can be used as a filler for bioplastics.

In Indonesia, glutinous rice starch (*Oryza sativa glutinosa*) is widely found. and can be obtained at low prices. White glutinous rice starch contains 99% amylopectin and 1-2% amylose [9], which affect the stability of bioplastics and compactness, respectively [10]. The high amylopectin levels can facilitate the starch gelatinization process and cause a lot of space that can be filled by the other biopolymer to bind [8]. In bioplastic production, the glutinous rice starch containing high amylopectin acts as a matrix.

Several investigations related to the development of bioplastics from organic materials have been carried out. However, no information on the use of bamboo leaf containing biosilica as a filler and glutinous rice starch with high amylopectin as a matrix in bioplastics production. Therefore, this study was conducted to determine the effect of using glutinous rice starch reinforced with bamboo leaf powder on the psycho-mechanic characteristics and biodegradability of bioplastic composite by considering the best composition.

2. Research Methods

2.1 Materials

The glutinous rice was obtained from a local market in Yogyakarta, Indonesia. It

was sieved to reach a uniform size in 40 mesh. The bamboo leaf waste was provided on plantation land in Rembang, Central Java, Indonesia. They were cleaned, milled, and sieved to powder form in size 100 mesh. Aquadest and glycerol from food-grade, UniChem Candi, Indonesia were purposed for bioplastic production.

2.2 Methods

This study was carried out in a schematic diagram as depicted in Figure 1. Concisely, the methods involved several main steps, namely experiment preparation, bioplastic production, physical characteristics evaluation, and mechanical properties evaluation. The psycho-mechanic characteristics were used to predict the best composition of bioplastic composite from glutinous rice starch reinforced with bamboo leaf powder.

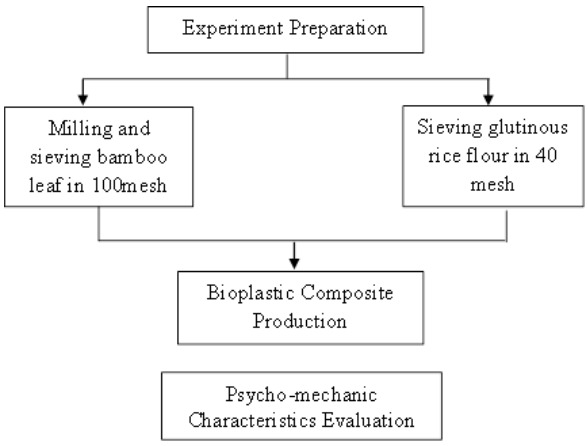

Figure 1. The schematic diagram of the research

2.3 Bioplastics Composite Production

The bioplastic composites were produced by adding bamboo leaf powder in glutinous rice starch under various composition ratios, namely 0, 1, 3, 5, and 7 % (w/w), respectively. They were dispersed in 100 ml aquadest. The process was carried out on a hot plate at around 90^{o}C temperature and 436 rpm stirring speed using a magnetic stirrer for 10 minutes. Approximatly 30% plasticizer was added by volume of glycerol for each weight of glutinous rice starch, successively and the solution was stirred again until homogeneous. The molding process was carried out using a 25x25cm tray and dried at 50^{o}C for 24 hours. Subsequently, the bioplastic composites that had been removed from the mold were evaluated for their physical and mechanical characteristics [13,18].

2.4 Physical Characteristics Evaluation

The physical characteristics analyzed were thickness, moisture content, hardness, density, and water vapor transmission rate. The thickness of the bioplastic composite was measured by a micrometer with an accuracy of approximately 0.0001 mm. The sample was cut at a size of 2×2 cm^2 and tested at 10 different points. The thickness bioplastic was determined using equation 1 [13].

$$\text{Thickness} = \frac{Sum\ of\ measured\ value}{10} \quad \text{.....(1)}$$

The hardness tests are used to evaluate response under compressive load. Generally, the hardness of most plastic materials is measured using a durometer scale of Shore D. Testing was carried out at 5 different points on the sample. The hardness value of the bioplastic is expressed as the average of the measurement results [12].

The density value can be determined by the mass and volume ratio of the sample. The mass (m) of the sample was weighed using an analytical balance with an accuracy of 0.0001 g. The volume of the sample was calculated based on the

area (A) and thickness (d) value of the bioplastic [13].

The moisture content is the amount percentage of water in a material. Meanwhile, the moisture content of bioplastic was measured by gravimetric analysis for 24 hours at 105°C using a drying oven [14]. It can be calculated based on initial and final weight data during drying as expressed in equation 2 [13].

$$\text{Moisture Content} = \frac{W_1 - W_2}{W_1} x\ 100\ \% \quad \text{.....(2)}$$

The water vapor transmission rate (WVTR) test is used to measure the permeability of bioplastic under specific conditions of temperature and relative humidity [15]. The samples were cut at a size of 2×2 cm^2 and conditioned into a desiccator filled with distilled water with humidity (RH) of 80%. The WVTR was analyzed by weighing the samples every 2 hours for 24 hours. The WVTR value of the bioplastic was obtained by comparing the specimen weight (W) to the area of specimen (A) and 24 hours of time (t) as stated in equation 3.

$$\text{WVTR}\ (g/m^2) = \frac{W}{A\,x\,t} \quad \text{.....(3)}$$

2.5 Mechanical Characteristics Evaluation

The mechanical characteristic test for bioplastics-based glutinous rice starch reinforced with bamboo leaf powder was carried out by measuring the tensile and elongation.

Tensile strength is the amount of maximum force as the ability of the material to hold the strain before breakage [12]. The instrument used for testing tensile strength was Universal Testing Machine (Shimadzu, Japan). Furthermore, the specimen was elongated with a certain load and speed before breakage. The maximum force required to break the specimen is recorded as F. The value of tensile strength (τ) was obtained from the ratio of maximum force (N) to the cross-sectional area of the specimen (width x thickness) mm^2. The tensile strength was quantified by equation 4.

$$\tau\ (MPa) = \frac{F_{max}}{A} \quad \text{.....(4)}$$

Elongation is an extension in length of the specimen to break under tension. It was expressed as a percentage of the length before breaking when stretched. The elongation measurement is carried out simultaneously with the tensile test. The percentage of elongation was obtained using equation 5.

$$E\ (\%) = \frac{\Delta L}{L_o} \quad \text{.....(5)}$$

2.6 Biodegradability Evaluation

The biodegradable was evaluated using a decomposition test by burial in the ground [16]. The sample was cut at a size of 4×4 cm^2 and buried in the soil at a 10 cm depth. The weight loss was measured by weighing the sample daily for 7 days. The biodegradation of bioplastics was obtained using equation 6 for weight loss.

$$\text{Biodegradibility} = \frac{W - W_o}{W_o} x\ 100\% \quad \text{.....(6)}$$

3. Results and Discussion

This study aims to evaluate the quality of bioplastic composite from glutinous rice starch reinforced with bamboo leaf powder, especially psycho-mechanic characteristics. The experimental

results showed the effect of using bamboo leaf powder on the quality of bioplastic. It was also discovered that glutinous rice starch can be an alternative raw material for making bioplastics due to the high amylopectin that acts as a matrix in bioplastic. Meanwhile, bamboo leaf powder is a source of biosilica used as filler.

3.1 Physical Characteristics Bioplastic

The physical characteristics of bioplastic, namely thickness, moisture content, hardness, density, and water vapor transmission rate were used to evaluate the quality. The results showed that the addition of bamboo leaf powder affects the thickness, hardness, and density of the bioplastic as presented in Table 1.

The higher amount of bamboo leaf powder caused an improvement in the thickness, density, and hardness value of the bioplastic. Table 1 revealed that the highest thickness of the bioplastic, which is 0.3419 mm was obtained using 7% bamboo leaf powder. Previous studies have stated that thickness can influence the characteristics of the composite [17], while bamboo leaf powder is used as an additive that contains high biosilica [18]. Silica is an amorphous molecule with a relatively large particle size, which can affect the thickness of the bioplastic [13]. The results showed that the percentage concentration of added filler obtained different thicknesses [19,23]. Hence, the higher the filler concentration, the more thickness the bioplastic will produce. This showed that thickness is one of the characteristics of bioplastics that impact its physical and mechanical properties [19].

Table 1. Effect of bamboo leaf powder amount on the thickness, hardness, and density of the bioplastic

Bioplastic Sample	Amount of Bamboo Leaf Powder (w/w) %	Thickness (mm)	Hardness (Shore D)	Density (g/cm^3)
A	0	0.2167	11	1.2615
B	1	0.2486	12	1.3812
C	3	0.2810	17	1.3889
D	5	0.3180	20	1.4203
E	7	0.3419	21	1.4611

In line with the result of thickness, Table 1 informs that the high addition of biosilica in bioplastics can enhance the value of hardness. The highest hardness value was 21 Shore D in addition to 7% bamboo leaf powder content. The hardness value also was influenced by the thickness of bioplastics. Consequently, the higher bioplastic thickness causes an increase in the hardness value, which shows the response of the material under compressive load [12].

The density values in polymer indicate the compactness of the composite materials. Density is one of the requirements to determine the quality of packaging bioplastics. Based on Table 1, the density of bioplastics was significantly affected by the increasing concentration of bamboo leaf powder. In this study, bioplastics that was not added bamboo leaf powder had a relatively low-density value of 1.2615 g/cm^3.

The density of bioplastic composites increased the higher the volume fraction of nanosilica was added [8]. Moreover, the high-density value is also related to the thickness of the bioplastic. Density increases with increasing thickness. Oluwasina *et al*. [13] stated that thickness influences the density value due to the presence of additive particles in bioplastics.

The low percentage of moisture content in bioplastics as a packaging material has a longer shelf life and can protect against spoilage due to microbial activity [20]. Bioplastic is often expected to have relatively low moisture content. In this study, the lowest value was recorded at 10.3% with the addition of 7% bamboo leaf powder. Oluwasina et al. [13] explained that amorphous silica can enhance the moisture content of bioplastics compared to other additives. However, the percentage of moisture content in the bioplastics decreased with further addition of silica concentration as revealed in Figure 2. Since the bamboo leaf powder contains biosilica which tends to be hydrophobic [8], little amount of moisture content was trapped in the bioplastic. Furthermore, the hydrophobic material decreases the solubility [20].

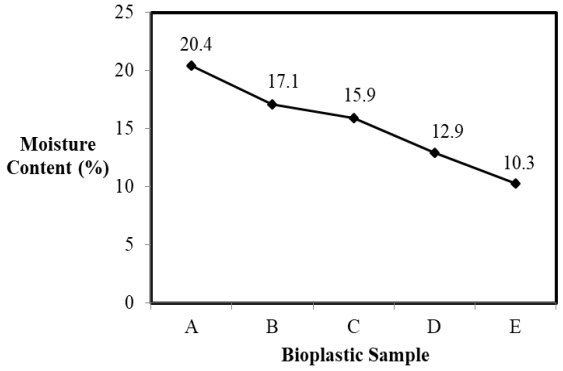

Figure 2. The percentage of bioplastic moisture content (wet basis) from glutinous rice starch reinforced with bamboo leaf powder

The WVTR of bioplastic composite from glutinous rice starch reinforced with different concentrations of bamboo leaf powder is depicted in Figure 3. The results showed that the WVTR value gradually reduced with increasing bamboo leaf powder content in the range of 9.421-15.124 g/m^2. Figure 3 revealed that the highest WVTR value was 15.124 g/m^2 in the control treatment without bamboo leaf powder. Meanwhile, the lowest value was 9.421 g/m2 in the treatment with 7% bamboo leaf powder content. These results indicate that bamboo leaf powder containing biosilica had a positive influence on the WVTR value of bioplastics-based glutinous rice starch.

Several studies have reported that the addition of a small filler in the polymer matrix can reduce WVTR value significantly [11]. The biosilica as filler tends to be hydrophobic and improves the moisture barrier properties of bioplastics. This is because it creates tortuous pathways to block the moisture diffusion pathways [13]. Kavoosi et al. [22] discovered that the water vapor diffusion process in biofilm depends on the hydrophilic-hydrophobic properties of their components and the degree of cross-linking. The biosilica will fill the pores in the amylopectin structure of the composite matrix glutinous rice starch, which makes a compact crosslinking structure. It was also reported that the hydrogen bonds between the oxygen atoms of biosilica and glutinous rice starch matrix in bioplastics composites can reduce the permeability to water vapor [17]. Furthermore, the thickness of the bioplastic affects the permeability to water vapor. This showed that the thicker the bioplastic film, the lower the WVTR value [8].

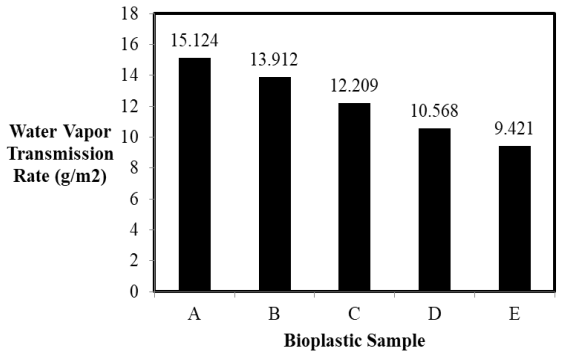

Figure 3. The water vapor transmission rate of bioplastic composite from glutinous rice starch reinforced with bamboo leaf powder

3.2 Mechanical Characteristics of Bioplastic

The mechanical characteristic test for bioplastics-based glutinous rice starch reinforced with bamboo leaf powder was carried out by measuring the tensile and elongation value. It is expected that the addition of filler in bioplastics composites significantly increases the mechanical strength especially tensile strength and elongation value [20]. The effect of bamboo leaf powder content on tensile strength in glutinous rice starch bioplastics is depicted in Figure 4.

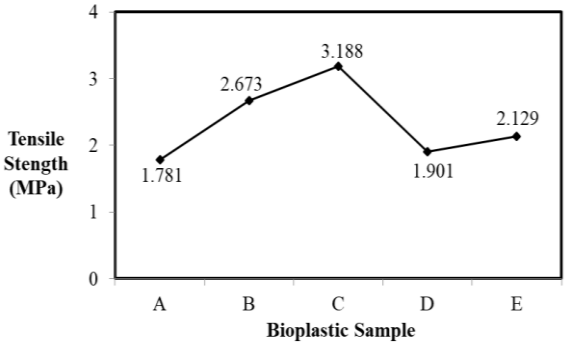

Figure 4. The effect of bamboo leaf powder content on tensile strength in glutinous rice starch bioplastics

Figure 4 informs that increasing content of bamboo leaf powder as a source of biosilica added to bioplastics in certain limits causes higher tensile strength values. In this study, the tensile strength increased to a maximum value of 3.188 MPa with the addition of 3% bamboo leaf powder. However, the value of tensile strength decreased when bamboo leaf powder content of more than 3% was added.

The higher addition of bamboo leaf powder as a source of biosilica increases the particle interaction, which makes the material stronger. Torabi and Nafchi [11] confirmed that nanosilica as a filler can enhance the mechanical performance of bioplastic due to their interaction with hydroxyl groups and other hydrogen or Van der Wall's bonds of starch to improve molecular strength. A previous report stated that the interactions of hydrogen generate molecular interactions that are getting stronger and harder to break because the process requires a lot of energy [23].

The amylose content of glutinous rice starch also affects the compactness of polymer networks in bioplastics to increase the mechanical properties [24]. However, there is a certain limit that the addition of filler cannot improve the mechanical properties of the composite. Generally, when the filler added exceeded a certain limit, it can create large agglomerates on the filler particles. This causes the reduction of interaction between the filler and the matrix in bioplastic composite [8]. Based on the results, the highest tensile strength of bioplastic was 3.188 MPa and did not meet the SNI 7188.7:2016 standard for moderate properties (10-100 MPa).

Elongation at the break of material shows an extreme extension in length of the specimen to break under tension associated with the initial length [20]. In most cases, elongation has a contrasting relation with tensile strength [11]. The influence of bamboo leaf powder content

on elongation percentage in glutinous rice starch bioplastics is shown in Figure 5.

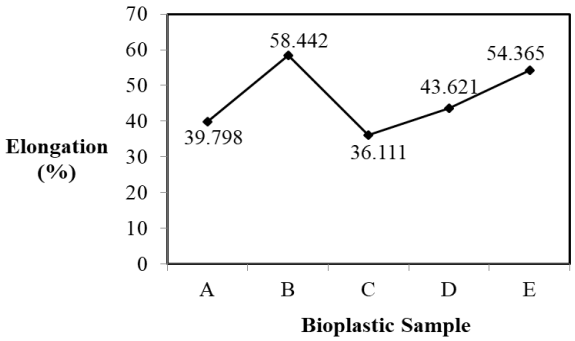

Figure 5. The effect of bamboo leaf powder content on elongation percentage in glutinous rice starch bioplastics

The addition of bamboo leaf powder in 0, 1, 3, 5, and 7% (w/w) significantly increased the tensile strength with a slight improvement in elongation. The higher value of elongation at break in bioplastic indicates it is more deformable [12]. The results also showed that the elongation percentage of bioplastic in various ratios of glutinous rice starch and bamboo leaf powder was around 39.798-58.442% and met the plastic standard of SNI 7188.7:2016 (21 - 220%) [25].

3.3 Biodegradability of Bioplastic

Biodegradability evaluation for plastics was carried out to ensure proper degradation in the environment [26]. Biodegradation of bioplastics is determined by the weight loss mass during the soil burial process at a certain time due to the activity of microorganisms. Generally, starch is a food source for microorganisms.

These microorganisms can damage the molecular structure of bioplastics, leading to the degradation and production of carbon dioxide [27]. Furthermore, microorganism enzymes can also break down polymer chains into monomers, which produce various organic compounds that are safe for the environment. The biodegradability of bioplastics from glutinous rice starch reinforced with bamboo leaf powder is revealed in Figure 6.

Based on Figure 6, the percentage of bioplastic biodegradation of glutinous rice starch at various concentrations of bamboo leaf powder was 70% and was not significantly different for 7 days of soil burial. This value has met the standard of biodegradability of bioplastics based on SNI 7188.7:2016. According to the Indonesian National Standard, the biodegradation value of bioplastics must be more than 60% during the 7-day testing process. Therefore, bioplastics from glutinous rice starch reinforced with bamboo leaf powder can be used as biodegradable plastic.

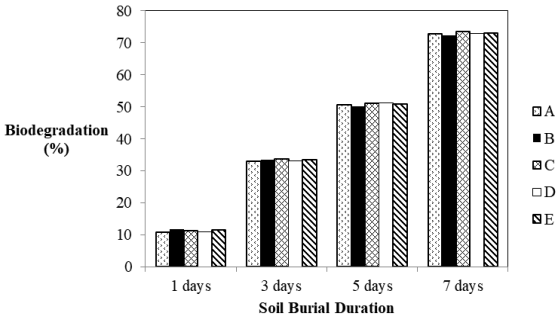

Figure 6. Biodegradability of bioplastics from glutinous rice starch reinforced with bamboo leaf powder

4. Conclusion

The results showed that the addition of bamboo leaf powder can improve the physical and mechanical properties of bioplastics. The addition of bamboo leaf powder to a reinforced bioplastic composite of glutinous rice starch enhanced the thickness and tensile strength significantly. Meanwhile, the value of density, elongation, and water vapor transmission rate showed a slight increase.

More than 70% of the bioplastics also degraded for 7 days. The best treatment was obtained on composite bioplastic with 3% bamboo leaf powder. However, the highest tensile strength value of 3.188 MPa of bioplastic had not reached the SNI standard for moderate properties, which ranged from 10 to 100 MPa.

References

[1] Proshad, R., Kormoker, T., Islam, M. S., Haque, M. A., Rahman, M. M., & Mithu, M. M. R. (2018). Toxic effects of plastic on human health and environment : A consequences of health risk assessment in Bangladesh. *International Journal of Health*, 6(1), 1–5. doi: 10.14419/ijh.v6i1.8655

[2] Selvamurugan, M., & Sivakumar, P. (2019). Bioplastics – An Eco-friendly Alternative to Petrochemical Plastics. *Current World Environment*, 14(1), 49–59. doi: 10.12944/cwe.14.1.07

[3] Ministry of Environment and Forestry. (2020). *National Plastic Waste Reduction Strategic Actions for Indonesia*. Republic of Indonesia. Retrieved from https://wedocs.unep.org/bitstream/handle/20.500.11822/32898/NPWRSI.pdf?sequence=1&isAllowed=y

[4] Landi, T., & Arijanto, A. (2017). Perancangan Dan Uji Alat Pengolah Sampah Plastik Jenis Ldpe (Low Density Polyethylene) Menjadi Bahan Bakar Alternatif. *Jurnal Teknik Mesin Undip*, 5(1), 1–8.

[5] Zoungranan, Y., Lynda, E., Dobi-Brice, K. K., Tchirioua, E., Bakary, C., & Yannick, D. D. (2020). Influence of natural factors on the biodegradation of simple and composite bioplastics based on cassava starch and corn starch. *Journal of Environmental Chemical Engineering*, 8. doi: 10.1016/j.jece.2020.104396

[6] Aminullah, Rohaeti, E., & Irzaman. (2015). Reduction of High Purity Silicon from Bamboo Leaf as Basic Material in Development of Sensors Manufacture in Satellite Technology. *Procedia Environmental Sciences*, 24, 308–316. doi: 10.1016/j.proenv.2015.03.040

[7] Silviana, S., & Bayu, W. J. (2018). Silicon Conversion from Bamboo Leaf Silica by Magnesiothermic Reduction for Development of Li-ion Baterry Anode. *MATEC Web of Conferences*, 156, 0–3. doi: 10.1051/matecconf/201815605021

[8] Warsiki, E., Setiawan, I., & Hoerudin, H. (2020). Sintesa Komposit Bioplastik Pati Kulit Singkong-Partikel Nanosilika Dan Karakterisasinya. *Jurnal Kimia dan Kemasan*, 42(2), 37–45. doi: 10.24817/jkk.v42i2.3535

[9] Pillai, S. R., Venkatachalapathy, N., Kumar, K. S., & Pare, A. (2021). Effect of roasting and cooking on physiochemical properties of black rice soluble extract. *International Journal of Chemical Studies*, 9(1), 2848–2852. doi: 10.22271/chemi.2021.v9.i1an.11655

[10] Nisah, K. (2017). Study Pengaruh Kandungan Amilosa dan Amilopektin Umbi-Umbian terhadap Karakteristik Fisik Plastik Biodegradable dengan Plastizicer Gliserol. *BIOTIK: Jurnal Ilmiah Biologi Teknologi dan Kependidikan*, 5(2), 106–113. doi: 10.22373/biotik.v5i2.3018

[11] Torabi, Z., & Nafchi, A. M. (2013). The Effects of SiO2 Nanoparticles on Mechanical and Physicochemical Properties of Potato Starch Films. *The Journal of Chemical Health Risks*, 3(1), 33–42. Retrieved from http://www.jchr.org/article_544018.html

[12] Nandiyanto, A. B. D., Fiandini, M., Ragadhita, R., Sukmafitri, A., Salam, H., & Triawan, F. (2020). Mechanical and biodegradation properties of cornstarch-based bioplastic material. *Materials Physics and Mechanics*, 44(3), 380–391. doi: 10.18720/MPM.4432020_9

[13] Oluwasina, O. O., Akinyele, B. P., Olusegun, S. J., Oluwasina, O. O., & Mohallem, N. D. S. (2021). Evaluation of the effects of additives on the properties of starch-based bioplastic film. *SN Applied Sciences*, 3(4). doi: 10.1007/s42452-021-04433-7

[14] Reddy, J. P., & Rhim, J. W. (2014). Characterization of bionanocomposite films prepared with agar and paper-mulberry pulp nanocellulose. *Carbohydrate Polymers*, 110, 480–488. doi: 10.1016/j.carbpol.2014.04.056

[15] Bahtiar, A., Kurniati, M., Sari, Y. W., & Winarti, C. (2018). Surface morphology and water vapour transmission rate analysis of protein-based bioplastic. *IOP Conference Series: Earth and Environmental Science*, 187(1). doi: 10.1088/1755-1315/187/1/012015

[16] Wahyuningtiyas, N. E., & Suryanto, H. (2018). Properties of Cassava Starch based Bioplastic Reinforced by Nanoclay. *Journal of Mechanical Engineering Science and Technology*, 2(1), 20–26. doi: 10.17977/um016v2i12018p020

[17] Zhang, R., Wang, X., & Cheng, M. (2018). Preparation and characterization of potato starch film with various size of Nano-SiO2. *Polymers*, 10(10), 9–12. doi: 10.3390/POLYM10101172

[18] Olawale, O. (2020). Bamboo leaves as an alternative source for silica in ceramics using Box Benhken design. *Scientific African*, 8, e00418. doi: 10.1016/j.sciaf.2020.e00418

[19] de Azêvedo, L. C., Rovani, S., Santos, J. J., Dias, D. B., Nascimento, S. S., Oliveira, F. F., … Fungaro, D. A. (2021). Study of Renewable Silica Powder Influence in the Preparation of Bioplastics from Corn and Potato Starch. *Journal of Polymers and the Environment*, 29(3), 707–720. doi: 10.1007/s10924-020-01911-8

[20] Marichelvam, M. K., Jawaid, M., & Asim, M. (2019). Corn and rice starch-based bio-plastics as alternative packaging materials. *Fibers*, 7(4), 1–14. doi: 10.3390/fib7040032

[21] Sorrentino, A., Tortora, M., & Vittoria, V. (2006). Diffusion behavior in polymer-clay nanocomposites. *Journal of Polymer Science, Part B: Polymer Physics*, 44(2), 265–274. doi: 10.1002/polb.20684

[22] Kavoosi, G., Dadfar, S. M. M., & Purfard, A. M. (2013). Mechanical, Physical, Antioxidant, and Antimicrobial Properties of Gelatin Films Incorporated with Thymol for Potential Use as Nano Wound Dressing. *Journal of Food Science*, 78(2). doi: 10.1111/1750-3841.12015

[23] Setiani, W., Sudiarti, T., & Rahmidar, L. (2013). Preparasi Dan Karakterisasi Edible Film Dari Poliblend Pati Sukun-Kitosan. *Jurnal Kimia VALENSI*, 3(2), 100–109. doi: 10.15408/jkv.v3i2.506

[24] Haryanto, & Saputri, A. E. (2016). Pengembangan Bioplastik Dari Tepung Tapioka Dan Tepung Beras Ketan Putih. *Techno*, 17(2), 104–110.

[25] Simarmata, E. O., Hartiati, A., & Harsojuwono, B. A. (2020). Karakteristik Komposit Bioplastik Dalam Variasi Rasio Pati Umbi Talas (Xanthosoma sagittifolium)-Kitosan. *Jurnal Ilmiah Teknologi Pertanian Agrotechno*, 5(2), 75. doi: 10.24843/jitpa.2020.v05.i02.p05

[26] Saputra, M. R. B., & Supriyo, E. (2020). Pembuatan Plastik Biodegradable Menggunakan Pati Dengan Penambahan Katalis ZnO dan Stabilizer Gliserol. *Pentana*, 1(1), 41–51.

[27] Rahman, A. R., Syamsu, K. S., & Isroi, I. I. (2019). Biodegradability of Bioplastic in Natural Environment. *Jurnal Pengelolaan Sumberdaya Alam dan Lingkungan (Journal of Natural Resources and Environmental Management)*, 9(2), 258–263. doi: 10.29244/jpsl.9.2.258-263

CHEESA: Chemical Engineering Research Articles
ISSN **2614-8757 (Print)**, ISSN **2615-2347 (Online)**
Available online at: http://e-journal.unipma.ac.id/index.php/cheesa

Research Article

Synthesis and Characterization of SCDs/TiO_2 Composite

Sintesis dan Karakterisasi Komposit SCDs/TiO_2

Anthoni B. Aritonang[1*)], Ajuk Sapar[1)], Heni Puspita Sari[1)], Puji Ardiningsih[1)], Adhitiyawarman[1)]
[1)]Universitas Tanjungpura, Chemistry Department, Indonesia

****correspondence email*:** anthoni.b.aritonang@chemistry.untan.ac.id

Received: 18 September 2022;
Revised: 09 December 2022;
Accepted: 09 December 2022;

doi: *10.25273/cheesa.v5i2.13915.92-100*

Abstract

Synthesis of sulphur-doped carbon nanodots immobilized on the TiO_2 surface (SCDs/TiO_2) composite was carried out using the sol-gel method with SCDs and titanium tetraisopropoxide (TTIP) as precursors. SCDs were prepared from citric acid monohydrate, urea, and sodium disulphite using the microwave technique. SCDs/TiO_2 was then visually observed under UV 365 nm and characterized by UV-Vis diffuse reflectance spectrophotometry (UV-Vis/DRS), Photoluminescence (PL) spectroscopy, Fourier transform infrared (FT-IR), and X-ray diffraction (XRD). The SCDs/TiO_2 composite product had a brown solid with a green luminescent under UV light. Furthermore, UV-Vis/DRS for variations in SCDs concentrations of 0.5%; 1.25%, and 2.5% showed Eg values of 2.33 eV, 2.14 eV, and 1.61 eV, respectively. The results showed that SCDs caused the maximum emission peak (λ_{Em}) to redshift and also affected the intensity of PL TiO_2. There was also a shift in the absorption peak towards the visible light region. Based on the results, the 0.5% SCDs/TiO_2 was the optimum concentration with the lowest intensity as an indication of separation of the (e^-) and (h^+) charge pairs, which greatly enhanced the photocatalytic efficiency.

Keywords: microwave; photoluminescence; SCDs; sol-gel; TiO_2

Abstrak

Telah disintesis komposit sulfur karbon nanodots terimobilisasi pada permukaan TiO_2 (SCDs/TiO_2) menggunakan SCDs dan titanium tetraisopropoksida (TTIP) sebagai prekursor dengan metode sol-gel. SCDs dipreparasi dari asam sitrat monohidrat, urea dan natrium disulfit dengan metode microwave. SCDs/TiO_2diamati secara visual di bawah sinar UV 365 nm dan dikarakterisasi dengan metode UV-Vis diffuse reflectance spectrophotometry (UV-Vis/DRS), spektroskopi photoluminescence (PL), Fourier transform infrared (FT-IR) dan X-ray diffraction (XRD). SCDs/TiO_2 berupa padatan cokelat dan memiliki pendaran hijau di bawah sinar UV. Hasil pengukuran dengan UV-Vis/DRS, SCDs pada rasio konsentrasi SCDs/TiO_2 0,5% 1,25% dan 2,5% memberikan nilai Eg berturut-turut 2,33 eV; 2,14 eV dan 1,61 eV. Penambahan SCDs mengakibatkan puncak serapan bergeser ke arah sinar tampak. Karakteristik photoluminescence diketahui 0,5% SCDs/TiO_2 merupakan konsentrasi optimum yang memberikan intensitas paling rendah sebagai indikasi pemisahan pasangan muatan (e^-) dan (h^+) paling baik dengan meningkatkan efisiensi fotokatalisis.

Kata kunci: *microwave; photoluminescence; SCDs; sol-gel, TiO_2*

1. Introduction

Titanium dioxide (TiO_2) is a semiconductor material, commonly used in photocatalytic processes due to its high thermal stability and environmental friendliness [1]. Photocatalytic activity of TiO_2 is also often applied to destroy microorganisms and degrade organic compounds in air and water [2]. Furthermore, this material has 3 forms of crystal structure, namely rutile, anatase, and brookite [3]. The anatase form is commonly used, and it has a bandgap energy of 3.0-3.2 eV, which is equivalent to the wavelength of UV light < 380 nm [4].

A previous study reported that only 5% of UV light produced by the sun reaches the earth, while 45% is visible light [5]. This indicates that modifications are needed, such as the use of the photocatalytic activity of TiO_2 in the visible light absorption region. This can be performed by doping metal cations in its structure to reduce the band gap energy (Eg), thereby absorbing visible light energy. Metal cations as a dopant in the TiO_2 structure can accelerate the recombination of charge pairs (e^-) and (h^+) because they act as recombination centers [6].

Combining TiO_2 with other semiconductor materials with lower Eg can suppress the charge pair recombination process. One of the materials that have the potential to inhibit the recombination process is carbon nanodots (CDs) due to their high electronic conductivity, electron storage capacity, visible light absorption, and chemical stability [7]. CDs can also be used as strong energy transfer components in photocatalyst designs [8][9]. CDs that are composited on TiO_2 act as an electron transfer facility on the surface of titanium oxide, hence, the charge pairs (e^-) and (h^+) formed can be separated [10]. Kumar et al [8] reported that CDs/TiO_2 nanocomposites synthesized by the hydrothermal method have a more ability to degrade methylene blue comparedTiO_2-P_{25}. Titirici et al [11] succeeded in synthesizing N-doped CDs/TiO_2 using the solvothermal method. Furthermore, the composite obtained was used for the photoelectrochemical oxidation of water. Martins et al [12] also synthesized a similar product, which had high photocatalytic activity against methylene blue degradation and N conversion.

Sulphur (S) quantum dots (SQD) has unique optical properties, can absorb visible light, is non-toxic, and has the potential to be used as an alloy for photocatalysts [13]. The development of CDs materials is often carried out using S doping, which forms SCDs. Loukanov et al [14] reported that there was an improvement in the fluorescence properties of the product as metal cation sensors.

This study used the sol-gel method to synthesize SCDs/TiO_2 composite because it is easy to carry out and uses simple equipment [15]. Furthermore, it focused on the composition of SCDs in TiO_2 to obtain the optimum combination with good photocatalytic activity under visible light illumination.

2. Research Methods

2.1 Tools and Materials

The tools were used in this study included a 750 Watt Panasonic NNSM32HMTTE microwave, oven, furnace, Fourier transform infrared (FT-IR) Shimadzu IR Prestige 21, Photoluminescence (PL) Spectrophotometer Horiba FluoroMax 4, UVGL-55 Handheld UV Lamp 365 nm,

Ultra Violet-Visible Spectrophotometer (UV-Vis) Shimadzu UV-1280, Ultra Violet-Visible Diffuse Reflectance Spectrophotometer (DR/UV-Vis) Agilent Cary 60, and X-ray diffraction (XRD) X'Pert PRO PANalytical.

Meanwhile, the materials used were distilled water (H_2O), acetic acid (CH_3COOH; Merck), citric acid monohydrate ($C_6H_8O_7.H_2O$; Merck), acetylacetone ($C_5H_8O_2$; Merck), ethanol (C_2H_5OH; 97%, Merck), sodium disulfite ($Na_2S_2O_5$; Merck), urea (CH_4N_2O; Sigma Aldrich), and titanium tetraisopropoxide (TTIP; 97%, Sigma Aldrich).

2.2 Procedure

SCDs were synthesized using the microwave method [13]. A total of 2 g citric acid monohydrate, 4 g urea, 1 g sodium disulphite, as well as sodium disulphite: citric acid monohydrate with a ratio of 0.5 (w/w) were dissolved in 60 mL of distilled water, and stirred using a magnetic stirrer for 5 minutes. Subsequently, the solution was heated in a 450 W microwave on high mode for 12 minutes, and dried in an oven at 100 °C for 10 minutes to produce 1.3 g SCDs powder.

The SCDs/TiO_2 composite was synthesized using the sol-gel method based on the method proposed by Sugiarti et al [16]. The Ti(OH)n sol was prepared by mixing 2 solutions, namely A and B. Solution A was a mixture of 26.5 mL ethanol, 2 mL acetic acid, and 2 mL of distilled water, while B was prepared from 7.5 mL TTIP, 26.5 mL ethanol, and I mL acetylacetone in a reflux flask. Furthermore, solution A was dropped slowly into B while stirring using a magnetic stirrer. The reflux process was then carried out at 55 °C for 2 hours to produce a light yellow Ti(OH)n sol, which was aged for several days to form a Ti(OH)n gel. The product was dried in an oven at 80 °C, followed by calcination at 450 °C for 3 hours to produce TiO_2 in the form of white powder.

A total of 0.4 g TiO_2 powder was mixed with SCDs at ratios of 0.5, 1.25, and 2.5% (w/w). Subsequently, 5 mL of distilled water was added to the mixture while stirring for 20 minutes, followed by drying in an oven at 80 °C for 12 hours to produce a powder-shaped SCDs/TiO_2 composite. The resulting composite was then characterized using UV-Vis/DRS, PL, FT-IR, and XRD.

3. Results and Discussion

SCDs composite synthesis was carried out using the microwave heating method [13] with citric acid monohydrate as carbon chain precursor and urea as CDs surface passivation agent. Furthermore, sodium disulphite was the source of sulphur (S), which served as a dopant in the CDs structure.

Citric acid reacts with urea to form a citric acid amide. Heating with microwave energy triggers a carbonization process, which causes dehydration and deammoniation of the hydroxyl and amino groups in intermolecular compounds [16]. Furthermore, the carbon chains undergo rearrangement to form nanosheet structures and grow into quantum dots/nanodots SCDs material [17]. SCDs solids still contain water, which was used as a solvent, and then dried in an oven at 100 °C [14]. Based on observations of the luminescence properties of SCDs using UV light illumination (λ = 365 nm), a yellowish-green color was produced during the process. The emergence of this color was due to competition between various emission centers (bright edge states) that

dominate the optical properties of SCDs [18].

The synthesis of TiO_2 was carried out based on the method proposed by Aritonang et al. [4], starting with the preparation of $Ti(OH)_4$ sol using solution B containing titanium tetraisopropoxide (TTIP) precursor in ethanol solvent. Acetylacetone was then added to the mixture [16], and it was refluxed at 55 ^oC, followed by calcination to form sol [17-18]. This process produced white TiO_2 crystals, as previously reported by Aritonang et al [19]. The composite was synthesized by mixing TiO_2 with SCDs at various concentration ratios of 0.5-2.5, which led to the production of a light brown solid SCDs/TiO_2 composite, as illustrated by Li et al [20].

3.1 UV-Vis/DRS Characterization

UV-Vis/DRS characterization as a relationship (%) of reflectance to wavelength is shown in Figure 1. Furthermore, TiO_2 gave an absorption peak in the region below 380 nm. The results also showed that the addition of SCDs on TiO_2 widened the peak to the visible light region [18].

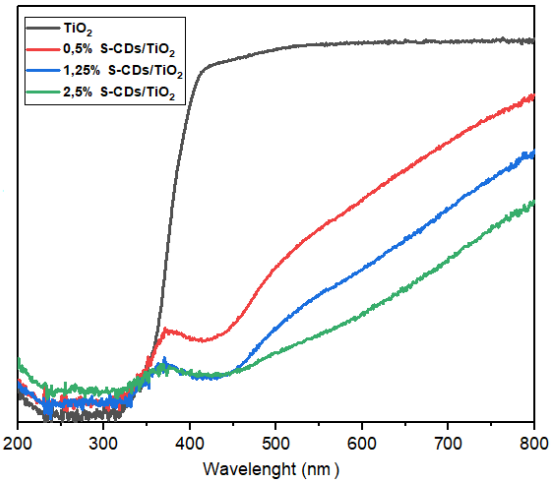

Figure 1. Spectra %R versus Wavelength (nm): TiO_2 and SCDs/TiO_2

The band gap energy of the SCDs/TiO_2 composite was determined using the Tauc equation (1):

$$(\alpha h\upsilon)^2 = B\,(h\upsilon - Eg) \quad \text{.....(1)}$$

Where, α is the absorbance coefficient, $h\upsilon$ is photon energy, B is constant, and Eg is bandgap energy. The value of α can be substituted with the Kubelka-Munk coefficient into equation (2).

$$(Kh\upsilon)^{1/n} = B(h\upsilon - Eg) \quad \text{.....(2)}$$

The graph of the relationship between $(Kh\upsilon)^{1/2}$ to hυ produced a band gap energy (Eg), which is presented in Table 1.

Table 1. Bandgap Energy Value

Material	Eg (eV)
TiO_2	3,27
0,5% SCDs/TiO_2	2,33
1,25% SCDs/TiO_2	2,14
2,5% SCDs/TiO_2	1,61

Based on Table 1, the band gap energy of TiO_2 was 3.27 eV, and this is in line with the results of Linsebigler et al [6]. The Eg values of SCDs/TiO_2 composite at a CDs ratio of 0.5 %; 1.25 % and 2.5% were 2.33 eV, 2.14 eV, and 1.61 eV, respectively. A low Eg value indicates the formation of SCDs/TiO_2 composite. Furthermore, the lower the band gap energy generated, the lower the energy required to excite electrons from the valence to the conduction band. Based on the Eg value, the SCDs/TiO_2 composite at the three concentration ratios was estimated to be active when illuminated with visible light.

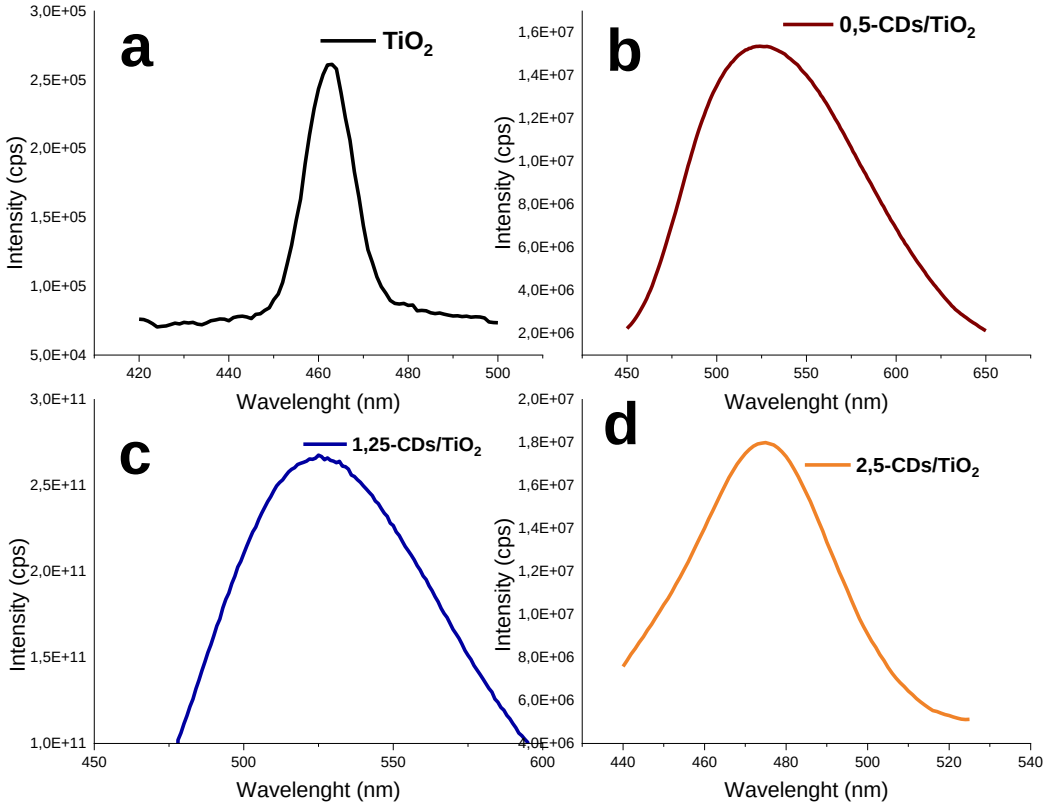

Figure 2. Photoluminescence spectra: (a) TiO_2; SCDs-TiO_2 with a CDs ratio of (b) 0.5%, (c) 1.25% and (d) 2.5%.

3.2 Photoluminescence (PL)

The measurements of the PL spectra of TiO_2 and SCDs/TiO_2 at various SCDs concentration ratios are presented in Figure 2. Based on Figure 2a, TiO2 gave a PL absorption peak at 460 nm. The calculation results of Eg showed that the combination of SCDs in a titanium oxide matrix with a concentration ratio of 0.5 and 1.25% (w/w) caused a shift in the PL absorption peak to the visible region (>400 nm). Huang et al [21] also stated that the interaction between SCDs and TiO_2 occurs physically (couple heterojunction) on the composite surface, and this led to a decrease in Eg. However, the addition of SCDs at a concentration of >1.5% caused an insignificant shift due to particle agglomeration.

The fluorescence emission absorption peak of the SCDs/TiO_2 composite was formed due to the recombination of photoelectron (e^-) and photo hole (h^+) charge pairs induced by photons [22]. Based on Table 2, SCDs/TiO_2 composite with an SCDs ratio of 0.5% had the lowest intensity of $1.53x10^7$ cps, and the lower the value obtained, the better the charge pair separation [8][11]. The PL emission analysis on the three SCDs/TiO_2 samples showed that the composite with a CDs ratio of 0.5% has photocatalytic activity under light illumination with the highest efficiency, which corresponds to the Eg value.

Table 2. λEm and TiO_2 and SCDs/TiO_2 emissions

Sample	λEm (nm)	Intensity (cps)
TiO_2	463	$2,61x10^5$
0,5% SCDs/TiO_2	524	$1,53x10^7$
1,25% SCDs/TiO_2	525	$2,6x10^{11}$
2,5% SCDs/TiO_2	475	$1,92x10^7$

3.3 FT-IR Spectrophotometry

The FT-IR spectrophotometry characterization of the SCDs/TiO_2 composite is shown in Figure 3.

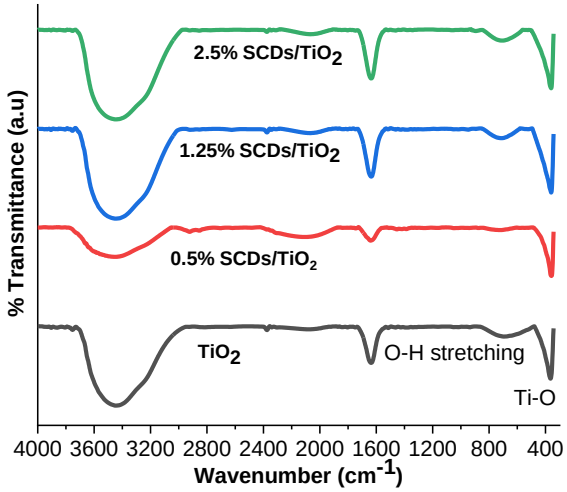

Figure 3. FT-IR spectra of TiO_2 and SCDs/TiO_2 composites

The absorption peaks of TiO_2 and the SCDs/TiO_2 composite observed at wave numbers 3446-3459 cm^{-1} were the stretching vibrations of the O-H groups [14]. Furthermore, the absorption at wave numbers 1635-1640 cm^{-1} was an O-H bending vibration due to the uptake of water vapor [23].

Absorption at wave numbers 696-718 cm^{-1} was a stretching vibration of Ti-O [29,30]. TiO_2 and SCDs/TiO_2 composites were observed for absorption peaks at wave number 412 cm^{-1} as a characteristic of Ti-O stretching vibration [24][6]. The results showed that the combination of SCDs with TiO_2 does not cause a shift in the titanium oxide absorption peak. This indicated that the interaction of these materials occurs physically on the surface, and does not distort the TiO_2 structure.

3.4 X-ray diffraction (XRD)

Characterization with the XRD method aimed to determine the phase structure and size of the crystallites. Furthermore, XRD analysis was carried out on TiO_2 as well as 0.5, 1.25, and 2.5 (w/w) SCDs/TiO_2. The results of XRD characterization of TiO_2 and SCDs/TiO_2 are presented in Figure 4.

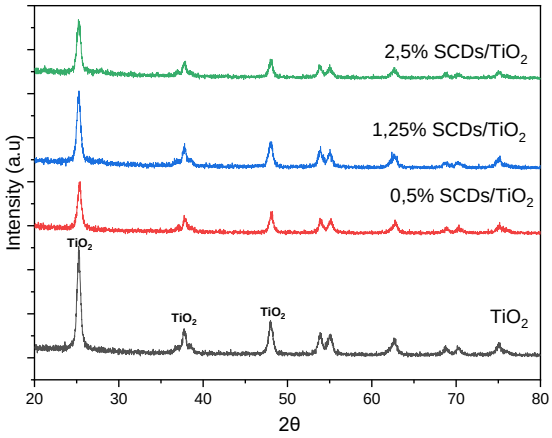

Figure 4. XRD diffractogram of TiO_2 and SCDs/TiO_2 composite

The TiO_2 and SCDs/TiO_2 diffractograms showed that there were similarities in the three highest peaks produced, namely in the range of 2θ 25°, 37°, and 48°. These peaks indicated that TiO_2 had an anatase crystal phase, which was similar to the JCPDS database catalog No. 01-075-8897, and this was in line with the results obtained from Aritonang et al [19]. The similarity of the diffraction angle peaks produced by SCDs/TiO_2 and TiO_2 showed that no new compounds were formed from the SCDs/TiO_2 composite. The size of the crystallites was then determined using the Deybe-Scherrer equation (3) [4].

$$D = k\lambda / B\cos\theta \quad \text{.....(3)}$$

Where, D is the crystal thickness (size) (nm), k is a material constant with value < 1 (common value is 0.9), λ is the X-ray wavelength during measurement (nm), B is the width of the half-peak on the diffractogram, and θ is derived from the graph data of 2θ on the diffractogram. The

calculation results of the crystallite size are presented in Table 3.

Table 3. Size of TiO_2 and SCDs/TiO_2 crystallites

Material	2 θ	d (nm)	D (nm)
TiO_2	25,2834 37,8352 48,1053	0,2597	4,045
0,5% SCDs/TiO_2	25,2772 37,6632 47,9844	0,2502	3,938
1,25% SCDs/TiO_2	25,3332 37,7934 48,0287	0,2596	3,942
2,5% SCDs/TiO_2	25,3648 37,7796 48,0902	0,2598	3,946

Table 3 shows that the addition of SCDs decreased the size of TiO_2 crystallites, but there was no 2θ shift in angular position. Therefore, the formation of the composite does not occur in the anatase TiO_2 crystal phase transformation. The results showed that 0.5% SCDs/TiO_2 had the smallest crystallinity size of 3.938 nm compared to TiO_2 and other composites. This indicated that 0.5% SCDs is the optimum concentration for the production of composites. These findings were supported by PL characteristic data and UV-Vis/DRS spectrum analysis results. The addition of SCDs at a concentration of 2.5% increased the crystallinity size of TiO_2. This was due to the inhomogeneous mixture of SCDs and TiO_2 from the physical mixing process.

4. Conclusion

The SCDs/TiO_2 composite produced is a brown solid, which has a green glow under 365 nm UV light. Furthermore, the UV-Vis/DRS characteristics include band gap energy values of 2.33, 2.14, and 1.61 eV for the 0.5%, 1.25%, and 2.5% composites, respectively. The results showed that SCDs caused a shift in the absorption peak of the visible region. PL characteristics also revealed that 0.5% SCDs/TiO_2 is the optimum concentration, which gave the lowest intensity. Based on XRD diffractogram analysis, this product has an anatase crystalline structure with a crystallite size of 3.938 nm.

Acknowledgment

The authors are grateful to the Dean and Head of the Chemical Research Laboratory, Faculty of Mathematics and Natural Sciences, Universitas Tanjungpura, for supporting this study.

References

[1] Dastan, D., & Chaure, N. B. (2014). Influence of Surfactants on TiO2 Nanoparticles Grown by Sol-Gel Technique. *International Journal of Materials, Mechanics and Manufacturing*, 2(1), 21–24. doi: 10.7763/ijmmm.2014.v2.91

[2] Tussa'adah, R., & Astuti. (2015). SINTESIS MATERIAL FOTOKATALIS TiO 2 UNTUK PENJERNIHAN LIMBAH TEKSTIL. *Jurnal Fisika Unand*, 4(1), 91–96.

[3] Dambournet, D., Belharouak, I., Ma, J., & Amine, K. (2011). Template-assisted synthesis of high packing density SrLi2Ti 6O14 for use as anode in 2.7-V lithium-ion battery. *Journal of Power Sources*, 196(5), 2871–2874. doi: 10.1016/j.jpowsour.2010.11.011

[4] Patil, S. M., Deshmukh, S. P., Dhodamani, A. G., More, K. V., & Delekar, S. D. (2016). Different Strategies for Modification of Titanium Dioxide as Heterogeneous Cata lyst in Chemical Transformations. *Current Organic Chemistry*, 21(9), 821–833. doi: 10.2174/1385272820666161013151816

[5] Karim, S., Pardoyo, P., & Subagio, A. (2016). Sintesis dan Karakterisasi TiO2 Terdoping Nitrogen (N-Doped TiO2) dengan Metode Sol–Gel. *Jurnal Kimia Sains dan Aplikasi*, 19(2), 63–67. doi: 10.14710/jksa.19.2.63-67

[6] Linsebigler, A. L., Lu, G., & Yates, J. T. (1995). Photocatalysis on TiO2 Surfaces: Principles, Mechanisms, and Selected Results. *Chemical Reviews*, 95(3), 735–758. doi: 10.1021/cr00035a013

[7] Kumar, M. S., Yasoda, K. Y., Kumaresan, D., Kothurkar, N. K., & Batabyal, S. K. (2018). TiO2-carbon quantum dots (CQD) nanohybrid: Enhanced photocatalytic activity. *Materials Research Express*, 5(7). doi: 10.1088/2053-1591/aacbb9

[8] Li, H., He, X., Kang, Z., Huang, H., Liu, Y., Liu, J., … Lee, S. T. (2010). Water-soluble fluorescent carbon quantum dots and photocatalyst design. *Angewandte Chemie - International Edition*, 49(26), 4430–4434. doi: 10.1002/anie.200906154

[9] Qin, Y., Wen, J., Zheng, L., Yan, H., Jiao, L., Wang, X., … Zhu, C. (2021). Single-atom-based heterojunction coupling with ion-exchange reaction for sensitive photoelectrochemical immunoassay. *Nano Letters*, 21(4), 1879–1887. doi: 10.1021/acs.nanolett.1c00076

[10] Yao, Y., Li, G., Ciston, S., & Lueptow, R. M. (2008). Photoreactive TiO2Carbon Nanotube.pdf, 42(13), 4952–4957.

[11] Luo, H., Dimitrov, S., Daboczi, M., Kim, J. S., Guo, Q., Fang, Y., … Titirici, M. M. (2020). Nitrogen-Doped Carbon Dots/TiO2 Nanoparticle Composites for Photoelectrochemical Water Oxidation. *ACS Applied Nano Materials*, 3(4), 3371–3381. doi: 10.1021/acsanm.9b02412

[12] Martins, N. C. T., Ângelo, J., Girão, A. V., Trindade, T., Andrade, L., & Mendes, A. (2016). N-doped carbon quantum dots/TiO2 composite with improved photocatalytic activity. *Applied Catalysis B: Environmental*, 193, 67–74. doi: 10.1016/j.apcatb.2016.04.016

[13] Ning, K., Sun, Y., Liu, J., Fu, Y., Ye, K., Liang, J., & Wu, Y. (2022). Research Update of Emergent Sulfur Quantum Dots in.

[14] Loukanov, A., Mladenova, P., Udono, H., Miskolczy, Z., Angelov, A., Biczók, L., & Nakabayashi, S. (2018). Sulfur doped fluorescent carbon dots as nanosensors for rapid and sensitive monitoring of calcium in hard water. *Journal of Chemical Technology and Metallurgy*, 53(3), 473–479.

[15] Aritonang, A. B., Krisnandi, Y. K., & Gunlazuardi, J. (2018). Modification of TiO2 nanotube arrays with N doping and Ag decorating for enhanced visible light photoelectrocatalytic degradation of methylene blue. *International Journal on Advanced Science, Engineering and Information Technology*, 8(1), 234–241. doi: 10.18517/ijaseit.8.1.2342

[16] Syafei, D., Sugiarti, S., Darmawan, N., & Khotib, M. (2017). Synthesis of TiO2/carbon nanoparticle (C-dot) composites as active catalysts for photodegradation of persistent organic pollutant. *Indonesian Journal of Chemistry*, 17(1), 37–42. doi: 10.22146/ijc.23615

[17] Hou, J., Li, H., Wang, L., Zhang, P., Zhou, T., Ding, H., & Ding, L. (2016). Rapid microwave-assisted synthesis of molecularly imprinted polymers on carbon quantum dots for fluorescent sensing of tetracycline in milk. *Talanta*, 146, 34–40. doi: 10.1016/j.talanta.2015.08.024

[18] Ruan, H., & Zhou, L. (2022). Synthesis of Fluorescent Sulfur Quantum Dots for Bioimaging and Biosensing. *Frontiers in Bioengineering and Biotechnology*, 10(May), 1–7. doi: 10.3389/fbioe.2022.909727

[19] Aritonang, A. B., Pratiwi, E., Warsidah, W., Nurdiansyah, S. I., & Risko, R. (2021). Fe-doped TiO2/Kaolinite as an Antibacterial Photocatalyst under Visible Light Irradiation. *Bulletin of Chemical Reaction Engineering & Catalysis*, 16(2), 293–301. doi: 10.9767/bcrec.16.2.10325.293-301

[20] Li, H., Liu, J., Qian, J., Li, Q., & Yang, J. (2014). Preparation of Bi-doped TiO2 nanoparticles and their visible light photocatalytic performance. *Cuihua Xuebao/Chinese Journal of Catalysis*, 35(9), 1578–1589. doi: 10.1016/S1872-2067(14)60124-8

[21] Huang, K., Chen, L., Deng, J., & Xiong, J. (2012). Enhanced visible-light photocatalytic performance of nanosized anatase TiO 2 doped with CdS quantum dots for cancer-cell treatment. *Journal of Nanomaterials*, 2012. doi: 10.1155/2012/720491

[22] Kudhier, M. A., Alkareem, R. A. S. A., & Sabry, R. S. (2021). Enhanced photocatalytic activity of TiO2-CdS composite nanofibers under sunlight irradiation. *Journal of the Mechanical Behavior of Materials*, 30(1), 213–219. doi: 10.1515/jmbm-2021-0022

[23] Wang, L., Zhu, S. J., Wang, H. Y., Qu, S. N., Zhang, Y. L., Zhang, J. H., … Sun, H. B. (2014). Common origin of green luminescence in carbon nanodots and graphene quantum dots. *ACS Nano*, 8(3), 2541–2547. doi: 10.1021/nn500368m

[24] Pratiwi, E., Harlia, H., & Aritonang, A. B. (2020). Sintesis TiO2 terdoping Fe3+ untuk Degradasi Rhodamin B Secara Fotokatalisis dengan Bantuan Sinar Tampak. *Positron*, 10(1), 57. doi: 10.26418/positron.v10i1.37739

CHEESA: Chemical Engineering Research Articles
ISSN **2614-8757 (Print)**, ISSN **2615-2347 (Online)**
Available online at: http://e-journal.unipma.ac.id/index.php/cheesa

Research Article

Analysis of Pyrolytic Product Distribution for B3 and Non-B3 Medical Waste Pyrolysis

Analisis Distribusi Produk Pirolitik pada Pirolisis Limbah Medis B3 dan Non-B3

Tri Nur Rezeki[1)], Abrar Ridwan[1*)], Wahyu Meka[2)], Yulia Fitri[3)], Rain Agri Mahendra[1)], Munawir Hamzah[3)], Laras Sita Widara[3)], Azzalya Putri Athala[3)]
[1)]Universitas Muhammadiyah Riau, Department of Mechanical Engineering, Indonesia
[2)]Institut Teknologi Sepuluh Nopember, Department of Chemical Engineering, Indonesia
[3)]Universitas Muhammadiyah Riau, Department of Physics, Indonesia

**correspondence email*: abrar.ridwan@umri.ac.id

Received: 14 October 2022;
Revised: 08 December 2022;
Accepted: 09 December 2022;

doi: *10.25273/cheesa.v5i2.14134.101-110*

Abstract

The coronavirus disease (COVID-19) has badly impacted many sectors, particularly medical waste generation in healthcare facilities. The increasing amount of medical waste poses a serious threat to health and environmental sustainability. Pyrolysis as a superior thermochemical technology is an effective solution for treating both B3 medical waste and non-B3 medical waste. The waste used in this study has good characteristics, as indicated by the low water and high fixed carbon content. The pyrolysis process yields products with economic value, such as solid, liquid, and gas products. Therefore, this study aims to determine the levels of products that can be produced from B3 and non-B3 medical waste. The results showed that rubber bands produce the highest proportion of liquid products at 44%, the highest solid products were obtained from LDPE plastic waste with a proportion of 65%, while the highest gas product was produced by mask waste at 45%. Based on the results, waste with high product yields can be used as an alternative energy source, such as gasoline, LPG, briquettes, and battery-based materials.

Keywords: alternative energy; medical waste; pyrolysis; thermal technology

Abstrak

Virus corona (COVID-19) memberikan dampak buruk bagi banyak sektor, terutama pada timbulan sampah medis di fasilitas pelayanan kesehatan. Meningkatnya jumlah limbah medis merupakan ancaman serius bagi kesehatan dan kelestarian lingkungan. Pirolisis sebagai teknologi termokimia yang unggul merupakan solusi efektif untuk pengolahan limbah medis baik limbah medis B3 maupun limbah medis non-B3. Sampah yang digunakan dalam penelitian ini memiliki karakter sampah yang baik. Hal ini ditunjukkan dengan kadar air yang rendah dan kadar karbon tetap yang tinggi. Tujuan dari penelitian ini adalah untuk mengetahui kadar produk yang dapat dihasilkan dari limbah medis B3 dan limbah medis non-B3. Hasil penelitian diketahui karet gelang menghasilkan proporsi produk cair tertinggi sebesar 44%, sedangkan produk padat tertinggi diperoleh dari limbah plastik LDPE dengan proporsi 65% dan produk gas tertinggi diperoleh dari limbah masker dengan proporsi 45%. Limbah dengan hasil produk yang tinggi memiliki potensi untuk dimanfaatkan sebagai sumber energi alternatif seperti bensin, gas lpg, briket dan bahan dasar baterai.

Kata kunci: energi alternatif; limbah medis; pirolisis; teknologi termal

1. Introduction

Coronavirus disease 2019 (COVID-19) is a deadly virus whose existence was first reported in Indonesia in March 2020. Subsequently, census information on the number of people who have contracted and recovered from the disease has been integrated into statistical data comprehensively by various credible public or private institutions to increase public awareness. Similar information related to the census of medical waste, which is also important must be given more attention by the community. This will reduce the increasing impacts of medical waste generation. Previous data on medical waste showed an increase in the capital city of DKI Jakarta from March 2020 to July 2021, with a total of seven to ten thousand tons. This includes masks, gloves, bandages, tissues, plastic, paper, syringes, personal protective equipment (PPE), and patient food waste [1]. The World Health Organization [2] stated that medical waste is a hazardous material containing radioactive, toxic, or infectious substances. Medical waste management should be performed using safe and environmentally friendly methods [3].

Several management practices related to technology, such as chemical disinfection, sanitary landfill, incineration, and pyrolysis, have emerged in various developed and developing countries [4,5]. Indonesia, as a developed country, prefers incineration which has the advantages of reducing the capacity and quantity of waste significantly and sterilizing them as a whole [6]. However, organic wastes such as polychlorinated dibenzo-p-dioxins and dibenzofurans (PCDD/Fs), polycyclic aromatic hydrocarbons (PAHs), inorganic emissions, as well as ash containing toxic metals are generated during waste incineration. They cause secondary pollution to the environment, which threatens human health [7,8].

Thermochemical conversion has many advantages over traditional waste incineration methods, which are mainly related to increased air pollution, generation of value-added products, and energy [5]. Another advantage is that the operation uses a temperature which can be adjusted as needed, thereby potentially reducing the risk of alkaline volatilization [9]. One of the thermochemical conversions which utilize the instability of organic components in medical waste is the pyrolysis method [10]. This method uses raw materials that are heated at high temperatures under low oxygen conditions and produces synthetic gas (syngas), which is then condensed and converted into pyrolysis oil. The liquid product has properties that are very close to commercial transportation fuels which can be improved and modified to become an alternative energy source [11].

Previous studies have assessed the pyrolysis concept as the most appropriate method for treating medical waste because it is considered safe and environmentally friendly [5,8,12]. Medical waste generated by health services consists of 15% B3 medical waste which comprises hazardous and toxic materials, while the remaining 85% is considered non-B3 [13]. Non-hazardous medical waste resembles domestic/household materials, such as garden waste, food scraps, paper, plastic, cloth and rubber. Meanwhile, B3 medical waste such as medical masks and gloves arising from hospital medical activities, are pathogenic and infectious in nature [13]. Based on the explanation above, this study aims to perform pyrolysis of B3 and non-B3 medical waste to determine the levels of products in the form of liquid, solid, and gas

products. The results are expected to be used as an innovation in handling B3 and non-B3 medical waste in Indonesia.

2. Research Methods

2.1 Tools and materials

The raw materials were obtained from the nearest canteen and pharmacy around the Universitas Muhammadiyah Riau, between May and July 2022. They consist of B3 and non-B3 medical waste. B3 medical waste includes masks and gloves, while non-B3 includes rubber bands, LDPE plastic, HVS paper, cotton cloth, garden and food waste. The sample weight was determined by keeping half of the reactor volume (500 mL) which was then weighed. The proportion of each waste was placed in the reactor, as shown in Figure 1. Furthermore, the food waste in this study was dried beforehand at a temperature of 90 °C to get the maximum bio-oil and reduce the water content [14]. The next step is the enumeration process. The collected waste was chopped to a size of 5 mm to maximize waste in the heating furnace and accelerate thermochemical reactions [15].

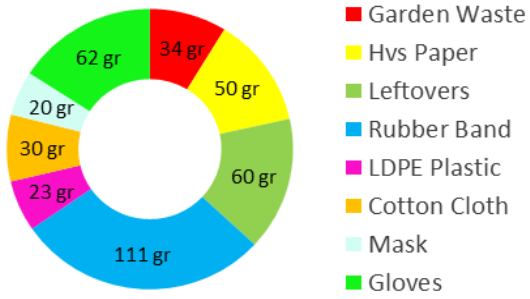

Figure 1. The proportion of medical waste

The laboratory-scale pyrolysis equipment consisting of several components was used as shown in Figure 2. The chopped medical waste was placed into the neck flask reactor 3 (1) which has a volume of 1000 mL. The heating furnace (2) is a horizontal frequency electromagnetic heating device with an inner diameter of 106 mm, a height of 61 mm, and is equipped with a temperature controller (30-450 °C). Nitrogen (3) was fitted with a hose and regulator to adjust the nitrogen flow rate, while the condenser (4) used was a Liebig-type with a length of approximately 60 cm that utilizes the flow rate of tap water as a cooling source. Meanwhile, the liquid product container (5) used was a glass two-neck flask with a volume of 500 mL.

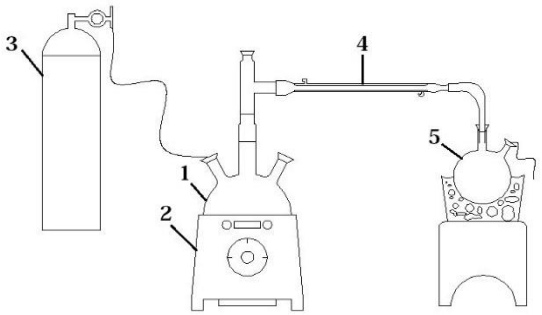

(1). Reactor (2). Electromagnetic heating furnace (3). Nitrogen (4). Condenser (5). Liquid product container

Figure 2. Pyrolysis equipment schematic

2.1.1 Characteristics of Medical Waste

A feasibility test for B3 and non-B3 medical waste is an important step before performing the pyrolysis process. The characteristics of medical waste were determined using the proximate test based on ASTM D 1762-84 standardization. The proximate test was used to determine the content contained in B3 and non-B3 medical waste. This includes water, ash (fly ash), volatile, and fixed carbon [16].

2.2 Procedure

The first step before the pyrolysis process is to ensure that all equipment sets are properly installed. Chopped B3 and non-B3 medical waste were put in the reactor which was placed into a heating furnace with the temperature set at 400 °C. The pyrolysis time starts counting after the

heating temperature is set and turned on. Furthermore, nitrogen was added to help push the syngas out through the condenser pipe at a flow rate of 0.5 L/min. Nitrogen also has the function of minimizing the presence of air in pyrolysis equipment. Airtight conditions can help the pyrolysis process break down complex hydrocarbon compounds into smaller molecules [5].

The cooling system uses two stages, the first is a source of water that flows into the condenser, while the second is a mixture of ice and salt, which is placed under the liquid product collector. Liquid components were separated from volatile products by condensation and collected in specific devices, the solid product was obtained from the pyrolysis residue, while non-condensable gas flowed through the exhaust hose. Furthermore, the process continued until the temperature reached 400 °C. The pyrolysis time and equipment were stopped when no more syngas and liquid were produced. These steps were carried out for all samples of B3 and non-B3 medical waste.

The products obtained from the pyrolysis process were mainly solid (charcoal), liquid (oil) and gas. The percentage of each product produced was calculated using equations 1, 2, and 3.

The liquid product was collected in an oil reservoir under the condenser, and the percentage yield was calculated using equation 1.

$$\%Liquid = \frac{Liquid\ mass}{Initial\ mass} X\ 100\% \quad \textbf{.....(1)}$$

The solid product (charcoal) is the combustion residue produced through the pyrolysis process and collects in the reactor. The percentage can be calculated using equation 2.

$$\%Charcoal = \frac{Charcoal\ mass}{Initial\ mass} X\ 100\% \quad \textbf{.....(2)}$$

Gas is the result of a pyrolysis process that cannot be condensed. The gas product from each raw material can be calculated using equation 3.

$$\%Gas = 100 - \%Liquid - \%Charcoal \quad \textbf{.....(3)}$$

Table I. Proximate Test Results

Waste	Water Content (%)	Volatile Content (%)	Ash Content (%)	Fixed Carbon (%)
Mask	2.24	63.85	15.38	18.52
Gloves	2.31	68.08	13.37	16.22
Garden Waste	6.95	64.11	24.15	4.77
Leftovers	26.95	70.06	2.51	0.47
HVS Paper	3.02	65.54	19.20	12.23
Cotton Cloth	10.01	80.40	5.09	14.51
Rubber Band	1.20	60.26	18.97	20.76
LDPE Plastic	5.38	89.62	4.32	0.66

3. Results and Discussion

3.1 Characteristic Test Results

The results obtained for the water, ash, volatile, and fixed carbon test for B3 and non-B3 medical waste are shown in Table I. B3 medical waste including gloves and masks had an average water content of 2.27%, while non-hazardous medical waste such as garden and food waste, paper, rubber, cloth, as well as LDPE plastic had an average water content of 8.91%. High water content is an unwanted substance during the pyrolysis process. This is because it can increase the need for heat and

slow down the process. The B3 and non-B3 medical waste had a water content below 10% meaning that they have the potential to be processed by the pyrolysis method based on Silva et al. [17].

B3 medical waste had an average ash content of 14.37%, while that of non-B3 was 12.37%. Ash content is an impurity for the product obtained during pyrolysis and it has non-flammable properties. Therefore, high content will reduce the performance of the pyrolysis tool. The samples used in this study had an ash content below 15% which implies that the waste will have production effectiveness when processed by the pyrolysis method [17].

Volatile contents are substances that easily evaporate and they determine the burning ability of fuel [18]. Gloves and masks have an average volatile content of 65.96%, while that of garden and food waste, paper, rubber, cloth, as well as LDPE plastic was 71.66%. The sample used in this study had a volatile content below 76% indicating that they have good potential to be processed by pyrolysis, according to Liu et al. [19].

Meanwhile, fixed carbon is the remaining amount left after the volatile and ash content test. It is an important component of waste because high fixed carbon indicates the potential to be used as an energy source [18]. Gloves and masks have an average fixed carbon value of 17.37%, while that of garden and food waste, paper, rubber, cloth as well as LDPE plastic was 8.91%. The higher the fixed carbon content produced, the higher the potential for the waste to be used as an energy source.

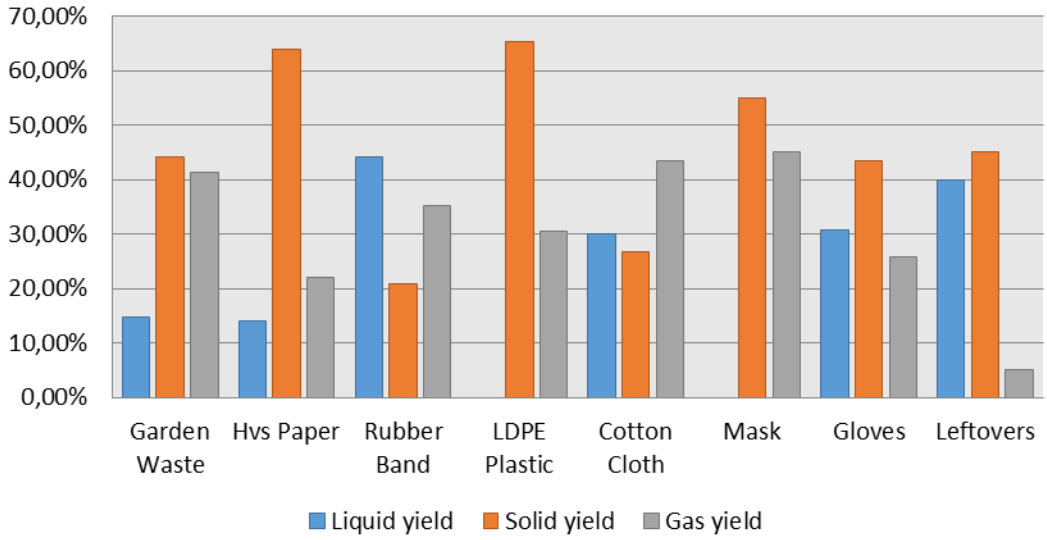

Figure 3. Percentage of pyrolysis products

3.2 Pyrolysis Product Results

The pyrolysis process produces liquid, solid, and gas products as shown in Figure 3. Based on the results, gloves produced liquid, solid, and gas products at 400 °C with a trial time of 90 minutes. The liquid product has a thick texture caused by the aromatic compounds contained in the glove. The highest product obtained was 43% solid, 30% liquid, and 25% gas. A glove (medical glove) is a plastic polymer of the nitrile rubber type. Therefore, the identified medical plastics can be recycled into fuel energy because they are thermoplastic polymers with a high oil content [20].

The mask produced wax, solid, and gas with a trial time of 110 minutes, while the highest product was 55% solid and 45% gas. This waste is made of polypropylene containing paraffin [21] which causes the liquid product to freeze and form wax. The pyrolysis of disposable face mask waste at low temperatures ranging from 350-450 °C will produce wax and light liquid products, while at high temperatures between 450-600 °C, gas and liquid products will be obtained [22]. In this study, masks pyrolyzed at 400 °C did not produce liquid products due to the low temperature.

The residues produced liquid, solid, and gas products with an experimental time of 75 minutes. The highest product from food waste was 45% solid, 40% liquid, and 5% gas. A similar result was found in a study conducted by Amrullah et al. [23] who obtained a solid product of 57% and a liquid of 41% at a temperature range of 400 °C. This is because the high water content in the food waste caused the heating in the reactor flask to slow down, leading to an increase in solid products.

Garden waste produced liquid, solid, and gas products with an experimental time of 60 minutes. Based on the results, the highest product was 44% solid, 15% liquid and 41% gas. A similar result was also obtained from the pyrolysis of leaf and twig waste by Novita et al. [24] namely 35% solid, 30% liquid and 35% gas product at a temperature range of 400 °C. Furthermore, the content of lignin, cellulose and water in garden waste causes gas and solid products to increase [25]. According to Shen et al. [26], the liquid product can be increased [26]by reducing the particle size to 0.3-1.3 mm. This size is smaller than the size used in this study, which is 5 mm.

HVS paper was found to contain liquid, solid, and gas products with a trial time of 60 minutes. The highest product was 64% solid, 14% liquid, and 22% gas. Paper is made from cellulose which is found in wood. The high cellulose content causes an increase in solid pyrolysis products [27]. The liquid product can be increased by reducing the particle size, according to a review by Guedes et al. [28].

Furthermore, cotton fabrics produced liquid, solid, and gas with a trial time of 30 minutes. The product obtained included 30% liquid, 27% solid, and 43% gas. A similar result was also obtained in the pyrolysis of cotton fabric by Ma et al. [29] which produced a liquid product of 24% in the temperature range of 400-500 °C. Cotton fabric is a textile product made from cotton fiber. It has the property of absorbing water (hygroscopic) and heat resistance. The temperature setting of 400 °C in the pyrolysis process is considered capable of degrading cotton fabric waste into liquid products.

Rubber bands were found to contain liquid, solid, and gas products with an experimental time of 108 minutes. The highest product was 44% liquid, followed by 21% solid and 35% gas. Rubber bands have the highest proportion of liquid products because they contain 80% pure rubber, 3% protein, and 2% fatty acids. Moreover, Aragaw and Mokenenen [20] stated that rubber-based waste contains high oil.

LDPE plastic produced wax, solid, and gas products with a trial time of 130 minutes. Based on the results, the highest product was 65% solid and 30% gas. The TPA (Terephthalic Acid) content and the high calorific value of plastic waste cause the combustion process to occur faster and produce more wax. Furthermore, the TPA is sublime and molecules from its isomer which are burned into gas will experience

freezing in the reactor flask and condenser, eventually forming a solid wax [30]. Another factor that caused the formation of wax solids is the low-temperature setting [22] which greatly affects the products obtained from plastic waste [31]. The results of liquid products in this study are shown in Figure 4.

Figure 4. Pyrolysis liquid product

3.3 Potential Energy

Products obtained from the pyrolysis process offer many opportunities to be exploited. According to Czajczyńska et al. [14], the liquid product from the pyrolysis of paper biomass, cotton cloth, as well as garden and food waste consists mostly of acids, sugars, alcohols, ketones, aldehydes, phenols, furans, and other mixed oxygen compounds. Meanwhile, glove and rubber band waste contains isoprene, toluene, xylene, trimethylbenzene, and limonene. The liquid product has the potential to be used as an alternative fuel because it has a high calorific content and value. Surono and Ismanto [32] determined the calorific value of liquid products produced from the pyrolysis of PET, PP, and PE plastic waste. The result showed that PP-type plastic has a high heating value of 46.5 Mj/kg. This calorific value is equivalent to those of premium gasoline with a value of 44.0 Mj/kg.

According to Czajczyńska et al. [14], gas products from HVS paper biomass waste, cotton cloth, as well as garden and food waste consist of CO, CO_2, and light hydrocarbons. Meanwhile, products from rubber band waste, LDPE plastic, gloves, and masks contain CO_2, ethane, propane, paraffin, olefin, and carbon. The gas product produced in this study has an average of 30.75% and is considered to have great potential as an alternative gas fuel to replace LPG, in line with Klinghoffer and Castaldi [33].

The pyrolysis process is usually maximized to obtain liquid and gas, while solid products or charcoal are produced from the rest of the combustion process. Besides, the solid products contain a matrix rich in activated carbon content [34] and are widely used as solid fuel briquettes[35] or as a base material for batteries [36].

4. Conclusion

The pyrolysis process in this study produced liquid, solid, and gas products using the same temperature of 400 °C. The highest liquid product was obtained from non-B3 rubber band medical waste with a yield of 44%. Furthermore, liquid products were not obtained from LDPE plastic and masks because the content in the waste does not match the temperature applied, hence, only solid wax was produced. The highest solid product was obtained from LDPE plastic waste, with a yield of 65%, while the lowest was produced from rubber band waste with a yield of 21%. Moreover, the highest gas product was obtained from mask waste, with a proportion of 45% while the lowest was produced from food waste, with a yield of 18%.

Products from the pyrolysis process offer many opportunities to be used as alternative energy sources. Based on the percentage yields obtained, the liquid product with the greatest potential to be converted into gasoline is the rubber band waste with a yield of 44%. The gas products with the best potential to be converted into fuel was obtained from masks with a percentage of 45%. Finally, LDPE plastic waste with a yield of 65% has the greatest potential to be converted into solid fuel briquettes and battery base materials.

Suggestion

Future studies should pay more attention to the characteristics of the waste and the temperature to obtain maximum bio-oil. Moreover, inappropriate particle size will affect the production of pyrolysis oil.

Acknowledgment

The authors are grateful to the Education Fund Management Institution through the Merdeka Learning Campus Merdeka program for providing support during this project. Moreover, the authors are grateful to all parties who helped in the writing process of this study, especially the supervisor. Hopefully, this study can provide benefits for all and sundry

References

[1] Rachmat, R., & Nadjib, M. (2022). Implementasi kebijakan pengelolaan limbah medis infeksius pada era COVID-19. *Journals of Ners Community*, 13(4), 449–458. doi: 10.55129/jnerscommunity.v13i4.2088

[2] WHO. (2018). Limbah perawatan kesehatan. *World Health Organization*. Retrieved September 24, 2022, from https://www.who.int/news-room/fact-sheets/detail/health-care-waste

[3] Kriswibowo, A., Wahyuningtiyas, A., Wandira, N., & Prasetyo, K. (2021). Kerjasama pemerintah dan swasta dalam pengelolaan limbah medis Covid - 19 di Kota Madiun. *Public Inspiration*, 6(1), 8–18. doi: 10.22225/pi.6.1.2021.8-18

[4] Ali, S. A., Parvin, F., Al-Ansari, N., Pham, Q. B., Ahmad, A., Raj, M. S., … Thai, V. N. (2021). Sanitary landfill site selection by integrating AHP and FTOPSIS with GIS : a case study of memari municipality, India. *Environmental Science and Pollution Research*, 28, 7528–7550. doi: 10.1007/s11356-020-11004-7

[5] Dharmaraj, S., Ashokkumar, V., Pandiyan, R., Halimatul Munawaroh, H. S., Chew, K. W., Chen, W. H., & Ngamcharussrivichai, C. (2021). Pyrolysis: An effective technique for degradation of COVID-19 medical wastes. *Chemosphere*, 275, 130092. doi: 10.1016/j.chemosphere.2021.130092

[6] Purwanti, A. A. (2018). Pengelolaan limbah bahan berbahaya dan beracun rumah sakit di RSUD Dr.Soetomo surabaya. *Jurnal Kesehatan Lingkungan*, 10, 291–298.

[7] Sitompul, P. P. E. (2021). Menilik kebijakan pengolahan limbah B3 fasilitas pelayanan kesehatan selama pandemi COVID-19 di Provinsi Jawa Barat. *Dinamika Lingkungan Indonesia*, 8(1), 73–79. doi: 10.31258/dli.8.1.p.73-79

[8] Fang, S., Jiang, L., A, P. L., Bai, J., & Chang, C. (2020). Study on pyrolysis products characteristics of medical waste and fractional condensation of the pyrolysis oil. *Energy*, 195, 116969. doi: 10.1016/j.energy.2020.116969

[9] Matsakas, L., Gao, Q., Jansson, S., Rova, U., & Christakopoulos, P. (2017). Green conversion of municipal solid wastes into fuels and chemicals. *Electronic Journal of Biotechnology*, 26, 69–83. doi: 10.1016/j.ejbt.2017.01.004

[10] Aini, N., Jamilatun, S., & Pitoyo, J. (2022). Pengaruh tipe biomasa pada produk pirolisis : a review. *Agroindustrial Technology journal*, 06(01), 89–101. doi: 10.21111/atj.v6i1.7559

[11] Wajdi, B., Safiruddin, Novianti, B. A., & Zahara, L. (2020). Pengolahan sampah plastik menjadi Bahan bakar minyak (BBM) dengan metode pirolisis sebagai energi alternatif. *Kappa Jurnal*,

4(1), 100–112. doi: 10.29408/kpj.v4i1.2156

[12] Qin, L., Han, J., Zhao, B., Chen, W., & Xing, F. (2018). The kinetics of typical medical waste pyrolysis based on gaseous evolution behaviour in a micro-fluidised bed reactor. *Waste Management and Research*, 36(11), 1073–1082. doi: 10.1177/0734242X18790357

[13] WHO. (2018). Health-care waste. *WHO*. Retrieved August 17, 2022, from https://www.who.int/news-room/fact-sheets/detail/health-care-waste

[14] Czajczyńska, D., Anguilano, L., Ghazal, H., Krzyżyńska, R., Reynolds, A. J., Spencer, N., & Jouhara, H. (2017). Potential of pyrolysis processes in the waste management sector. *Thermal Science and Engineering Progress*. doi: 10.1016/j.tsep.2017.06.003

[15] Syamsiro, M., Hadiyanto, A. N., & Mufrodi, Z. (2016). Rancang bangun mesin pencacah plastik sebagai bahan baku mesin pirolisis skala komunal. *Jurnal Mekanika dan Sistem Termal (JMST)*, 1(2), 43–48.

[16] Gao, N., Sipra, A. T., & Quan, C. (2020). Thermogravimetric analysis and pyrolysis product characterization of municipal solid waste using sludge fl y ash as additive. *Fuel*, 281, 118572. doi: 10.1016/j.fuel.2020.118572

[17] Silva, J. D. O. da, Santos, D. E. L., Abud, A. K. de S., & Oliveira, A. M. de. (2020). Characterization of acerola (Malpighia emarginata) industrial waste as raw material for thermochemical processes. *Waste Management*, 107, 143–149. doi: 10.1016/j.wasman.2020.03.037

[18] Sukarta, I. N., Sastrawidana, I. D. K., Putu, N., & Ayuni, S. (2018). Proximate analysis and calorific value of pellets in biosolid combined with wood waste biomass. *Journal of Ecological Engineering*, 19(3), 185–190. doi: 10.12911/22998993/86153

[19] Liu, X., Chen, M., & Wei, Y. (2015). Kinetics based on two-stage scheme for co-combustion of herbaceous biomass and bituminous coal. *Fuel*, 143, 577–585. doi: 10.1016/j.fuel.2014.11.085

[20] Aragaw, T. A., & Mekonnen, B. A. (2021). Current plastics pollution threats due to COVID-19 and its possible mitigation techniques: a waste-to-energy conversion via Pyrolysis. *Environmental Systems Research*, 10, 1-11. doi: 10.1186/s40068-020-00217-x

[21] Sari, G. L. (2018). Kajian potensi pemanfaatan sampah plastik menjadi bahan bakar cair. *Al-Ard: Jurnal Teknik Lingkungan*, 3(1), 6–13. doi: 10.29080/alard.v3i1.255

[22] Qureshi, M. S., Oasmaa, A., Pihkola, H., Deviatkin, I., Tenhunen, A., Mannila, J., … Laine-Ylijoki, J. (2020). Pyrolysis of plastic waste: Opportunities and challenges. *Journal of Analytical and Applied Pyrolysis*, 152(February), 1048. doi: 10.1016/j.jaap.2020.104804

[23] Amrullah, A., Ristianingsih, Y., Mursadin, A., & Abdi, C. (2015). Studi eksperimental bio oil berbahan baku limbah sisa makanan dengan variasi temperatur pirolisis. *Proceeding Seminar Nasional Tahunan Teknik Mesin XIV*, (Snttm Xiv), 7–14.

[24] Novita, S. A., Santosa, S., Nofialdi, N., Andasuryani, A., & Fudholi, A. (2021). Parameter operasional pirolisis biomassa. *Agroteknika*, 4(1), 53–67. doi: 10.32530/agroteknika.v4i1.105

[25] Ridhuan, K., Irawan, D., & Inthifawzi, R. (2019). Proses pembakaran pirolisis dengan jenis biomassa dan karakteristik asap cair yang dihasilkan. *Turbo*, 8(1), 69–78. Retrieved from http://ojs.ummetro.ac.id/indeks.php/turbo

[26] Shen, J., Wang, X. S., Garcia-Perez, M., Mourant, D., Rhodes, M. J., & Li, C. Z. (2009). Effects of particle size on the fast pyrolysis of oil mallee woody biomass. *Fuel*, 88(10), 1810–1817. doi: 10.1016/j.fuel.2009.05.001

[27] Awad, M., Moustafa-farag, M., Wei, L., Huang, Q., & Liu, Z. (2020). Effect of garden waste biochar on the bioavailability of heavy metals and growth of brassica juncea (L .) in a multi-contaminated soil. *Arabian Journal of Geosciences*, 13, 1–12. doi: 10.1007/s12517-020-05376-w

[28] Guedes, R. E., Luna, A. S., & Torres, A. R. (2018). Operating parameters for bio-oil production in biomass pyrolysis: A review. *Journal of Analytical and Applied Pyrolysis*. Elsevier B.V. doi: 10.1016/j.jaap.2017.11.019

[29] Ma, W., Rajput, G., Pan, M., Lin, F., Zhong, L., & Chen, G. (2019). Pyrolysis of typical msw components by Py-GC / MS and TG-FTIR. *Fuel*, 251(April), 693–708. doi: 10.1016/j.fuel.2019.04.069

[30] Savira, F. L., & Hendriyanto, O. (2018). Pirolisis sampah plastik sebagai bahan bakar alternatif dengan penambahan sampah ranting. *Jurnal Envirotek*, 9(2). doi: 10.33005/envirotek.v9i2.966

[31] Kurniawan, E., & Nasrun. (2017). Karakterisasi bahan bakar dari sampah plastik jenis high density polyethelene (HDPE) dan low density polyethelene (LDPE). *Jurnal Teknologi Kimia Unimal*, 3(2), 41–52.

[32] Surono, U. B., & Ismanto. (2016). Pengolahan sampah plastik jenis PP, PET dan PE menjadi bahan bakar minyak dan karakteristiknya. *Jurnal Mekanika dan Sistem Termal*, 1(1), 32–37. Retrieved from http://e-journal.janabadra.ac.id/index.php/JMST%0AOriginal

[33] Klinghoffer, N. B., & Castaldi, M. J. (2013). Gasification and pyrolysis of municipal solid waste (MSW). *Waste to Energy Conversion Technology*. doi: 10.1533/9780857096364.2.146

[34] Riandis, J. A., Setyawati, A. R., Sanjaya, A. S. (2021). Pengolahan Sampah Plastik Dengan Metode Pirolisis menjad Bahan Bakar Minyak. *Jurnal Chemugry*, 5(1), 8–14. doi: 10.30872/cmg.v5i1.4755

[35] Yanti, R. N., Ratnaningsih, A. T., & Ikhsani, H. (2022). Pembbuatan bio-briket dari produk pirolisis biochar cangkang kelapa sawit sebagai sumber energi alternatif. *Jurnal Ilmiah Pertanian*, 19(1), 11–18. doi: 10.31849/jip.v19i1.7815

[36] Nanda, S., Dalai, A. K., Berruti, F., & Kozinski, J. A. (2016). Biochar as an exceptional bioresource for energy, agronomy, carbon sequestration, Activated Carbon and pecialty Materials. *Waste and Biomass Valorization*, 7, 201-235. doi: 10.1007/s12649-015-9459-z

Kampus 3 Universitas PGRI Madiun
Jl. Auri No 14-16 Kartoharjo Madiun
Email: cheesa@unipma.ac.id
http://e-journal.unipma.ac.id/index.php/cheesa